High-Capacity Short-Range Optical Communication Links

Tatarczak, Anna

Publication date:
2016

Document Version
Publisher's PDF, also known as Version of record

High-Capacity Short-Range Optical Communication Links

Anna Tatarczak

Supervisor:
Professor Idelfonso Tafur Monroy

Delivery Date: September 1st, 2016

DTU Fotonik
Department of Photonics Engineering
Technical University of Denmark
Building 343
2800 Kgs. Lyngby
DENMARK

DTU Fotonik
Institut for Fotonik

Abstract

Over the last decade, we have observed a tremendous spread of end-user mobile devices. The user base of a mobile application can grow or shrink by millions per day. This situation creates a pressing need for highly scalable server infrastructure; a need nowadays satisfied through cloud computing offered by data centers. As the popularity of cloud computing soars, the demand for high-speed, short-range data center links grows. Vertical cavity surface emitting lasers (VCSEL) and multimode fibers (MMF) prove especially well-suited for such scenarios. VCSELs have high modulation bandwidths, are energy efficient, reliable, and cheap to fabricate. MMFs are highly tolerant to coupling misalignment and bending. However, because of the large spectral width of VCSELs and, consequently, chromatic and modal dispersion effects in the fiber, the VCSEL–MMF links have a limited bandwidth–distance product: their achievable distance is limited to 100 m at 25 Gbps for non-return-to-zero (NRZ) signaling.

This thesis introduces several methods to tackle this limitation and increase the capacity of a VCSEL–MMF link based on intensity modulation (IM)/direct detection (DD). First, we apply the MultiCAP modulation format to increase the transmission net rate to 65.7 Gbps over 100 m MMF using a single VCSEL and equalization at the receiver. Second, we demonstrate that using a novel block-based 8-dimentional/8-level (BB8) advanced modulation format improves the receiver sensitivity compared to to the equally spectrally efficient PAM-4 modulation format. Single VCSEL transmission over 100 m is demonstrated at 54.5 Gbps. Third, we explore the potential of extending the transmission reach by using a lower chromatic dispersion region with a pre-emphasized 1060 nm VCSEL. Fourth, we discuss short-range wavelength division multiplexing where the total capacity is the product of the single wavelength's capacity and the number of wavelengths. The presented simulations and experiments validate the capacity improvement it introduces. Finally, we apply selective modal launch

to the multimode VCSEL–multimode fiber scenario. This way, we achieve 10 Gbps over 400 m and then confirm the approach in an optimized system at 25 Gbps over 300 m.

The techniques described in this thesis leverage additional degrees of freedom to better utilize the available resources of short-range links. The proposed schemes enable higher speeds and longer distances of the IM/DD optical interconnects.

Resumé

I de seneste 10 år der der sket en eksplosion i udbredelsen af mobile bredbåndsenheder. Antallet af brugere af en mobil applikation kan variere med flere millioner fra dag til dag. Dette stiller krav om en kraftigt skalérbar serverinfrastruktur; et krav der i dag imødekommes ved hjælp af såkaldt cloud-computing 'afvikling i skyen' i datacentre. I takt med at cloud-computing bliver mere og mere populært stiger behovet for højhastigheds datacenterforbindelser med kort rækkevidde. 'Vertical cavity surface emitting lasers' (VCSELs) og multimodefibre (MMF) er særligt velegnede for sådanne forbindelser. VCSELs har høj modulationsbåndbredde, de er energieffektive, og de er billige at massefremstille. Multimodefibre er meget tolerante overfor bøjninger og koblingsunøjagtigheder. Til gengæld betyder VCSELernes store optiske linjebredde sammen med multimodefiberens modal- og kromatiske dispersion at disse VCSEL–MMF er begrænsede i forhold til deres båndbredde-rækkevidde produkt. I praksis begrænser dette deres anvendelighed til 100 m ved 25 Gbps under anvendelse af såkaldt non-return-to-zero (NRZ) modulation.

I denne afhandling introduceres adskillige nye metode til at gennembryde denne begrænsning og øge kapaciteten af VCSEL-MMF forbindelser baseret på intensitetsmodulation og direkte detektion (IM/DD). Først anvendes modulationsformatet MultiCAP til at øge dataraten til 70.4 Gbps over 100 m MMF hvor en enkelt VCSEL genererede signalet. Derefter demostrerer vi at man ved at anvende et nyt blokbaseret 8-dimesionelt/8-niveau (BB8) modutationsformat kan forbedre modtagerfølsomheden i forhold til systemer, der anvender PAM-4 modulation, der har tilsvarende spektral effektivitet. Vi demonstrerer enkelt-VCSEL transmission over 100 m MMF ved 56 Gbps. Derefter udnytter vi muligheden for at forøge transmissionsrækkevidden ved at anvende 1060 nm området hvor den kromatiske dispersion er lavere. Som det næste diskuterer vi bølgelængdemultipleksning for korte forbindelser, hvor forbindelsens samlede kapacitet

er den enkelte kanals datarate ganget med antallet af kanaler. Vi præsenterer numeriske simuleringer samt eksperimenter der demonstrerer dette. Til slut anvender vi selektiv modalexcitation i VCSEL–MMF systemer, og opnår derigennem 10 Gbps over 400 m. Vi bekræfter denne fremgangsmåde ved i et optimeret system at transmittere 25 Gbps over 300 m.

Teknikkerne, som er beskrevet i denne afhandling drager fordel yderligere frihedsgrader til bedre at udnytte til forhåndenværende ressourcer i korte forbindelser. De foreslåede metoder åbner for højere hastigheder og længere rækkevidde for IM/DD forbindelser.

Acknowledgements

First, I would like to thank my supervisor, Idelfonso Tafur Monroy, for the support and encouragement through all these years. His supervision from my bachelor studies till the end of my PhD was imaginative, visionary, challenging, and overall, inspiring.

I would like to thank people I have learnt a lot from while working together over the course of my PhD. Special thanks to Miguel, Mario and Xiaofeng from DTU as well as Roberto, Chris, and Sascha from Finisar. I learnt focus, determination, stubbornness, and problem solving thanks to your support, faith in me, as well as countless hours spent in the lab together. Thank you for being motivating, and patient. Moreover, I would like to thank my short-term collaborators, Vladimir, Ruslan, Simon, and Seba with whom I have shared an intense experiment experience, a lot of fun, knowledge and music. I would like to thank Jesper who has always been helpful and supportive from the beginning of my journey in the optics world. Thanks to all of the members of Metro Access group at DTU Fotonik.

Great thanks to my friends and flatmates for bearing with me through the years when I was always late or not there, because there was something to finish at work. Special thanks to Piotr B. for being always ready to share a different perspective, for introducing a taste of objectivity in my subjective world.

I would like to thank my sister Agnieszka, for all that time spent on writing and sharing. Thanks to my parents for their faith in me. Last, but not least to my best friend and a partner, Piotr. For being supportive but critical, for challenging me and helping me grow. For always being there for me.

Summary of Original Work

This thesis is based on the following original publications:

PAPER 1 Tatarczak, A.; Lu, X.; Tafur Monroy, I., "Improving the Capacity of Short-Reach VCSEL-based MMF Optical Links," *LAOP*, 2016.

PAPER 2 Tatarczak, A.; Reza Motaghiannezam, S. M.; Kocot, C.; Hallstein, S.; Lyubomirsky, I.; Askarov, D.; Daghighian, H.M.; Nelson, S.; Tafur Monroy, I.; Tatum, J.A., "Reach Extension and Capacity Enhancement of VCSEL based Transmission over Single Lane MMF Links," submitted to *Journal of Lightwave Technology*, 2016.

PAPER 3 Tatarczak, A.; Iglesias Olmedo, M.; Zuo, T.; Estaran, J.; Bevensee Jensen, J.; Xu, X.; Tafur Monroy, I., "Enabling 4- Lane Based 400 G Client-Side Transmission Links with MultiCAP Modulation," Advances in Optical Technologies, vol. 2015, Article ID 935309, 2015.

PAPER 4 Lu, X.; Tatarczak, A.; Tafur Monroy, I., "Eight Dimensional Optimized Modulation for IM-DD 56 Gbit/s Optical Interconnections Using 850 nm VCSELs," Optical Communication (ECOC), 2014 European Conference on, pp. , September 2016.

PAPER 5 Tatarczak, A.; Zheng, Y.; Rodes, G.A.; Estaran, J.; Lin, Chin-Han; Barve, A.V.; Honore, R.; Larsen, N.; Coldren, L.A.; Tafur Monroy, I., "30 Gbps bottom-emitting 1060 nm VCSEL," *Optical*

Communication (ECOC), 2014 European Conference on, pp. 1, 3, September 2014.

PAPER 6 B. Cimoli, J. Estaran, G. A. Rodes, A. Tatarczak, J. J. Vegas Olmos, and I. Tafur Monroy, "100G WDM Transmission over 100 meter Multimode Fiber," in *Asia Communications and Photonics Conference 2015*, OSA Technical Digest, paper ASu2A.89, 2015.

PAPER 7 Tatarczak, A.; Usuga Castaneda, M.; Tafur Monroy, I., "OAM - enhanced Transmission for Multimode Short-Range Links," Proc. SPIE 9390, Next-Generation Optical Networks for Data Centers and Short-Reach Links II, 93900E, March 2015.

PAPER 8 Tatarczak, A.; Lu, X.; Rommel, S.; Rodriguez, S.; Vegas Olmos, J.J.; Monroy, I.T., "Radio-over-Fiber Transmission over 400m MMF," submitted to *JOCN*.

Other scientific reports associated with the project:

[PAPER 9] Lyubopytov, V. S.; Tatarczak, A.; Lu, X.; Kutluyarov, R. V.; Rommel, S.; Sultanov, A. K.; Monroy, I. T., "Optical-domain Compensation for Coupling between Optical Fiber Conjugate Vortex Modes," in 2015 Conference on Lasers and Electro-Optics Pacific Rim, Optical Society of America, 2015, paper PDP T12 1001, 2015.

[PAPER 10] Iglesias Olmedo, M.; Tatarczak, A.; Tianjian Zuo; Estaran, J.; Xiaogeng Xu; Tafur Monroy, I., "Towards 100 Gbps over 100m MMF using a 850 nm VCSEL," *Optical Fiber Communications Conference and Exhibition (OFC)*, 2014, pp.1,3, March 2014.

[PAPER 11] Kocot, C.; Motaghian, R.; Tatarczak, A.; Lyubomirsky, I.; Hallstein, S.; Askarov, D.; Daghighian, H.; Nelson, S.; Tatum, J., "SWDM Strategies to Extend Performance of VCSELs over MMF," in *Optical Fiber Communication Conference*, OSA Technical Digest (online) (Optical Society of America, 2016), paper Tu2G.1.

[PAPER 12] Lu, X.; Tatarczak, A; Rommel, S.; Rodriguez, S.; Vegas Olmos, J. J.; Tafur Monroy, I., "Microwave Photonics Technologies Supporting High Capacity and Flexible Wireless Communications Systems," in Asia Communications and Photonics Conference 2015, OSA Technical Digest, paper ASu1J.5, 2015.

[PAPER 13] Tatarczak, A.; Lu, X.; Rommel, S.; Rodriguez, S.; Vegas Olmos, J.J.; Monroy, I.T., "Radio-over-Fiber Transmission Using Vortex Modes," in Microwave Photonics (MWP), 2015 International Topical Meeting, pp.1-3, 2015.

Other scientific reports:

[C1] Zuo, T.; Tatarczak, A.; Olmedo, M.I.; Estaran, J.; Jensen, J.B.; Qiwen Zhong; Xiaogeng Xu; Tafur Monroy, I., "O-band 400 Gbit/s Client Side Optical Transmission Link," *Optical Fiber Communications Conference and Exhibition (OFC)*, 2014, pp.1,3, March 2014.

[C2] Jurado-Navas, A.; Tatarczak, A.; Lu, X.; Vegas Olmos, J.J., Garrido-Balsells, J.M.; Tafur Monroy, I., "850-nm Hybrid Fiber/Free-Space Optical Communications using Orbital Angular Momentum Modes," Opt. Express 23, 33721-33732, 2015.

Contents

Glossary

B2B back to back. 33

BB8 Block-based 8-dimentional/8-level. 33

BER bit error rate. 26–28, 40, 45–47, 50

BW bandwidth. 44

CAP carrierless amplitude phase. 31

CCD charge-coupled device. 40

CD chromatic dispersion. 13, 35

DAC digital-to-analog converter. 44

DD direct detection. i, 6, 27, 33, 41, 45

DFE decision feedback equalizer. 26

DMD differential mode delay. 17–20, 40

DMT discrete multitone. 26, 27, 31

DSA digital storage analyzer. 45

DSP digital signal processing. 45

EB effective bandwidth. 21

EMB effective modal bandwidth. 20, 21, 37

EMBc calculated effective modal bandwidth. 20

EML externally modulated laser. 44

ER extended range. 44, 45

FEC forward error correction. 27, 28, 30, 31, 44, 45, 47

FFE feed forward equalizer. 25, 26, 28

FIR finite impulse response. 31

FSO free-space optics. 47

GD group delay. 16

IM intensity modulation. i, 6, 27, 33, 41

ISI inter-symbol interference. 16, 17, 30

LED light emitting diode. 21

LMS least mean square. 24, 26

LR long range. 44, 45

MMA multi-modulus algorithm. 45

MMF multi mode fiber. 5, 6, 15, 16, 18, 21–24, 26–28, 30, 31, 33–41, 43–47

MUX multiplexer. 44

NA numerical aperture. 16

NRZ non return to zero. 6, 27, 28, 30, 31, 33, 43

PAM pulse amplitude modulation. 25–27, 30, 31, 33, 34, 37, 40, 41, 43–45

PAPR peak-to-average power ratio. 31, 32

PD photodiode. 5, 14–16, 43, 46

QSFP quad small form-factor pluggable. 33

QW Quantum Well. 8

RIN relative intensity noise. 12, 13, 27, 30

RoF radio over fiber. 43, 47

RX receiver. 24–26, 28, 45

SIR signal to interference ratio. 40

SLM spatial light modulator. 39, 40, 46, 47

SMF single mode fiber. 16, 36, 44

SNR signal-to-noise ratio. 24, 26, 27, 32, 44, 45

SOA semiconductor optical amplifier. 45

SR short range. 44, 45

SWDM short-wave wavelength division multiplexing. 23, 31, 37, 38, 40, 41, 43, 44, 46

TX transmitter. 24, 25, 28, 38, 41

VCSEL vertical cavity surface-emitting laser. 5–14, 19–22, 24, 25, 27, 28, 30, 33–35, 37, 40, 41, 43–47

WDM wavelength division multiplexing. 35, 44–46

Chapter 1

Introduction

The aim of this PhD study was to investigate various methods for improving the capacity of short-range optical links. The considered schemes are based on intensity modulation (IM)/direct detection (DD), vertical cavity surface-emitting laser (VCSEL), and multi mode fiber (MMF). This thesis consists of an introduction and a collection of original published articles preceded by their summary. The following introduction briefly describes the topics tackled in the main research papers from the system perspective.

1.1 Problem statement

With the growing popularity of bandwidth consuming applications such as cloud computing or online gaming, computation has moved from the distributed devices towards data centers. This puts pressure on the capacity of short-range data center optical interconnects. An interconnect includes a driver circuit, VCSEL, MMF, and a photodiode (PD). High bandwidth multimode 850 nm GaAs VCSELs are typically used in the interconnects to satisfy the high-speed requirement. The capacity of such 850 nm VCSEL–MMF links, defined as bandwidth–distance product, is limited by modal and chromatic dispersion effects. Increasing the speed lowers the achievable transmission distance; conversely, longer links can only operate at lower bitrates. Currently, 10 Gbps VCSELs are used in data centers and they support the optical links up to 300 m [1]. However, with the 25 Gbps optical interconnects becoming available [2,3] the transmission distance becomes limited. The IEEE standard defines 100 m as the 25 Gbps reach. The majority of the existing data center connections are below 100 m [4]. Yet, a solution for an improved link capacity is required to support future

interconnects speeds (40 Gbps), increasing data center sizes [5], and already implemented longer links (100m – 300m). Installing parallel lanes is a popular approach. Although viable, this solution is short-term because the optical packaging of components with multiple lanes becomes increasingly complex and there is no sufficient space for the interconnect ports [6]. Moreover, the rewiring is costly and the space in the data centers limited.

This work tackles the problem of limited capacity of short-range links by employing solutions that do not require installing additional fibers.

I focus on the VCSEL–MMF based solutions because these devices are currently utilized in more than 85% of short-range data center links [7]. The proposed schemes is based on IM/DD to satisfy the low complexity and energy consumption requirements.

1.2 Applications

The majority of high-speed short-range optical links is implemented in the data centers. They have to be high-speed, densely packaged, and energy efficient. There are several new standards that cover high-speed VCSEL–MMF types of links. IEEE 802.3bm aims at supporting 100 Gbps (4x25) 100 m OM4 and 70 m OM3 using non return to zero (NRZ) [1]. Infiniband EDR suggests 1, 2, or 12 parallel lanes with 25 Gbps in each [8]. Fiber channel 32GFC requires transceivers at 28 Gbps supporting 100 m OM4 [9].

VCSEL–MMF links are also used as low-rate, low-cost antenna MMF links. They feed the signal from a cell cabinet to the antenna. Antenna link capacities are standardized by LTE standard, i.e. the 43rd band of the LTE standard is defined as 1 Gbps at a 3.7 GHz carrier. In the future, RoF systems will use higher carrier frequencies (starting with 5GHz [10]) to increase capacity. Some of the techniques for capacity improvement as in the high-speed interconnects, e.g. based on optical design, can be applied to lower speed, longer antenna links.

Short-range MMF links are also implemented for inter-building connections, e.g. in big company buildings. The speed of these connections is usually defined by customers. These types of links are supported by a physical layer Ethernet standard, 10GBASE-SR.

Papers 1–7 aim at data center application and Paper 8 at the antenna link scenario, where the RoF signal is transmitted over MMF.

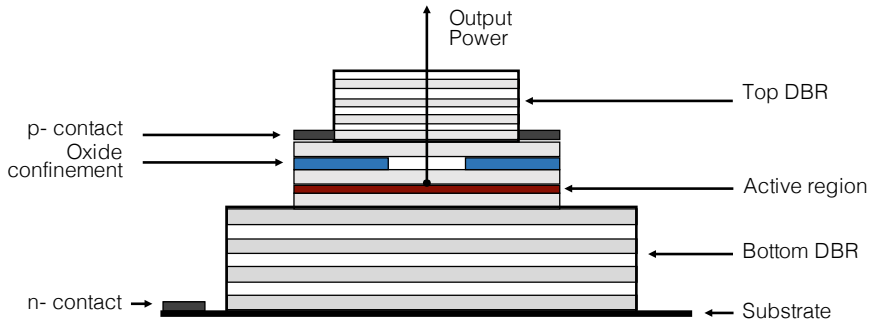

Figure 1.1: GaAs VCSEL structure [16].

1.3 Vertical cavity surface emitting laser

Vertical Cavity Surface Emitting Lasers have been used in the telecom industry for over two decades. Because they emit light through the top surface they offer a number of improvements over edge-emitting lasers:

- They do not need to be packaged before characterization. Thus, testing can be performed on wafer—earlier in the production stage and the production is more cost-effective.
- They can be integrated in densely spaced arrays with small interchannel crosstalk [11, 12].
- The cavity of VCSEL is small and typically a single longitudinal mode is generated.

Furthermore, they can be modulated with high frequencies [13], have a low threshold current (for short wavelengths even below 1 μA [14]) and power consumption, and are highly reliable through their long lifetime [15]. Additionally, VCSEL's beam is symmetric, has a low divergence, and therefore is easy to collimate.

1.3.1 Structure

Figure 1.1 shows an example structure of a multimode VCSEL. The structure is placed on a substrate and has two electrical contacts: p-contact and n-contact. In between two distributed Bragg reflectors (top DBR and bottom DBR) there is an active region. The mirrors provide optical feedback and the active region provides the gain [17].

DBRs are highly reflective mirrors used for current injection [18]. They include interchanging high and low refractive index layers where the light is partially reflected at each interface. The layers closest to the active region have a lower refractive index than the active region. DBRs vertically confine the light and enable an increased reflection coefficient.

The active region must provide gain sufficient to overcome optical losses in the medium and power sufficient for lasing. It usually consists of a pin-heterojunction and Quantum Well (QW). The QW were first demonstrated in a VCSEL structure in Reference [19]. The carriers in QW are confined to one dimension and free in two other dimensions due to the quantum confinement effect [20]. Carriers are 'trapped' in the lowest conduction and valence band states, and separated from each other by higher band states. This provides high carrier density. Typically, a VCSEL structure features multiple QWs to provide sufficient gain.

The oxide layer is added in the structure to confine both optical modes and current in the transverse direction. The transverse confinement region is called the oxide aperture. The confined current and modes are guided to the active region [21].

The cavity length of high-speed VCSELs is usually designed to be the shortest possible to increase the modulation bandwidth. The smaller the cavity, the higher confinement factor Γ and the stronger the carrier — photon interaction. The resonance in the longitudinal direction (limited by DBRs) is created when optical field repeats itself after the round-trip in the cavity. Therefore, the smallest cavity length equals to $1/2\lambda$ and the second smallest cavity length equals to λ. Typically used is $3/2\lambda$ Because of the short cavity, there is typically only one longitudinal mode which falls into gain bandwidth. In the transverse direction, however, the oxide aperture diameter is multiple times longer than the wavelength to improve output power. In case of 850 nm GaAs devices is it often more that 10 times longer. Consequently, multiple transverse modes with different wavelengths are created, broadening the optical spectrum [22].

The original VCSEL structure was proposed in 1988 in Reference [23] and has been under development ever since. GaInAsP/InP and AlGaAs-/Ga/As were the first materials used for VCSEL fabrication. They supported VCSEL wavelengths in a region from 750 nm to 980 nm. VCSELs based on InGaAs were introduced in the 90's supporting longer wavelengths, i.e. 1550 nm and 1300 nm [24]. In parallel, high bandwidth 850 nm VCSELs were studied and commercialised [25,26]. Currently GaAs 850 nm VCSELs are used in 95% of all optical data links below 1000 m [27]. VC-

SELs used during the course of this PhD include multimode 850 nm VC-SELs based on GaAs (Papers 2 – 4, 7, 8, 10, 11, 13, and C2), and a multimode 1060 nm VCSEL based on GaAs/AlAs and InGaAs (Paper 5).

1.3.2 Rate equations

The behavior of carriers and photons in the laser cavity can be described using a reservoir model introduced by Coldren in [28]. This model describes the intrinsic dynamics of a semiconductor laser. According to the model, there are two reservoirs in the active region: 1) a carriers (N) reservoir of a volume V, 2) a photons (N_p) reservoir of a volume V_p. They are related to each other through the confinement factor Γ: $V = \Gamma \cdot V_p$.

The number of carriers in the reservoir increases by $\eta_i I/q$ (when the current is injected to the laser) and by the carriers generated from the absorbed photons at the rate $R_{12}V$. η_i is the injection efficiency and I/q is number of carriers injected to the laser. The number of carriers decreases due to non-radiative recombination at the rate $R_{nr}V$, spontaneous emission recombination at the rate $R_{sp}V$, and stimulated emission recombination at the rate $R_{21}V$. The carrier number rate equation summarises these processes in the carrier reservoir:

$$V\frac{dN}{dt} = \frac{\eta_i I}{q} - (R_{sp} + R_{nr})V - (R_{21} - R_{12})V \tag{1.1}$$

The number of photons in the photons reservoir increases due to stimulated emission recombination at the rate $R_{21}V$, and spontaneous emission at the rate $R'_{sp}V$. It decreases due to the photon absorption at the rate $R_{12}V$ and due to light emission. Photons leave the laser cavity at the rate N_pV_p/τ_p. τ_p is the photon lifetime. The photon rate equation summarises processes in the photon reservoir:

$$V_p\frac{dN_p}{dt} = (R_{21} - R_{12})V - \frac{N_pV_p}{\tau_p} + R'_{sp}V \tag{1.2}$$

Dividing Equation 1.1 and Equation 1.2 by the carrier reservoir volume size V and replacing the term $R_{21} - R_{12}$ by $v_g g N_p$ results in density rate equations:

$$\frac{dN}{dt} = \frac{\eta_i I}{qV} - (R_{sp} + R_{nr}) - v_g\Gamma_r g N_p \tag{1.3}$$

$$\frac{dN_p}{dt} = \left(\Gamma v_g \Gamma_r g - \frac{1}{\tau_p}\right) N_p + \Gamma R'_{sp} \tag{1.4}$$

$\Gamma = \frac{V}{V_p}$ — confinement factor
v_g — group velocity
g — gain
τ_p — photon lifetime
N — carrier density
N_p — photon density
η_i — internal quantum efficiency
V — active region volume
q — electric charge
$R_{sp} = N/\tau$ — spontaneous emission rate
R_{nr} — non-radiative recombination rate
R'_{sp} — rate of photons emitted into mode of interest

There are different solutions of the rate equations for the following VCSEL states: DC, small signal modulation, and large signal modulation. Large signal modulation is used during the transmission experiments. The following subsections will address DC and small signal modulation solutions. A strict analysis would require a rate equation for each photon density of each mode and a rate equation for the carrier density, resulting for a laser with N modes in (2N+1) equations. Yet, a single-mode rate equation was experimentally verified to be a good approximation of the multimode behaviour [29].

The carrier and photon densities depend on one another and therefore the photons and carriers reservoirs are coupled. The coupled increase and decrease of N and N_p results in 'ringing of the output power' [28] at a certain frequency. The 'ringing' frequency depends on the bias current, photon lifetime, and carrier lifetime [30]:

$$f_r = \frac{1}{2\pi}\sqrt{\frac{v_a a_N}{qV_p}\Gamma\Gamma_r\eta_i(I_L - I_{th})} \tag{1.5}$$

$a_N = \frac{\partial g}{\partial N}$
I_L — laser bias
I_{th} — laser threshold current

Factor D describes the relation between f_r and the bias current:

$$f_r = D\sqrt{I_L - I_{th}} \tag{1.6}$$

A damping effect occurs in lasers analogously to the RLC circuit. Damping factor γ is proportional to the resonance frequency and related to the carrier lifetime [31]:

$$\gamma = Kf_r^2 + \frac{1}{\tau} \tag{1.7}$$

K — gain compression factor

D and K factors are figures of merit used for comparing lasers and for fitting laser models parameters to the measured behaviour. High resonance frequencies can be reached at low bias currents for a high D factor, indicating high bandwidth and energy efficiency of the device. The relaxation oscillation peak is less damped for a lower K factor. Very low K factor is one of the indicators that there will be overshoots in the optical eye diagram.

1.3.3 Characterization

In this section, I introduce several ways of characterizing VCSELs. I used these methods throughout the course of my PhD and in Papers 2 – 5, 7–8, 10–11, 13, and C1.

Static characterization

The working range of the laser can be defined based on the laser's DC characterization. All of the injected carriers are used for the spontaneous emission and the non-radiative recombination under the small, below threshold, current condition. There is only spontaneous emission output. The stimulated emission recombinations occur when the number of injected carriers exceeds the spontaneous and non-radiative losses. The current level at which the stimulated emission starts occurring is referred to as the threshold current I_{th}. For currents higher than I_{th} the carriers are used mostly in the stimulated emission and the output power increases linearly with applied current (above threshold behavior). The steady state solution of the rate equations describes the output power P_o in the linear range as a function of the bias current [30]:

$$P_o = \eta_d \frac{h\nu}{q}(I - I_{th}) \tag{1.8}$$

η_d — quantum efficiency

$h\nu$ — energy of a photon

q — elementary charge

The output power saturates for high bias current values due to thermal effects. The DC characterization allows to choose an operating bias current for the system. If a linear characteristic is essential the bias current is chosen in the middle of the linear range.

Frequency response

A laser's frequency response, or scattering parameter S_{21}, can be measured using small signal analysis. A small amplitude modulation is used to drive the laser. The photons are created due to the stimulated emission. The spontaneous emission into the lasing modes is not taken into account in the small signal analysis. A laser transfer function has been derived in [28] from the rate equation for photons and carriers density (Equation 1.3 and Equation 1.4) and has the following form of a second order damped system:

$$H_L(\omega) = \frac{{\omega_r}^2}{{\omega_r}^2 - \omega^2 + j\omega\gamma} \tag{1.9}$$

H_L — transient function of the laser
$\omega_r = 2\pi \cdot f_r$
γ — damping factor

Equation 1.9 describes VCSEL frequency response considering only intrinsic effects of the laser. At high frequencies VCSEL has parasitic resistances and capacitances that will reduce the modulation response. Additional poles need to be added to the equation to describe the extrinsic effects that include parasitics response. These vary for different lasers and have to be defined separately based on the device design and electrical contacts circuit. A simple approximation uses a single additional pole with a parasitics cut-off frequency f_p [32].

Relative intensity noise

The spontaneous emission processes are considered in the relative intensity noise description. They were neglected in the small signal analysis for simplicity but the random carrier and photon recombinations occur under all applied current conditions. Variations in carrier density result in a broadening of the laser pulse, referred to as frequency noise, while variations in photon density lead to intensity variations, referred to as relative intensity noise (RIN). RIN is a quantification of the constant variations of the photon densities and can be expressed as a relation between the squared photon density fluctuations and squared average photon density [28]. RIN can be observed in the steady state as laser output power fluctuations:

$$RIN = \frac{\delta P(t)^2}{{P_0}^2} \tag{1.10}$$

The frequency domain expression of RIN is based on the rate equations. It includes an additional spontaneous emission constant B, as compared to small signal analysis:

$$RIN(f) = \frac{Af^2 + B}{(f_r^2 - f^2)^2 + (\frac{\gamma}{2\pi})^2 f^2} \tag{1.11}$$

f_r — resonance frequency
γ - damping factor
A — constant
B — constant

Intensity noise severely limits the digital and analog modulation performance. It is one of the main limitations especially for the multilevel schemes described in the following sections because it broadens the signal levels and impacts the vertical eye opening.

Optical spectrum

The optical spectrum is the power versus wavelength response of a laser. The emission wavelength of the source can be measured using an optical spectrum measurement. The emission wavelength of the VCSEL rises with the increasing bias current as a result of internal heating. The spectral width (SW) of the laser source can be measured using the optical spectrum. A root-mean-square (RMS) deviation is a standardized measure to characterize a spectral width. σ_α is the RMS source spectral width expressed in nm. For multimode VCSELs, the RMS spectral width ranges up to 0.9 nm [33] due to multiple transverse modes. The increased SW consequently increases chromatic dispersion (CD) in the fiber and decreases its bandwidth. As a result, the fiber capacity decreases. This fiber related effect will be further addressed in Section 1.5.2.

1.3.4 Bandwidth limitations

The available modulation bandwidth supported by a VCSEL can be identified through the small signal analysis. VCSEL bandwidth is often given as a 3 dB bandwidth or f_{3dB}. f_{3dB} is the frequency where the response has decreased to half of its low-frequency value (-3 dB when plotted in the dB scale). VCSEL bandwidth can be limited by intrinsic factors such as thermal effects and damping or by the extrinsic factors [34]. The thermally limited 3 dB bandwidth can be described as [34]:

$$f_{3dB,Thermal} = \sqrt{1 + \sqrt{2}} f_{r,max} \tag{1.12}$$

for $\gamma << \omega_r$ where $f_{r,max}$ is a frequency for which the relaxation frequency saturates with increasing current. The damping limited 3 dB bandwidth is related to a the gain compression factor, K:

$$f_{3dB,damping} = \frac{2\pi\sqrt{2}}{K} \tag{1.13}$$

assuming $\gamma = \sqrt{2}\omega_0$ and $\gamma = Kf_0^2$

[34] defines parasitics limited frequency as:

$$f_{3dB,parasitics} = (2 + \sqrt{3})f_p \tag{1.14}$$

where f_p is a cut-off of the filter that describes parasitics.

A strong resonance peak in the modulation response due to low damping can partially compensate for the parasitic roll-off and, in turn, improve the total modulation bandwidth of the VCSEL [35].

1.4 Photodiode

Photodiodes convert the signal from the optical to the electrical domain using the photoelectric effect. In this section, I introduce the basic parameters of the PDs [36].

1.4.1 Responsivity

A photodetector is a semiconductor, in which an electron-hole pair is generated from each absorbed photon. The energy of a photon has to be higher than the bandgap energy $E_g = h\nu$. The presence of the electric field causes carriers to move and thus a photocurrent I_p to flow:

$$I_p = RP_{in} \tag{1.15}$$

P_{in} is the optical power at the input to the PD and R is its responsivity. R is related to wavelength λ as [36]:

$$R \approx \frac{\eta\lambda}{1.24} \tag{1.16}$$

where η is a quantum efficiency of the PD (the ratio between the absorbed and incident power). It can also be expressed using an absorption coefficient α and the PD's width W:

$$\eta = 1 - exp(-\alpha W) \tag{1.17}$$

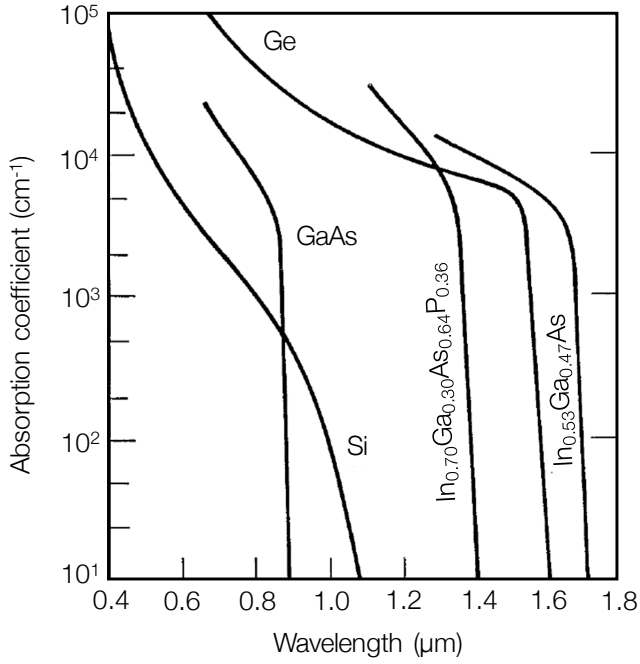

Figure 1.2: Absorption coeficient vs. wavelength. Figure adapted from [36].

The responsivity of the PD increases with λ until $E_g > h\nu$. The relation of absorption coefficient to the wavelength differs depending on the material. Figure 1.2 presents the absorption vs. wavelength dependence for several materials. The GaAs or Ge based PDs can be used for 850 nm short-range applications, as presented in Figure 1.2. Broadband photodiodes based on Indium are required for higher wavelengths.

1.4.2 Bandwidth

A PD's speed depends on the time necessary to transform the incident power into current. It is the rise time T_r in which electrons and holes travel to the electrical contacts and it is defined as the time in which the response increases from 10% to 90% of the final value. The smaller semiconductor width W, the shorter the travel time, and hence the bigger bandwidth. However, efficiency decreases with the decreasing W, as indicated in Equation 1.17. Consequently, responsivity decreases as well (Equation 1.16). Hence, there is a trade-off between the bandwidth of the PD and its responsivity.

The PDs used with MMF need to have a relatively large active area to support efficient coupling from the fiber core. As a result, they have smaller bandwidth than the single mode fiber (SMF) coupled PDs. PDs are one of the bandwidth limiting components in the optical interconnects.

1.5 Multimode fiber

Multimode fiber is a transmission medium used typically in short-range communication applications. Standard MMFs have a core diameter of 50 μm and a cladding diameter of 125 μm. The large core size of the MMF as compared to a SMF alows higher alignment tolerances, i.e. it is easier to launch light into the fiber. Lower connector cost, easier alignment, and a high tolerance to micro bending losses makes MMF based applications more cost efficient than those based on SMF. The numerical aperture (NA) ranges from 0.2 to 0.3 thus making the MMF a robust guiding medium. The core size is much larger than the wavelength of the light, and therefore multiple modes can propagate in the fiber core at different group velocities and with different group delays (GDs). The number of guided modes is determined by the wavelength, and the refractive index profile of the fiber. The achievable transmission distance and information capacity of the fiber are limited by the inter-symbol interference (ISI) caused by the modal and chromatic dispersion. Next sections describe these effects in detail.

1.5.1 Modal dispersion

Modal dispersion is an effect of different fiber modes travelling at different group velocities. The following description of modal dispersion is based on geometrical optics [36]. Fibers are divided into two main types, in terms of refractive index profile: fibers with step index and fibers with graded index. Figure 1.3 presents the difference in the profiles. The step index fiber has the same refractive index through the core, and the refraction occurs only at the core–cladding boundary. The refractive index of the graded index fiber gradually decreases from the fiber core center towards the cladding. In step-index fibers guiding is through complete internal reflection, whereas guiding for graded index fibers is through continuous refraction.

The rays can take several paths in the fiber, depending on the incident angle at the input to the fiber. The shortest path goes straight through the center of the core and has the length of the fiber L. This path is taken by the rays launched under the incident angle of 90°. The longest path in

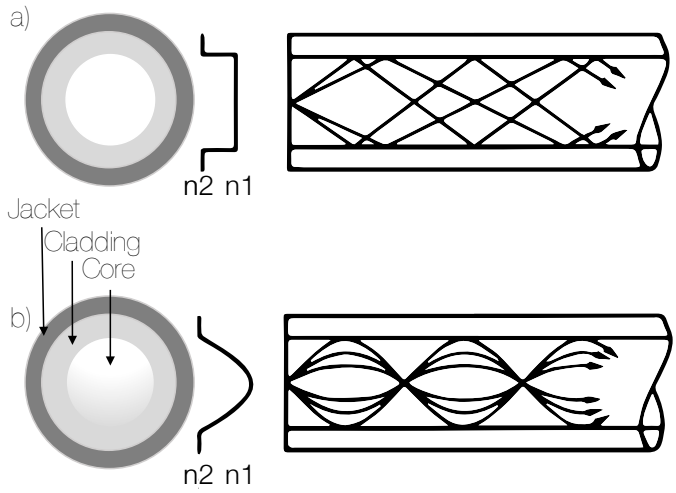

Figure 1.3: a) Step Index and b) graded index fibers.

the step index fiber is taken by the rays for which the angle of incidence on the cladding is ϕ_c, critical angle. Larger angle would result in beams leaving the fiber. The longest path length is equal to $L/sin\phi_c$. Two rays that take the shortest and longest paths arrive at the end of the step index fiber with the time delay ΔT [36]:

$$\Delta T = \frac{n_1}{c}\left(\frac{L}{sin\phi_c} - L\right) = \frac{L}{c}\frac{n_1}{n_2}\Delta \tag{1.18}$$

c — speed of light
n_1 — the refractive index of the fiber core
n_2 — the refractive index of the cladding
Δ is the fractional index change at the core-cladding interface, typically < 0.01.

The delay in arrival times described above is called differential mode delay (DMD). It causes a pulse broadening and ISI. The transmission is possible only if the delay ΔT is smaller than the bit slot of the information $T_B = 1/B$, where B is bitrate:

$$\Delta T < T_B \tag{1.19}$$

This condition gives a rough estimate of the maximum pulse spreading. The the maximum allowable pulse spreading in the implemented systems

is typically specified as $\Delta T = 10\% \cdot T_B$, but for the sake of simplicity I will use the condition from Equation 1.19.

$$B\Delta T < 1 \tag{1.20}$$

This fundamental limit defines the estimated capacity of the step index fiber derived from Equation 1.18:

$$BL < \frac{n_2}{n_1}\frac{c}{\Delta} \tag{1.21}$$

The graded index fibers with parabolic refractive indexes were introduced to reduce the DMD. The principle of the graded index fibers is presented in Figure 1.3 b. The refractive index is n_1 at the core center and gradually decreases to n_2 at the cladding. The refractive index profile can be described using the α profile:

$$n(\rho) = \begin{cases} n_1\left[1 - \Delta\left(\rho/a\right)^{\alpha}\right] & \rho < a \\ n_1(1-\Delta) = n_2 & \rho \geq a \end{cases} \tag{1.22}$$

a — the core radius

α — describes the index profile (is equal to 2 for parabolic index fibers).

In the graded index fibers the length of the shortest path is the same as in the step index fibers but the shortest path ray travels slower than the rays that take longer paths. The reason is that the refractive index is the largest in the very center of the core. The other rays take most of their longer paths in the medium or lower refractive index. The velocity for these rays changes along the path, because of the variation in the refractive index. The fiber capacity limit for graded index fibers is defined as [36]:

$$BL < 8c/n_1\Delta^2 \tag{1.23}$$

The index profile shape highly influences the achievable distance and the capacity of the fiber. Well optimized graded index fibers have a performance multiple times better than the step index fibers [37]. The profiles of commonly implemented MMFs, OM3 and OM4 fibers, are optimized for use with 850 nm multimode VCSELs. They will be addressed in Section 1.5.5.

It is possible to design a graded index fiber in a way that all of the rays from a single mode source arrive at the fiber end in the same time. The fiber can be designed to minimize the modal dispersion for the principal modes, there will, however, always be dispersion for higher order modes [38].

Additionally, the modal dispersion and modal coupling arises due to the imperfections of the MMF refractive index profile, additional modes related to the fiber bending, or when the operating wavelength of the source is not ideal, i.e. does not fit exactly the optimized fiber wavelength window.

1.5.2 Chromatic dispersion

Chromatic dispersion causes the group velocity of the mode to be frequency dependent. That means that different spectral components of a pulse travel with different group velocities. As a result, different spectral components of the pulse disperse during propagation and do not reach the fiber output at the same time. The pulse broadening due to chromatic dispersion for a single mode is defined as:

$$\Delta T = DL\Delta\lambda \tag{1.24}$$

D — a dispersion parameter expressed in ps/(km·nm)

L — a fiber length

$\Delta\lambda$ — a spectral width of the pulse, commonly treated also as a wavelengths range emitted by the laser.

Spectral width of the source was introduced in Section 1.3.3 and referred to as σ_α. The chromatic dispersion depends on the spectral width of the source, on the launch conditions [39], as well as on the silica properties for the specific wavelength. At 1300 nm chromatic dispersion is equal to 0 and the chromatic dispersion effect increases for higher and lower wavelengths. The chromatic dispersion at 850 nm is equal to -105 ps/nm/km. The maximum bitrate times distance, limited by chromatic dispersion, can be calculated in an analogous way to Equation 1.20:

$$BLD\delta\lambda < 1 \tag{1.25}$$

Spectral width includes the wavelengths of all of the transverse modes in multimode sources. Even though the chromatic dispersion at 850 nm is much higher than at higher wavelengths, it still has a smaller effect than the modal dispersion. The difference between the chromatic and modal dispersion for several fiber types is presented in Figure 1.4. The units from the figure (MHz·km) will be explained in the following subsection.

1.5.3 Fiber bandwidth

Effective modal bandwidth (EMB) is a metric popularly used to describe the fiber capacity limited by the modal dispersion [41]. It defines the maximum signaling rate multiplied by a distance and is expressed in MHz·km.

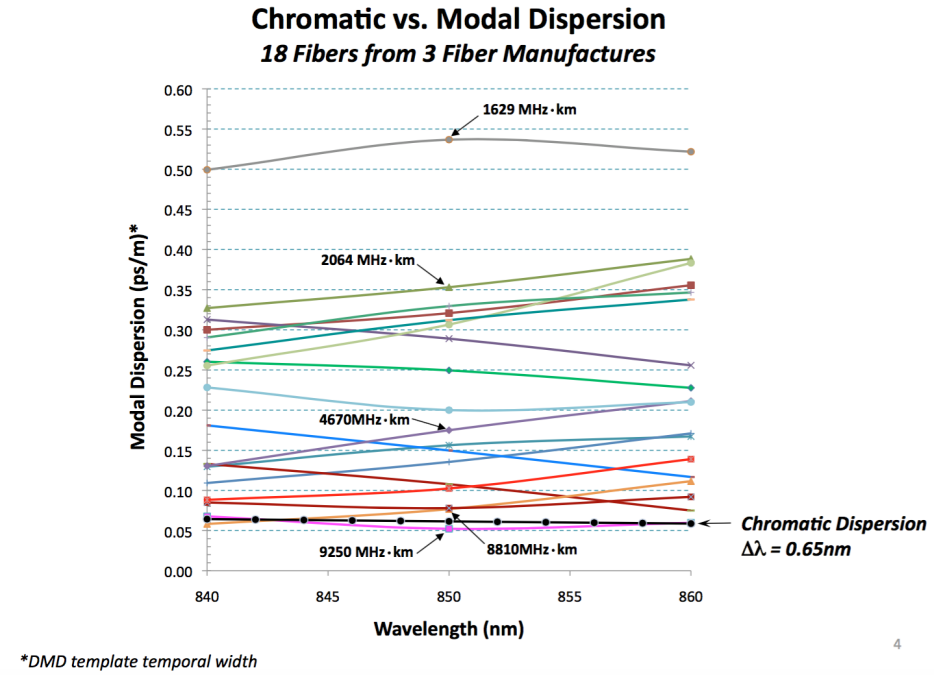

Figure 1.4: Chromatic vs. modal dispersion in OM3 and OM4 fibers. Figure adapted from [40].

DMD discussed in Section 1.5.1 could not be easily compared for different fibers because it depends on the fiber length, launch conditions, and mode structure of the VCSEL. EMB was created to easily compare fibers of different lengths. In order to measure a EMB of a fiber, telecommunication industry association (TIA) describes the method in a standard TIA FO 4.2.1 which is based on scanning the fiber core with a single mode pulses. The result is a DMD plot as a function of the radial position of the launched light. There are two standardized methods to estimate a fiber effective modal bandwidth (EMB). First is the DMD mask approach. The overall fiber delay is calculated by subtracting the slowest trailing edge from the fastest leading edge. The delay is expressed in units ps/m. Second, calculated effective modal bandwidth (EMBc), combines DMD measurement for fibers with the standard-compliant VCSELs. The output pulse is created for each fiber–VCSEL combination and EMB is calculated in units MHz·km. The second method allows for a better link performance predic-

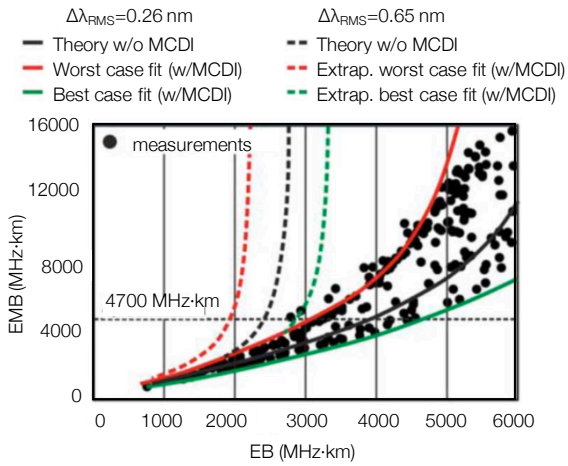

Figure 1.5: EMB vs. EB adapted from [44].

tion assuming launch created by a particular source, e.g. VCSEL. EMBc is indicated for five fibers in Figure 1.4.

Effective bandwidth (EB) combines the effects of modal and chromatic dispersion in the fiber [42], and can be used for reach predictions better than EMB [43]. It is also a better metric to approximate bandwidth of wideband fibers, which will be discussed in the following section. The modal and chromatic dispersion interaction (MCDI) is often not accounted for. Analogously to EMB, EB is expressed in MHz·km. The relation between effective bandwidth (EB) and EMB is presented in Figure 1.5 adapted from Molin et. al [44].

A traditional bandwidth metric is the over-filled launch (OFL) bandwidth. It was designed when MMF was used with systems based on light emitting diodes (LEDs). It is measured in the same way as EMB, but with an LED overfilling the core of the fiber instead of the laser. The light from LED is uniformly distributed in the core. This method however does not indicate the performance of the laser launch and does not serve as a prediction of the VCSEL-based system performance.

1.5.4 Losses

Losses in the fiber are defined as a reduction in signal power that reaches the receiver. The loss limits the transmission distance because of receiver sensitivity, i.e. the minimum power at which it recovers the signal correctly.

Power of the data stream propagating through the fiber is described by Beer's law [36]:

$$P_{out} = P_{in} exp(-\alpha_L L) \tag{1.26}$$

α_L — attenuation coefficient
P_{out} — output power
P_{in} — input power to the fiber
L — Fiber length.

The attenuation coefficient depends on the transmitted wavelength, increasing towards the lower wavelengths. A typical attenuation of silica at 1300 nm equals to 0.37 dB/km and at 850 nm to 2.89 dB/km. The maximum loss for standard MMFs (OM3, OM4) used in todays applications is standardized as 3.5 dB/km [45]. As the MMF link is usually limited to hundreds of meters by the dispersion, the losses are not a major concern in the short-range link design, yet important to consider for power budget design.

1.5.5 OM3 OM4 MMF

The 850 nm optimized MMFs, such as OM3 and OM4, are commonly used high-speed inter data center links. They have been standardized by TIA with a 850 nm VCSEL assumed as a source. An OM3 MMF has a modal bandwidth of 2 GHz·km [45] in the wavelength range of 780–920 nm, the graded-index core of 50 μm, and a maximum loss per km is 3.5 dB [45]. The modal bandwidth of an OM4 MMF is 4.7 GHz·km [46] at 850 nm. The core of OM4 MMF is typically graded-index and has a diameter of 50 μm. The α parameter of the refractive index profile (see Equation 1.22) for these two fibers is chosen to minimize the modal dispersion and therefore maximize the modal bandwidth at 850 nm. Their parameters and minimum guaranteed standardized distances are summarized in the Table 1.1. The maximum reach over these fibers depends on the spectral width of the source due the chromatic dispersion. The standard assumes 0.4 nm as the spectral width of the source. Figure 1.6 presents the maximum reach depending on the source's spectral width for OM4.

1.5.6 Wideband fibers

The index profile of the fibers described in the previous section was designed to support high speed and low dispersion at 850 nm. Lately, short-wave wavelength division multiplexing (SWDM) was introduced to improve the capacity and data density in MMF links [48]. Several works presented the

Fiber type	Min EMB (MHz·km)	OFL (MHz·km)	Distance (m)
OM3	2000	2000	100
OM4	4700	3500	125

Table 1.1: OM3 and OM4 MMF specifications for 850 nm transmission [45], [46].

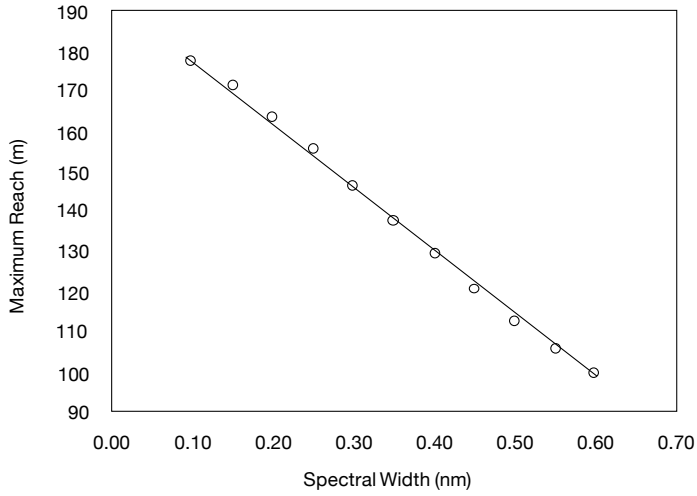

Figure 1.6: Maximum reach versus spectral width for OM4; figure adapted from [47].

SWDM transmitted at short wavelengths with the standard OM4 MMF [49]. However, the performance for the wavelengths higher than 900 nm was degraded due to discrepancy between the wavelength the index profile was optimized for and the transmitted wavelength. As a response, a few of fiber providers proposed an adjusted fiber design, which supports a wider range of wavelengths [13, 50]. The minimum required bandwidth of wideband fibers is defined in Reference [13]. The minimum bandwidth used for OM4 fibers at 850 nm was applied for wavelengths in the range from 850 nm to 950 nm. This fiber type has been used in several experiments in Paper 2. Other examples of wideband fibers were demonstrated in References [51] and [44].

1.6 Equalization techniques

Equalization is used to compensate for frequency-dependent losses in a channel or a component. A linear equalizer has a frequency response reverse to that of the compensated component. As a result, the combination of the two has a flat frequency response and the signal quality is improved.

Equalizers can be fixed or adaptive. A fixed equalizer is relatively easy to implement, however it does not respond to a dynamically changing performance of a link. Adaptive schemes are more complex and power consuming, as they require a feedback on the channel performance. Yet, they provide a better performance for links: a) changing in time, or b) the performance of which is not easy to predict. For example, an adaptive compensation scheme can be a right choice for the MMF links, where the frequency response is strongly dependent on the launch type.

Equalizers can be implemented in both the analog and the digital domain. The analog implementations are less energy consuming but the digital equalizers enable higher flexibility. Both implementations can be adaptive. A digitally controlled resistors array can be introduced for the analog equalizers to enable a parameter variation [52]. The adaptive schemes of a digital implementation can be based on algorithms such as least mean square (LMS), where equalizer's parameters are adjusted with a predefined step to optimize a certain performance parameter. The performance parameter, e.g. signal-to-noise ratio (SNR), is monitored via a feedback loop [53].

Equalization can be used both on the transmitter and the receiver side. The frequency response of the channel is a sum of the responses of all of the link elements. Hence, the placement of the equalizer does not affect the ideal system's performance. In practice, however, the placement of the equalizer is crucial and depends on the application. The typical equalization schemes used at transmitter (TX) and receiver (RX) are briefly described in the following subsections.

1.6.1 TX equalization

A VCSEL based transmitter is limited by intrinsic or extrinsic factors described in Section 1.3.4. They result in a non-flat frequency response of the device, and hence slow rising and falling slopes of the waveform. Low damping of the laser often results in overshoots (ripples) in optical eye diagram of a VCSEL. These limitations can be mitigated with the TX equalizer. The TX equalizer can also partly compensate for the limited

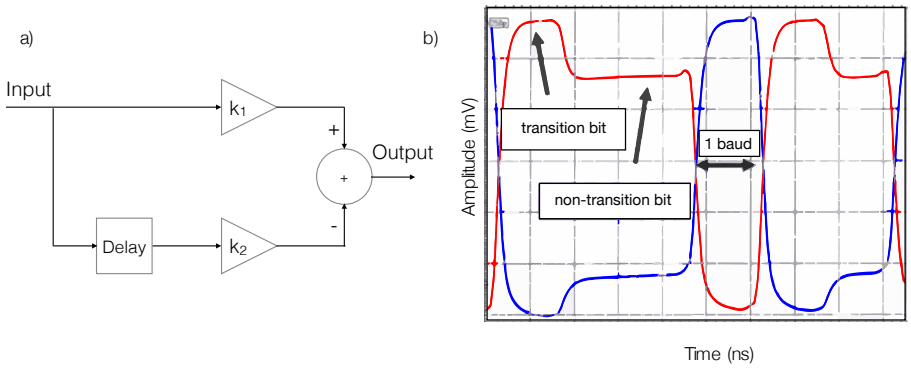

Figure 1.7: a) 2-tap FFE; b) A corresponding output waveform. Figure adapted from [52].

fiber link bandwidth, if it is known in advance. In case of the closed link scenarios, such as active cables in data centers, bandwidth of the fiber can be characterized in advance and corrected for at the TX.

Pre-emphasis and de-emphasis are low-cost, -power, and -complexity approaches to equalization and are based the feed forward equalizer (FFE) scheme. They can be implemented in both the digital and the analog domain (using an analog delay line). FFE gives different emphasis (weights) to the different frequency components. For example, low frequency components are de-emphasised and high frequency components are boosted in order to improve the slow rising and falling slopes in the transmitter's eye diagram. The low frequency components correspond to the sequences of the same bits (non-transition bits, e.g. 1, 1 and -1, -1). The high frequency components refer to the bits transitions (transition bits, -1,1 and 1, -1). The scheme for a 2-tap FFE is presented in Figure 1.7 a) and the corresponding equalized waveform is presented in Figure 1.7 b). The k_1 and k_2 are tap coefficients. Their values are chosen to improve the TX signal performance. TX coefficients are usually fixed because the feedback from the RX on the signal performance is rarely available. If it is, the coefficients can be changed adaptively.

Multiple implementation examples of TX FFE were published, such as a BiCMOS based 2-tap FFE implemented in a 71 Gbps NRZ VCSEL driver [13], and in a 40 Gbps NRZ VCSEL driver [54]. A one-tap pre-emphasis was demonstrated in a 25 Gbps VCSEL link in Reference [55]. Another CMOS based implementation for VCSEL based links was presented in Reference [56]. Pulse equalization technique was presented in Reference [57]. The

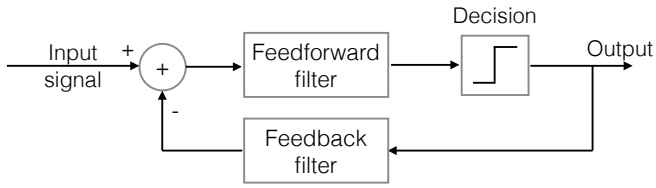

Figure 1.8: 1-tap FFE/DFE scheme. The graphic adapted from [53].

TX equalizers have also been implemented to optimize the performance of advanced modulation formats, e.g. pulse amplitude modulation (PAM)-4 in Reference [58].

1.6.2 RX equalization

Equalizers on the receiver side correct for a frequency response of a full channel. The FFE introduced in the previous section can also be used in the RX. Its performance, however, is limited in the noisy channels, e.g. after an MMF link when an SNR is low. The noise of the high frequency components is amplified together with the signal, further enhancing the noise and therefore degrading the achievable bit error rate (BER) [53]. A decision feedback equalizer (DFE) is often implemented together with FFE to further improve the quality of the received signal. The DFE improves the sensitivity and reduces the noise at the cost of the RX complexity [59]. It uses the information about the previous decision to set the threshold and decode the present bit. The knowledge of preceding bit is required. This feedback based approach allows for an accurate equalization of channels with a slow response. The tap coefficients of this scheme can be preprogrammed or adaptive. Adaptive schemes are more often used on the RX side because there is a convenient access to the feedback information on the received signal quality, e.g. SNR [60]. The schematic of a 1-tap FFE/DFE equalizer is presented in Figure 1.8. The optimization of the feedback filter taps is often performed using an LMS algorithm.

An example implementation of an FFE/DFE for short-range MMF links has been demonstrated in Reference [61]. The FFE/DFE has been optimized to find a trade-off between complexity and link capacity for the NRZ links [62] and the PAM-4 links [63]. The FFE/DFE combination for the discrete multitone (DMT) has been studied in Reference [64].

The advanced modulation formats presented in further sections require more complex equalizers. E.g. MultiCAP uses an equalizer based on an

adaptive K-means algorithm [65] combined with a DFE. Non-linear equalizers have also been recently proposed and applied to correct for the laser nonlinearities [66].

1.7 Modulation formats

Here I introduce several modulation formats used in the IM/DD short-range VCSEL MMF based links. Non-return-to-zero (NRZ) has traditionally been used in communication systems and, at the moment, it is the only modulation format implemented in the commercial modules. NRZ uses one bit per symbol. Advanced modulation formats that use multiple bits per symbol are proposed to improve short-range link capacity. The capacity can be improved multiple times at the cost of complexity, higher requirements in terms of SNR, and a higher energy dissipation of transceivers. The number of parallel optical lanes and transceivers can be minimized for all of the presented formats to reach the same capacity as NRZ.

Multiple types of advanced modulation formats were proposed for short-range links application. They can be multilevel and multidimensional. The most popular ones include: PAM (e.g. PAM-4, PAM-8) and DMT. Multiple amplitude levels are used in PAM, e.g. in PAM-4 four levels are utilized doubling the capacity of the link compared to NRZ. DMT uses multiple orthogonal subcarriers, each of ehich is modulated separately. Two novel modulation formats have been experimentally demonstrated and tested for short-range applications during the course of this PhD project: MutiCAP and BB8. This section includes an introduction to forward error correction (FEC), followed by the summary of record short-range transmissions presented in literature. The section ends with a brief description of the modulation formats used in Papers 1–8.

1.7.1 Forward error correction

The short-range transmission is assumed to be error-free at a BER<1e-12. However, the new multilevel modulation schemes are limited by e.g. laser's RIN. Consequently, BER level of 1e-12 can rarely be met within the existing power budget. Therefore, FEC, previously used in long-haul systems, gets the support of the short-haul community. FEC is a technique used in noisy channels where redundant information is encoded together with the message to improve the detection accuracy. FEC is included in the most recent Infiniband standard [67], and considered by a IEEE 802.3.bm

Bitrate (Gbps)	Transmission distance (m)	3 dB BW of VCSEL (GHz)	Equalization	Ref.
71	7	26	2-tap FFE TX	[13]
64	57	26	2-tap FFE	[72]
60	107	26	2-tap FFE	[72]
57	1	24	unequilized	[73]
43	100	24	unequilized	[73]

Table 1.2: State of the art for NRZ short-range transmissions; OM4 MMF was used in all of the presented experiments.

standard task force [1], as well as by the 32G and 128G Fibre Channel task force [68]. Net coding gain (NCG) of a coding scheme has to be analyzed together with the latency and overhead size to decide if FEC should be used in a specific scenario. The codes considered by the Ethernet 100GBASE-SR4 and used in the electrical backplane are Reed Solomon (RS) codes introduced in Reference [69]. Ethernet 100GBASE-KR4 and 100GBASE-KP4 [70] have adapted RS(528,514) and RS(544,514) codes, respectively.

In Paper 3 we use a 7% FEC with the input BER at 4.5e-3 [71]. In Paper 2 and 11 we employ KP4 FEC.

1.7.2 State of the art

State of the art VCSEL MMF link capacities for different modulation formats are summarized in Table 1.2 and Table 1.3. First, for the sake of comparison, the NRZ record transmissions are summarized in Table 1.2. All of the presented transmission results were error-free, i.e. reached BER of 1e-12. They were taken at the room temperature of 25 °C and the OM4 MMF was used for transmission.

Table 1.3 summarises the achieved bitrates and distances for five advanced modulation formats. In all of the presented examples a multimode 850 nm VCSEL and an MMF were used. All of the schemes required RX equalization.

Bitrate (Gbps)	Bitrate reported at BER of	Netrate (Gbps)	Transmission distance (m)	Fiber type	Ref.
PAM-4					
80	2e-3	70	2	OM4	[74]
60	2e-5	56.7	100	OM4	[75]
50	2e-5	48.7	200	OM4	[76]
52	2e-4	48.7	300	OM4*	Paper 2
8-PAM					
60	1.8e-4	56	50	OM4	[74]
37.5	1.5e-4	35.2	100	OM4	[77]
DMT					
74	1e-3	66	100	OM3	[78]
50	1e-3	44.6	200	OM3	[78]
46	1e-3	41	300	OM3	[78]
30	7e-4	27.2	500	OM4**	[79]
28	1e-3	25.4	1000	OM4**	[79]
MultiCAP					
107.5	3.8e-3	100.5	10 m	OM4	[80]
70.4	4.5e-3	65.7	100 m	OM4	Paper 3, 10
BB8					
56	2e-5	54.5	100	OM3	Paper 4

Table 1.3: State of the art for advanced modulation formats applied in the short-range links; Netrates are calculated by subtracting FEC overhead. * Wideband OM4; **MaxCap550 OM4 with EMB of 4700 MHz·km.

1.7.3 NRZ

Non-return-to-zero (NRZ) carries one bit per symbol and has two signal levels. It is nowadays the only modulation format used in commercially available transceivers. Its implementation is simple and therefore cost- and power-efficient. The capacity of the NRZ links has grown through the recent years with the increasingly improved VCSEL structures and, therefore, their higher bandwidths. However, the achievable distance for the high-speed VCSELs is limited by the fiber bandwidth. The capacities of the state of the art NRZ based short-range links are presented in Table 1.2. For the few meters long links the capacity is limited by the VCSEL's intrinsic or extrinsic behavior, e.g. Reference [72]. In case of longer links, the performance is limited by the dispersion of the fiber, e.g. Reference [72]. The highest bitrate presented with NRZ modulation over 7 m MMF is 71 Gbps [13]. At 100 m it is 60 Gbps [72]. The NRZ modulation was used during the course of this PhD project in Papers 2, 5–8, 10–11, 13, and C2.

1.7.4 PAM-4

The limited bandwidth–distance product of NRZ links led the short-range community to investigate advanced modulation formats to support longer links. PAM-4 offers doubling the capacity compared to NRZ with the same bandwidth. It is the least complex of the advanced modulation schemes presented in Table 1.3.

Realization

PAM-4 has four amplitude levels. Two additional voltage levels are introduced in between the maximum and minimum levels of NRZ. This results in reduced spacing between the levels and the twofold increase of the signal capacity. Gray coding, which has 1 bit difference between adjacent levels, is typically used to encode PAM-4 signals. One of the possible simple ways to realise PAM-4 is to couple together two decorrelated binary signals, one of them attenuated. Demodulation is performed by decoding the amplitude of the signal and using three decision thresholds to distinguish the symbol. All PAM-4 implementation examples presented in Table 1.3 required the FEC overhead and equalization. Physical layer integrated circuits (PHY) PAM-4 was used in Paper 2 and Paper 11 for PAM-4 realization.

Advantages and disadvantages

A clear advantage is the doubled spectral efficiency as compared to NRZ. PAM-4 reduces the bandwidth requirement and potentially extends the reach over MMF. A disadvantage is a tripled requirement on SNR that comes with closer spaced levels. This, in turn, puts a more stringent requirement on VCSEL's RIN and other noise sources in the link. With an increased number of levels, the ISI penalty increases together with the eye closure penalty [63, 74]. Therefore, PAM-4 transceivers need FEC and an equalization circuits. Consequently, they are more complex and energy consuming than NRZ transceivers.

Realization in short-range links

PAM-4 requires half of the bandwidth to reach the same bit rate as NRZ, and therefore is a solution for bandwidth limited channels such as MMF links. The PAM-4 systems realized in short-range scenario are presented in the Table 1.3. Paper 2 includes the PAM-4 results on an SWDM grid. PAM-4 shows an advantage over NRZ for links longer than 100 m, where the modal dispersion is dominant. The highest PAM-4 net rate reported is equal to 70 Gbps for 2 m and 56.7 Gbps for a 100 m transmission. NRZ outperforms PAM-4 for both these distances. At 200 m PAM-4 enables a net rate of 48.7 Gbps, which cannot be reached by NRZ.

1.7.5 MultiCAP

MultiCAP is a multiband approach to carrierless amplitude phase (CAP) modulation introduced in detail in Reference [81]. A single frequency band of CAP is broken into smaller sub-bands. It results in a multidimentional and multilevel modulation, which uses the advantages of both CAP and DMT. It inherits a low peak-to-average power ratio (PAPR) from CAP and an ability to fit the non-flat response of the channel from DMT.

Realization

Figure 1.9 presents the steps required to realize MultiCAP modulation. A data stream is first encoded into a constellation, for each band separately, using Gray coding. The constellation can be different in each band. Then, the signal is upsampled; sample rate depends on subcarriers' frequencies. In-phase (I) and quadrature (Q) components of the constellations create I and Q channels. I and Q channels for each frequency band are filtered by

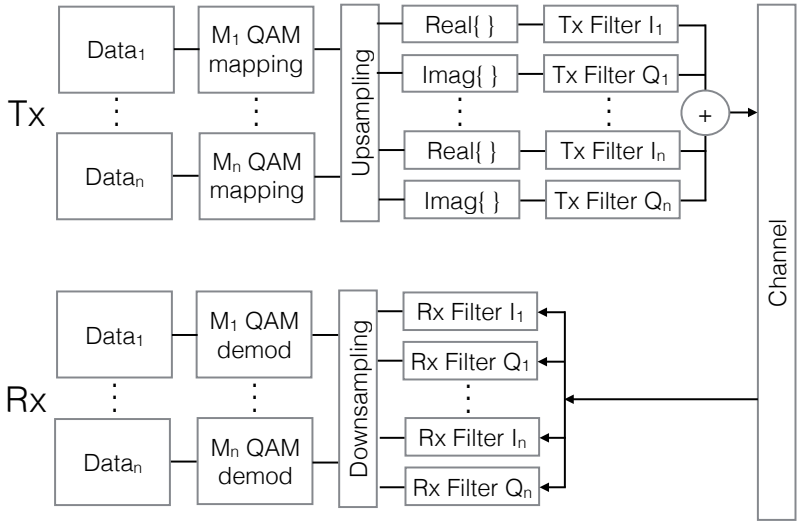

Figure 1.9: MultiCAP adapted from [81].

the orthogonal CAP filters. The filters are realized as orthogonal finite impulse response (FIR) filters in the experimental validation in Reference [81]. The number of filters and their characteristics need to be chosen during the implementation. The characteristics include: sin/cos frequency (frequency of the band), roll-off factor, and the filter's length. The signals from channels I and Q for all frequency bands are added and comprise a MultiCAP signal. On the receiver side, the inverted matched CAP filters separate the two channels for each frequency band. Demodulation is performed in baseband using the k-means algorithm [65].

Advantages and disadvantages

MultiCAP's advantage is the ability to fit non-flat system frequency response by choosing a different constellation order in different bands (bit loading) and a power level for each constellation (power loading) depending on the band's SNR. As presented in Reference [81], a 25 Gbps MultiCAP signal can tolerate bandwidth as low as 14 GHz. MultiCAP has also been presented to be more robust in the dispersive channels than a standard CAP. It inherits the CAP's low PAPR and an option of a simple analog implementation of the filters. Multiple bands require several narrow band filters. The main disadvantage of MultiCAP is the complexity, if the filters are implemented in the digital domain. The throughput flexibility of the

digital implementation comes at the cost of energy consumption. Moreover, the lack of the carrier results in a decrease in the horizontal eye opening. Another disadvantage that comes with using multiple closely spaced bands is the inter-band interference.

Realization in short-range links

MultiCAP provides high capacities in the IM/DD links (net rate of 100.5 Gbps for back to back (B2B) in Reference [80] and 65.7 Gbps for 100 m in Paper 3), outperforming both NRZ and PAM-4. A MultiCAP realization based on a single wavelength, single polarization, and direct detection (DD) optical link is presented in Paper 3. MultiCAP is a good choice for high capacity VCSEL MMF links, as it performs well in the bandwidth- and dispersion-limited channels [82].

1.7.6 BB8

The theoretical background for this modulation format has been presented in Reference [83] and it experimentally validated in Paper 4. BB8 is a block-based 8-dimentional/8-level format. It uses the properties of the modulation formats previously implemented in the coherent systems and applies them for the IM/DD applications. Two temporally adjacent symbols of four parallel optical lanes are used as the orthogonal basis of BB8. BB8 carries two bits per symbol, hence, has the spectral efficiency equivalent to PAM-4. A commercially available module quad small form-factor pluggable (QSFP) is an example of a potential application because it has four parallel uncorrelated lanes.

Realization

Block-based 8-dimentional/8-level (BB8) is optimized using an E8 lattice. E8 is the densest lattice and it maximizes the Euclidean distance between the pairs of transmitted points to avoid overlapping of the noise spheres [84]. In case of a short-range VCSEL based application, a solution for E8 optimization is limited by the extinction ratio of the VCSEL. The optimized modulation format BB8 has eight equally probable levels.

A sequence of 16 bits is mapped onto 8 symbols to implement BB8. A predefined mapping algorithm is introduced in Paper 4. Each symbol is modulated in 8 levels. The super symbol of BB8 is created of 8 symbols and forms four two-dimensional projections p, as presented in Figure 1.10.

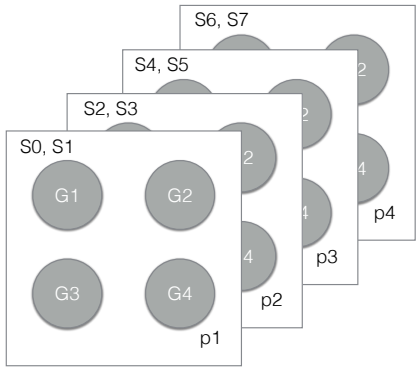

Figure 1.10: A BB8 super-symbol mapped on four projections with two symbols in each.

Four projections correspond to four parallel lanes. Every two symbols are projected in a constellation diagram in a projection p. The points in each projection are divided into four sub-groups $G1$-$G4$. The set of all constellation points is divided into two independent subsets: even and odd. The subsets are constructed with conditional combinations of $G1$, $G2$ (for even) and $G3$ and $G4$ (for odd). The transmitted signal is distributed among four independent lanes. After the transmission it is demodulated based on the conditional dependence of the subsets.

Advantages and disadvantages

BB8 carries two bits per symbol, has the spectral efficiency equivalent to PAM-4. Compared to PAM-4: it has a 1.5 dB asymptotic benefit, it is less prone to the noise in signal levels, it has an improved sensitivity, and, as a consequence, it has a lower power consumption and can be transmitted over higher distances. The mapping technique presented in Paper 4 includes a minimal alteration from PAM-4. The transceiver complexity is similar to PAM-4, but the issues related to parallelization can be expected.

Realization in short-range links

Paper 4 presents BB8 applied in a short-range application. As shown in Table 1.3, the demonstration for VCSEL–MMF link of BB8 included a 54.5 Gbps transmission over 100 m OM3 and OM4 MMFs. Because of its better sensitivity and tolerance to noise than PAM-4, BB8 is well suited for short-range VCSEL–MMF based applications.

1.8 Non-standard wavelengths for short-range communication

This section describes wavelengths higher than 850 nm applied in short-range MMF links. There are two basic motivations for moving towards higher wavelengths. First, CD is lower at higher wavelengths, thus enabling higher transmission distances. Second, the need for higher capacity drives the short-range community towards using multiple-wavelength solutions [85]. In the wavelength division multiplexing (WDM) scenario, several higher wavelengths have to be supported by the transceivers and the transmission medium.

Adding InGaAs quantum wells to a VCSEL increases its operating wavelength. VCSELs modified this way emit light from 860 to 1200 nm and offer a number of advantages: they can achieve a higher modulation bandwidth, have a higher differential gain, lower operating current density, lower operating voltage, higher reliability, improved thermal dissipation, and higher temperature stability [86].

PDs commonly used for 850 nm short-range links are GaAs based. Their responsivity ranges from 850 nm to 870 nm. Broadband detectors, such as InGaAs PDs, are required to support higher wavelengths. They operate in the range from 840 nm to 1300 nm; their responsivity increases with wavelength.

CD and attenuation of the silica fiber decreases for higher wavelengths allowing longer transmission distances. However, as explained in section 1.5.1, the further from 850 nm the wavelength is, the lower the modal bandwidth of the currently used MMFs. The fibers currently implemented in short-range links are optimized to support 850 nm sources and are not specified at wavelengths higher than 900 nm (Section 1.5.5).

1.8.1 1060 nm

Recent works improved transmission distances using a 1060 nm source [87]. A very good reliability performance has been presented for 1060 nm VCSELs in Reference [88]. Their energy efficiency has been studied in Reference [89]. The transmission loss at 1060 nm is 0.95 dB/km, compared to 3 dB/km at 850 nm. The chromatic dispersion at 1060 nm is equal to -37.4 ps/nm/km and at 850 nm it equals to -105 ps/nm/km. However, as explained in the beginning of the section, the fiber performance at 1060 nm is suboptimal due to the modal dispersion of MMF. OM4 sup-

Net baudrate (Gbaud/s)	Transmission distance (m)	Fiber type	EMB @1060 nm (MHz·km)	Ref.
25.78	1000	OM4*	9000	[87]
28	500	OM4*	4000	[90]
25	100	OM3	2800	[91]
24.34	200	OM3	4700	[91]
28	50	OM3	< 2000	[92] (Paper 5)

Table 1.4: State of the art for 1060 nm MMF transmissions. * OM4 optimized for 1060 nm.

ports wavelengths up to 900 nm, and above that wavelength the modal bandwidth decreases. Wideband MMFs need to be compatible with the previously standardized fibers, i.e. they must cover the operating window from 850 nm. The highest wavelength supported by wideband fibers is 980 nm because the refractive index profile can be optimized only for a limited range of wavelengths [42]. A promising alternative is a fiber specifically optimized for 1060 nm, with the refractive index profile of OM4 changed to support this wavelength, e.g. [90]. This solution would, however, require a separate standardization line.

Table 1.4 summarises the recent results obtained at 1060 nm with the corresponding fiber types. The record transmission over 1 km used an active optical alignment subassembly to centralize the optical power in the center of the MMF core [87]. Other researchers used either optical [91] or electrical [92] preemphasis.

1.8.2 WDM

Wavelength division multiplexing (WDM) is another method of increasing the capacity density per lane. It has long been employed in SMF based systems, together with tuneable transmitters, filters, and receivers [93–95], while MMF systems used parallel optics. A WDM signal is created by multiplexing signals at different wavelengths from multiple transceivers in a single optical lane. The short-wave WDM (SWDM) approach is currently of interest of the short-range community because it reduces the footprint and minimizes the number of fiber lanes used. Hence, improves the utilization

λ range (nm)	Bitrate in one λ (Gbps)	Transmission distance (m)	Fiber type	Ref.
850 - 940	10	300	WB-OM4	[3]
990 - 1080	10	300	OM3	[96]
990 - 1080	10	1	OM3	[97]
855 - 947	40	100	OM4*	[49]
855 - 947	26	200	OM4*	[49]
855 - 945	25	300	WB-OM4**	[48]
850 - 940	25	300	WB-OM4	Paper 2

Table 1.5: State of the art for SWDM4 MMF transmissions; wavelength spacing is 30 nm in all grids. *EMB that peaks >860 nm **EMB between 4000 - 9000 MHz·km.

of the data center fibers [48].

The lasers and broadband photodiodes technology for wavelengths higher than 850 nm is feasible and available, as explained at the beginning of the section. The bottleneck for the short-range WDM implementation with MMF is the modal bandwidth of the fiber. The OM4 fibers are standardized for 850 nm only, and their performance decreases for higher wavelengths. New wide-band fibers are proposed to tackle this problem, specifying the EMB in the wavelength window up to 980 nm [50], as described in Section 1.5.6. Multiplexers and demultiplexers are another challenge for SWDM implementation because of the data centers' temperature conditions. Temperature in data centers varies from 25 °C to 85 °C and this affects the temperature of uncooled VCSELs in the transceivers. The operating wavelength changes as a result of VCSEL's thermal drift. The multiplexer's and demultiplexer's pass-bands need to account for this wavelength fluctuation as well as for the source's spectral width.

A wavelength grid, channel spacing, and the fiber type need to be chosen to optimize SWDM system's performance, as discussed in Paper 6. Table 1.5 summarises several demonstrated SWDM4 systems (four wavelengths) with NRZ modulation format. Wavelength spacing in each of the demonstrated SWDM4 examples is 30 nm. There have been several demonstrations of WDM in combination with PAM-4. They will be addressed in the Section 1.10.

IEEE 802.3bs Task Force is currently discussing a 400 Gbit/s short-range systems. One of the proposed solutions is a combination of SWDM with parallel lanes [85]. Additionally, TIA has recently developed a new wideband fiber standard TR-42.12 for MMF to support wavelengths up to 950 nm. Both organizations consider the following wavelength grid: 850, 880, 910, 940 nm. This grid is used in the experimental demonstration in Paper 2.

1.9 Selective modal launch

The effect of modal dispersion is more pronaunced when the difference between velocities of different mode groups increases. The difference in velocities within a group is bigger for higher order modes than for lower order modes [98]. The propagation delay ΔT and, therefore, the modal dispersion effect can be minimized by reducing the number of fiber mode groups. Hence, the fiber bandwidth can be improved by precisely exciting fiber modes of the MMF. This dispersion mitigation technique redirects the light to the desired modes and, unlike electrical equalizers, does not amplify the noise. The selectively launched modes will not fully preserve in the MMF due to mode coupling. But the coupling will happen within the adjacent mode groups, where the velocity difference between modes is lower than the velocity difference for higher an lower order modes. As a result, the dispersion effect will be minimized even when mode coupling is present. Selective modal launch techniques are divided here into central launch and off-center launch.

1.9.1 Central launch

Central launch excites a few low order modes in the core of the MMF by launching a smaller beam waist into the center of an MMF. To do so, e.g. SM fiber is used at the TX side [99] or a single mode source is precisely coupled in into the MMF [100]. This technique has stringent mechanical alignment requirements to ensure central launch. It is very sensitive to bending and fiber core imperfections. The imperfections, which dominate in the center of the MMF refractive index profile, and bending result in exciting higher order modes. This method yields a performance superior to other types of launches, assuming correct launch conditions and no fiber bending. Recently, several works on the central launch of SM sources have

been presented and reached capacities of 54 Gbps over 1 km OM4 and 20 Gbps over 2 km OM4 [100, 101].

1.9.2 Off-center launch

Offset launch

An offset launch is one of the off-center launch techniques. In this approach, the beam is coupled to the MMF with an offset from the core center and excites higher order modes of the MMF. The difference of velocities between higher order modes is smaller than the corresponding velocity difference in the modes excited in the standard launch, yielding a higher bandwidth [102]. This technique requires high-tolerance connectors. A theoretical study and modeling of an optimal offset launch for graded index fibers is presented in Reference [103].

Selective launch

Selective modal launch assumes exciting only a fraction of fiber modes, in the adjacent mode groups. Selective modal launch has been presented in literature with a single mode source in a few wavelength regions, e.g. in 1550 nm [98], 1300 nm [104], 850 nm [105], and 640 nm [106]. The transmission performance of separately excited linearly polarized (LP) eigen modes of MMF modes has been studied in References [98, 98, 105–107].

Selective modal launch is performed in the following way: a single mode beam is collimated, goes through a phase plate or is reflected from an spatial light modulator (SLM), and refocused on an MMF. The beam is spatially modulated either by a phase plate or by an SLM. The phase plates are binary, and calculated for a specific wavelength of the mode. The phase of the phase plate bases usually on the Fourier transform of the far field modal pattern, because the modes in near and far fields are similar [98]. Phase mask is low cost, but not flexible (glass etching is fixed), e.g. Reference [104]. In SLM, a phase information is encoded in a calculated pattern. A beam modulated with this pattern will have a desired modal field. This expensive solution allows for much higher flexibility because the mask can be easily adjusted, but the resolution is limited by the matrix pixel size [107].

Several adaptive algorithms were proposed to find optimal launch conditions using SLM. The feedback loop reported on the signal performance and the phase mask was adjusted. In Reference [98], the SLM pixels were

flipped one by one, starting with the random setting. The optimization objective was to find the best mode shape in the far field. In Reference [108] the SLM pixels were flipped with the cryterion of maximum eye opening. In Reference [109] the objective was to find the trade-off between signal to interference ratio (SIR) and a minimum distance between signal levels.

In the experiments described in Paper 2, 7–8, and 11 the effectiveness of the beam modulation was first crudely confirmed in free space using a charge-coupled device (CCD) camera. Then, the optimal phase plate was chosen based on the BER performance after the transmission (Paper 7). In Paper 2 the phase plate design was chosen based on the numerical simulation of the DMD in Paper 2.

1.10 Combination of capacity improvement techniques

The techniques I described so far can be combined to vastly improve the capacity and meet the requirements of future interconnects. Here, I list a few record results. An impressive capacity of 49 Gbps over 2.2 km of OM4 MMF has been presented in Reference [110] by combining a DMT and a single mode VCSEL launched centrally. That same combination, but with a different single mode structure, resulted in a 72 Gbps transmission over 300 m of OM4 MMF [111]. Central launch into the fiber optimized for 1060 nm resulted in a record 1 km transmission at 25.78 Gbps [87]. 200 Gbps in a single lane using 25 Gbps components was enabled by the combination of PAM-4 and SWDM [50, 112]. 100 Gbps using SWDM2 was presented in References [63, 113]. This combination is presented also in Paper 2.

1.11 Main contributions and outline of the thesis

The work presented in this thesis has contributed the capacity improvement techniques to the state of the art in the area of short-range optical communication. The presented schemes are based on: equalization, advanced modulation formats, 1060 nm transmission over MMF, SWDM, and selective modal launch.

In the area of equalization, I designed a K-mean based DD equalizer on the receiver side for a MultiCAP modulation format, described in Paper 3. It enabled a net rate of 100 Gbps in 1300 nm range, higher by 6 Gbps

than in the previously presented unequalized system [114]. It was applied in a 850 nm short-range application and resulted in 65.7 Gbps transmission over 100 m OM3 as presented in Paper 3. Moreover, the thesis presents the results for a pre-emphasised 1060 nm transmission. The TX equalizer parameters were optimized based on the eye diagram opening and are presented in Paper 5.

Two novel advanced modulation formats were experimentally validated in short-range link during the course of this PhD: MultiCAP and BB8. The B2B capacities of 74.8 Gbps and 54.5 Gbps using a single VCSEL are reported, respectively. At the time of publication, the B2B result for MultiCAP was the record transmission in the IM/DD VCSEL–MMF link [82]. BB8 was first demonstrated in Paper 4 and presented to have receiver sensitivity higher by 1.5 dB than its counterpart of an equal spectral efficiency, PAM-4.

Next, the I experimentally validated the performance of a VCSEL–MMF link in the lower chromatic dispersion wavelength region, namely at 1060 nm. In collaboration with UCSB, we reported the 28 Gbps transmission over 50 m OM3, demonstrated in Paper 6. OM3 optimized for 850 nm is suboptimal for 1060 nm transmission, due to high modal dispersion. Our result was reported simultaneously with, at the time, the record 28 Gbps 1060 nm transmission over 500 m of the MMF optimized for 1060 nm [90] (Table 1.4). Additionally, an SWDM concept is theoretically introduced in the thesis in Paper 6. SWDM performance over wideband fibers is presented in Paper 2.

Finally, this PhD study contributed with an application of the selective modal launch technique to the 850 nm multimode VCSEL–MMF scenario. This concept, previously studied with the single mode sources [105], enabled a modal dispersion mitigation and hence the MMF bandwidth improvement. Primary 10 Gbps results over 400 m MMF have been presented in Paper 7–Paper 8 used the same technique for an RoF antenna link. I performed an experimental validation of the technique at 25.7 Gbps over 300 m in collaboration with Finisar. This result is presented in Paper 2. Overall, this PhD study provided an overview on the possible capacity improvements techniques that have been summarized in Paper 1.

This thesis is structured as follows: Chapter 1 introduces the context of the topic. It briefly describes the short-range links scenario, the devices, and the basics of the capacity improvement schemes implemented during this PhD project. Chapter 2 describes the main papers published as a result of this PhD study. To conclude, chapter 3 summarises the main

achievements of this research and provides an overview of the potential future work in the field of short-range high-speed optical communication.

Chapter 2

Description of papers

This thesis is based on a set of articles already published or submitted for publication in peer-reviewed journals and conference proceedings. The articles present the results I obtained during the course of my PhD studies together with my colleagues and collaborators. In **PAPER 1** I review the state-of-the-art for short-range VCSEL-MMF links. High-capacity short-range links, and their applications in data centers in particular, are studied and their performance is demonstrated experimentally in **PAPER 2** to **PAPER 7**. **PAPER 8** presents experimental results for an antenna multimode short-range link which carries radio over fiber (RoF) signal.

In **PAPER 1** I describe the main applications of the VCSEL-MMF links, including: data center links, antenna links, inter-, and intra- building links. I also explain a need for improving the capacity in existing optical networks and provide a literature review on the topic. The paper offers a comprehensive overview of the strategies developed further in this thesis: advanced modulation formats, equalization, and SWDM. Additionally, I outline the methods for improving the multimode link bandwidth, by using single- or quasi-single-mode sources or selective modal launch.

PAPER 2 reports and summarizes the experimental results for short-range data center applications. The results include MMF bandwidth improvement techniques based on: (1) SWDM transmission in combination with NRZ and PAM-4 and (2) selective modal launch. We describe and characterize the structure of VCSELs and PDs used for SWDM. Then, we present the reliability study results for these devices. In the SWDM-4 transmission experiment, we combine four NRZ 25.78 Gbps signals at different wave-

lengths in an external multiplexer (MUX). It allows 100 Gbps transmission in a single fiber lane. The experimental results include a 100 Gbps error-free unequalized transmission over 200 m wideband OM4 MMF, and a below FEC 100 Gbps transmission over 300 m wideband OM4 MMF. The second part of the SWDM experiment includes PAM-4 signalling. We modulate four VCSELs at different wavelengths with 22.5 Gbaud PAM-4 and consecutively transmit four wavelengths over 100 m wideband OM4, 300 m wideband OM4, and 200 m standard OM4. Additionally, we modulate two VCSELs at the outer wavelengths with 25.8 Gbaud PAM-4 and consecutively transmit two wavelengths over 300 wideband OM4. I worked on the experimental demonstration of selective modal launch in the multimode VCSEL-MMF scenario. We measure the bandwidth of the same 305 m fiber with the standard launch and the selective modal launch. Selective launch improves bandwidth by 2.1 GHz at -6 dB. We collate the experimental results with the simulation results run at a sample of 2300 OM3 MMFs. The simulations indicate that the bandwidth can be improved for 80% of the OM3 fiber spools using the selective modal launch technique. This paper is an extended version of the results published in **PAPER 11**.

In **PAPER 3** we provide an overview of a uniform solution for the 400 G Ethernet links that is based on the MultiCAP advanced modulation format. We apply the same modulation scheme in 20 km long range (LR) and 40 km extended range (ER) scenarios, using WDM lanes, and in short range (SR), using parallel optical lanes. MultiCAP increases capacity per lane and, therefore, decreases number of transceivers. It is a multi-level approach that employs multiple bands transmitted in baseband, each of them carrying a different modulation order. We use features of power and bit loading to account for the non-flat system frequency response and optimally use our setup. The paper summarizes results we obtained in O-band using externally modulated lasers (EMLs): 432 Gbps in a single lane transmitted over an unamplified 20 km SMF link and an amplified 40 km SMF link. In the 850 nm band, we use a multimode VCSEL of 10.1 GHz 3 dB BW to transmit 70.4 Gbps over 100 m OM3. That result shows the feasibility of transmitting 100 Gbps with a VCSEL of a higher bandwidth (BW). The listed results are below 7% FEC limit.

A digital-to-analog converter (DAC) generates MultiCAP signal in our experimental validation. We implement a 6-band MultiCAP configuration, where each band carries a different modulation order and therefore a different bit rate. The modulation orders range from 4 to 64, fitting the SNR

of the specific band. The MultiCAP signal occupies 26 GHz in LR and ER and 21 GHz in SR. We measure four WDM lanes for LR and ER scenarios and a single lane for SR. We demodulate the signal offline. The paper describes the equalization step of the RX digital signal processing (DSP). We implement an adaptive decision directed frequency domain equalization to mitigate the linear impairments. We compare the BER for unequalized system, for multi-modulus algorithm (MMA) equalizer, as well as the K-means based DD equalizer. The last one outperforms MMA by 0.0181 dB at the SNR level of 20 dB. SR scenario has a 3.6 dB power budget, whereas LR has 12.6 dB and ER with semiconductor optical amplifier (SOA) has 15.9 dB. We demonstrate the feasibility of using MultiCAP in all three scenarios. This paper contains an extended and more detailed description of the results presented in **PAPER 10** and **PAPER C1**.

In **PAPER 4** we introduce and experimentally validate a new modulation format — block-based 8-dimentional/8-level format — BB8. It uses super-symbols visualized in 8-dimentional space, carries 2 bits per symbol, and enables 56 Gbps transmission over 100 m MMF with the sensitivity 1.5 dB higher than PAM-4. We introduce the format, the bit-mapping and demapping, and a hyper space hard decision which is suitable for the specific experimental scenario. The modulation format design is a result of a trade-off between performance (maximum link capacity) and computational simplicity. We experimentally validate BB8 using an 850 nm VCSEL and an MMF. 65 GSa/s 8-bit AWG generates 520 mV_{pp} 28 Gbaud signal. The signal is transmitted over 100 m OM3 MMF and over 100 m OM4 MMF. PD serves as a receiver and a 33 GHz 80 GSa/s digital storage analyzer (DSA) captures the trace. The equalization in the RX consists of T/2 factional IIR filter with fixed taps. Using the same experimental setup, we compare the BB8 modulation format in terms of BER with PAM-4, which has the same spectral efficiency, and with PAM-8, which has the same number of levels. Our experimental study finds that, in the B2B scenario, the BB8 outperformes PAM-4. It does not result in the error floor which is observed for PAM-4. PAM-8 does not reach the 7% FEC limit, hence the transmission is unsuccessful. In 100 m 56 Gbps transmission, BB8 reaches the 2.7% FEC limit (BER of 2e-5) while PAM-4 reaches only 7% FEC (BER of 3.8e-4).

PAPER 5 reports on the 28 Gbps and 30 Gbps transmissions over the short-range communication data link obtained using a 1060 nm laser source.

We bias the 1060 nm bottom-emitting VCSEL at 3.77 mA and directly modulate it with the 0.55 V_{pp} pre-emphasised electrical signal. The optical signal is transmitted over 50 m of OM3 MMF and received by the InGaAs PD. We analyze BER in real time and we do not use post-equalization. We achieve the BER below 1e-4 and 1e-3 for 28 Gbps and 30 Gbps scenarios, respectively. This work explores the performance and characteristics of the non-standard short-range wavelength in the multimode medium. Moreover, we study the impact of the pre-emphasis on the transmission performance. The benefits of using the higher wavelength include lower fiber attenuation and high energy efficiency due to the low threshold current of the source. A disadvantage is fiber's higher modal dispersion compared to the 850 nm standard short-range region. The work indicates that the wavelength and the VCSEL used are suitable for the high speed transmission. Longer transmission distances could be obtained using 1060 nm optimized OM4 fiber. This work is a base for moving towards the wavelength division multiplexing in short-range.

PAPER 6 describes a simulation-based performance analysis of three short-wave WDM wavelength grids. The grids are based on four wavelengths with 30 nm inter-channel separation and enable 100 Gbps transmission. The simulated wavelengths of the sources range from 850 nm to 1120 nm. We study the 100 Gbps transmission performance over several types of MMF: OM2, OM3, and OM4. Our study finds that due to the modal bandwidth of the fiber there are different optimal SWDM grids for OM2 MMF type and for OM3, OM4 fiber types. We perform the simulations in OptSim using the existing fabricated VCSELs' parameters to simulate the transmission light sources.

PAPER 7 proposes and experimentally validates selective modal launch in the multimode VCSEL – multimode fiber scenario. We phase-modulate the multimode 850 nm VCSEL beam in the free space setup using an SLM and shape it as the orbital angular momentum (OAM) mode. We use three modes that carry different phase information. They are referred to as M1, M2, and M3. We compare their performance to the standard mode, referred to as M0, under the same launch and received optical power conditions. We consecutively launch the four modes to the multimode fiber and optimize the coupling to reach the maximum coupled optical power. We evaluate the different modes launched to MMF in terms of the frequency response as well as BER (small and large system analysis of the system). The 50 m OM3,

50 m OM4, 100 m OM3, and 200 m OM3 present the same performance for all of the tested launched modes. Then, 400 m OM3, 400 m OM4, and 400 m OM4 are tested and show an improved performance in terms of BER for higher order modes launched to MMF. Using M3 allows for the 10 Gbps transmission over 400 m OM3 with BER below a 7% FEC threshold. The system does not include equalization. The proposed launch results in exciting fewer modal groups of a fiber than in the central launch and therefore in improved performance.

PAPER 8 addresses a last-mile antenna link scenario for RoF signals, where the combination of free-space optics (FSO) and cost effective MMF is applied. FSO is used to remotely feed the antenna site, and then MMF to distribute the signal to the antenna. In the presented experiment, we modulate the 850 nm VCSEL with several RoF signals, of bitrates up to the 1.5 Gbps and carriers up to 10 GHz. We use an SLM to phase-modulate the VCSEL beam carrying RoF signal and create a donut-shaped beam. First, we transmit the beam through a 45 cm long FSO link and then launch it to MMF. We investigate the transmission performance for four independent types of launches over up to 400 m OM4.

The described above main scientific papers, **PAPER 1**–**PAPER 8**, are attached after the Section 3. Other related scientific papers, **PAPER 9**–**PAPER 11**, are attached in Appendix A–Appendix C.

Chapter 3

Conclusions and future work

3.1 Conclusions

This thesis proposes a number of capacity improvement schemes for short-range optical communication, such as equalization, advanced modulation formats, transmission at wavelength 1060 nm with a chromatic dispersion lower than 850 nm, SWDM, and selective modal launch. Higher capacity means that the existing optical networks can be used to transmit higher bitrates without the need of rewiring, and that new, longer links can be implemented without compromising the transmission speeds. Our findings have important implications for short-range data center links as well as antenna links: at a cost of additional complexity, the proposed methods enable the transition to the next generation, high-speed optical applications, e.g. SFP+.

Equalization techniques

The equalization schemes presented in this thesis mitigate fiber dispersion effects and correct for the frequency response of the devices. The results in **PAPER 5** provide an experimental demonstration of the pre-emphasis implemented in TX. We correct the bandwidth limited response of the 18 GHz VCSEL using pre-emphasis and transmit a 28 Gbps NRZ signal over 50 m OM3. The MultiCAP modulation format is supported by the equalization we developed and described in **PAPER 3**. Our k-means based equalizer is integrated in the receiver DSP algorithm. It outperforms the multi-modulus algorithm decision-directed equalizer in terms of BER. The comparison of the equalizers is presented in **PAPER 3** .

Advanced modulation formats

Advanced modulation formats allow more efficient usage of bandwidth by utilizing multiple amplitude levels and/or multiple dimensions. **PAPERS 2, 3**, and **4** present the performance of PAM-4 (48.7 Gbps over 300 m WB-OM4), MultiCAP (65.7 Gbps over 100m OM3), and BB8 (54.5 Gbps over 100m OM3), respectively. This work confirms that advanced modulation formats can be applied in short-range optical links and are a promising solution to vastly improve their capacity.

Non-standard wavelengths transmission

Transmission at wavelengths higher than 850 nm over MMF results in lower chromatic dispersion and, consequently, longer possible transmission distances. In **PAPER 3** we study the transmission at 1060 nm over OM3 MMF. Because the refractive index profile of OM3 is optimized for 850 nm, the modal bandwidth is limited for wavelength of 1060 nm. We achieved transmission over only 50 m OM3. This work stresses the importance of fiber structure optimization in supporting higher wavelengths.

A theoretical study of transmission performance of wavelengths 850 nm — 1060 nm over OM2, OM3, and OM4 is presented in **PAPER 6**. Our study finds optimal wavelength grids for an SWDM4 system for each fiber type. One of the grids is implemented and experimentally tested at 25 Gbaud/s. We present the experimental results in **PAPER 2** and show a potential of SWDM4 to quadruple the capacity in a single MMF link.

Selective modal launch

We introduce selective modal launch in the multimode VCSEL–multimode fiber scenario in **PAPER 7** and then use it in an RoF application in **PAPER 8**. Selective launch mitigates the modal dispersion effect and hence improves the fiber bandwidth for long MMF links of 400 m. We use beams with four different phase modulations in the experimental validation to find the optimal launch conditions. We use SLM in **PAPER 7** and **PAPER 8** for a phase mask optimization and the maximum BER as an optimization criterion. In **PAPER 2** we perform numerical simulations of fiber's DMD to find the optimal phase mask. For the experimental validation, we use a phase plate with a profile defined in the simulations. The study shows potential using simple phase modulation to selectively launch multimode VCSEL's light to the MMF and obtain improved fiber bandwidth.

3.2 Future work

Current challenges of the high speed short-range links are related to the limited bandwidth of the devices, i.e. VCSELs and MMF. The development of VCSELs has progressed rapidly during the course of this PhD project: record transmission bitrates for 850 nm VCSELs increased from 56 Gbps in 2013 [115] to 71 Gbps in 2016 [13]. The multimode fibers optimization and standardization have also progressed (TIA [45], IEEE [85]). A closer integration of the ICs and optics is necessary to continue this development. The impressive result of 71 Gbps with NRZ was achieved thanks to this approach [13]. The close integration in combination with the optimized equalization techniques will further decrease the impact of electrical connection on the bandwidth of the transceivers.

One of the directions which became clear during this PhD study is using 850 nm VCSELs with a decreased spectral width in multimode fiber based applications. Single- or quasi-single mode devices, not yet available during the course of this study, could be used with the presented capacity improvement techniques, i.e. advanced modulation formats (MultiCAP and BB8) as well as selective modal launch. The combination of these schemes with SM source is expected to provide further capacity improvement, as indicated in References [100, 110], but will require development of the optimization techniques.

A long term goal for the short-range links is an extension of the SWDM grid towards higher wavelengths to combine it with the existing 1300 and 1550 nm WDM grids and cover the full optical spectrum. Other possible future directions for data center short-range links, that are not directly related to this study, include multicore fibers, spatial division multiplexing, or silicon photonics.

Paper 1: Improving the Capacity of Short-Reach VCSEL-based MMF Optical Links

Tatarczak, A.; Lu, X.; Tafur Monroy, I., "Improving the Capacity of Short-Reach VCSEL-based MMF Optical Links," *LAOP*, 2016.

Improving the Capacity of Short-Reach VCSEL-based MMF Optical Links

Anna Tatarczak[1], Xiaofeng Lu[1], Idelfonso Tafur Monroy[1,2]

[1] *DTU Fotonik, Technical University of Denmark, Build. 343, DK-2800, Denmark*
[2] *ITMO University, St Petersburg, Russia*
atat@fotonik.dtu.dk

Abstract: We summarize strategies for increasing a capacity of short-reach links that base on an 850 nm VCSEL and an MMF. Presented methods include advanced modulation formats, equalization, WDM, quasi-single mode sources and a selective mode launch.
OCIS codes: 060.2330 Fiber optics communications; 060.4510 Optical communications

1. Introduction

A typical short-reach link bases on a cost-effective directly-modulated multimode 850 nm vertical cavity surface emitting laser (VCSEL), a multimode fiber (MMF) and a photodiode. The multimode 850 nm VCSELs are multiple times cheaper than commercially available 1300 nm laser sources. Besides cost efficiency, the 850 nm VCSELs have high modulation bandwidth. The recently demonstrated multimode 850 nm VCSEL supports a 71 Gbps transmission bitrate [1]. Additionally, the commercially available VCSELs present a high reliability and temperature performance [2] that indicate maturity of the VCSEL technology. The multimode fibers have higher coupling tolerance than single mode fibers because of a larger core size. Therefore the multimode solutions are widely implemented in the existing short-reach links such as data center links. The multimode fibers have a higher attenuation than the single mode ones. The attenuation is usually negligible because of a limited fiber length in the shot-reach applications. A main performance degradation factor for the short-reach links is a dispersion. A chromatic and a modal dispersion contribute to the signal degradation. The chromatic dispersion results in a different arrival times of different spectral components (wavelengths). Hence, the higher a spectral width of the source is, the higher the chromatic dispersion effect. The modal dispersion results in a pulse spreading due to different propagation velocities of different modes in the fiber. Because of the abovementioned factors, the VCSEL-MMF links have a limited bandwidth times distance product. The higher the number of longitudinal modes (a chromatic dispersion effect) and transverse modes (a modal dispersion effect), the more limited the fiber bandwidth. Sustaining the same quality of service involves a trade-off between the bitrates and the achievable distance: increasing the bitrate means the diminishing of the achievable distance and increasing the link length requires transmitting at lower bitrates. This paper reviews several methods enhancing the capacity of the short-reach links without a need for a costly rewiring. We will start with describing main applications of the VCSEL-MMF links. Then the solutions for increasing the bitrate in a single opical link will be presented and followed by the reach extension solutions.

2. Applications

The short-reach VCSEL-MMF links are used for multiple applications. The main one is a data center interconnect. The VCSELs are used in the data centers for over a decade due to their low cost, high modulation bandwidth, energy efficiency, low heat dissipation, good performance in high temperatures, easy testing on wafer and good reliability results. Another application that requires a cost effective short-reach solution is an antenna link. This type of link typically carries a radio over fiber (RoF) signal. Wired mobile backhaul and fronthaul segments of a wireless network were traditionally based on copper links. They have migrated to the optical fiber based links over the last years. The MMF links based on 850 nm VCSEL lasers meant for short distances up to 300 meters have been demonstrated as a feasible solution for the RoF applications [3]. Other applications employing the VCSEL-MMF infrastructure are intra-building client connections. These types of applications are supported by the physical layer of the 10GBASE-SR Ethernet standard. IEEE 802.3 standardizes 10 Gbps for the 300 m OM3 MMF links. IEEE 802.3bj proposes 25 Gbps for the 75 m OM3 MMF links. The RoF applications are standardized e.g. by LTE standard. The 43rd band of the LTE standard defines the speed of 1 Gbps at a 3.7 GHz carrier. Solutions which allow for the capaciy increase of the already widely implemented MMF links is of interest for both research and industry communities.

3. Enhanced capacity

A recent literature review suggests a number of ways to increase the bitrate in the optical link. One way is to improve a VCSEL structure and use a non-return-to-zero (NRZ) signaling [1]. An alternative is employing advanced modulation formats to increase the bitrate in the bandwidth-limited short-reach link. The NRZ signal can be replaced with the lower badwidth channel carrying a lower baud rate multilevel signal that results in the same capacity. A following paragraph summarizes the reported experimental results for the multilevel signaling used in the 850 nm multimode VCSEL MMF links. With a pulse amplitude modulation PAM-4 60 Gbps has been demonstrated for 100 m OM4 [4]. With a discrete multitone modulation (DMT) 74 Gbps has been obtained for 100 m OM3 link [5]. Using a MultiCAP signaling resulted in 70.4 Gbps over 100 m OM4 [6]. These technologies offer higher capacity at the cost of the high energy dissipation. PAM-4 offers doubling the capaciy, it is least complex of the described above advanced modulation schemes and therefore is currently considered for standardization.

An equalization is another technique used to increase speed in the short-reach links. It can be implemented both at the transmitter side, in a form of a pre-emphasis [7, 8] as well as on the receiver side [9]. Equalization on the transmitter side can be designed to compensate for a non-flat VCSELs frequency response, an overshoot in an optical eye diagram, a time jitter, etc. The receiver side equalization is usually implemented to correct for the chromatic and the modal dispersion effects. Several studies were performed to find the optimal equalization which allows highest link capacity for the NRZ [10] and PAM-4 [11]. The equalization is often used together with the advanced modulation formats to compensate for the non-flat channel response which characterizes the VCSEL MMF links.

A wavelength division multiplexing (WDM) improves the capacity of the single optical link multiple times by combining several signals at different wavelengths within the same fiber [12]. Various short wavelength WDM grids have been suggested and simulated for the optimal stort-reach link performance [13]. The mature VCSEL and PD technology is required to suppot all the WDM wavelengths. In general, higher wavelengths experience a lower attenuation and a lower chromatic dispersion. However, the fiber bandwidth is lower for higher wavelengths because the standard multimode fibers are optimized for 850 nm transmission. Wideband fibers have been designed to support higher wavelengths such as 980 nm in order to overcome this issue [14]. There have been multiple demonstrations that combine the previously described techniques [15, 16].

4. Enhanced transmission distance

The multimode link's bandwidth and the achievable transmission distance are limited by the chromatic and modal dispersion. The chromatic dispersion effect is more significant for the laser sources with a higher spectral width. A novel 850 nm VCSEL structure have been proposed to decrease the VCSEL spectral width and therefore increase the achievable transmission distance. A reported quasi-single mode VCSEL have a 20 dB side-modes suppression ratio [17]. Using the quasi-single mode 850 nm lasers over the multimode links allow for e.g. a 1 km transmission at 54 Gbps [18]. This technology requires a laser based on a high suppression ratio of the side-modes and hence has a low optical output power. Another technique which improves multimode link's bandwidth is a selective modal launch [19]. By launching modes from the source to a single fiber modal group the modal dispersion effect is reduced and the achievable transmission distance is increased [20].

5. Summary

The techniques that allow for increasing the capacity of the 850 nm VCSEL MMF links include the advanced modulation formats, the equalization, the wavelength division multiplexing, the side modes suppression of the laser source and the selective modal launch. By improving the capacity, the higher bitrates can be supported in the already implemented MMF links of the fixed lengths.

References

1. D. M. Kuchta, A. V. Rylyakov, F. E. Doany, C. L. Schow, J. E. Proesel, C. W. Baks, P. Westbergh, J. S. Gustavsson, and A. Larsson, "A 71-Gb/s NRZ Modulated 850-nm VCSEL-Based Optical Link," IEEE Photonics Technology Letters **27**, 577–580 (2015).
2. J. Guenter, B. Hawkins, R. Hawthorne, and G. Landry, "Reliability of VCSELs for $>$ 25Gb/s," in "Optical Fiber Communications Conference and Exhibition (OFC), 2014," (2014), pp. 1–3.
3. M. Sauer, A. Kobyakov, and J. George, "Radio Over Fiber for Picocellular Network Architectures," Journal of Lightwave Technology **25**, 3301–3320 (2007).

4. J. Castro, R. Pimpinella, B. Kose, Y. Huang, B. Lane, K. Szczerba, P. Westbergh, T. Lengyel, J. Gustavsson, A. Larsson, and P. Andrekson, "Investigation of 60 gb/s 4-pam using an 850 nm vcsel and multimode fiber," Journal of Lightwave Technology **PP**, 1–1 (2016).
5. B. wu, X. Zhou, N. ledentsov, and jun luo, "Towards 100 gb/s serial optical links over 300m of multimode fibre using single transverse mode 850nm vcsel," in "Asia Communications and Photonics Conference 2015," (Optical Society of America, 2015), p. ASu4C.3.
6. M. I. Olmedo, A. Tatarczak, T. Zuo, J. Estaran, X. Xu, and I. T. Monroy, "Towards 100 gbps over 100m mmf using a 850nm vcsel," in "Optical Fiber Communications Conference and Exhibition (OFC), 2014," (2014), pp. 1–3.
7. T. Lengyel, K. Szczerba, P. Westbergh, M. Karlsson, A. Larsson, and P. Andrekson, "Sensitivity improvements in an 850 nm VCSEL transmitter using a one-tap pre-emphasis electronic filter," in "Optical Communication (ECOC), 2015 European Conference on," (2015), pp. 1–3.
8. C. L. Schow, A. V. Rylyakov, B. G. Lee, F. E. Doany, C. Baks, R. A. John, and J. A. Kash, "Transmitter pre-distortion for simultaneous improvements in bit-rate, sensitivity, jitter, and power efficiency in 20 Gb/s CMOS-driven VCSEL links," in "Optical Fiber Communication Conference and Exposition (OFC/NFOEC), 2011 and the National Fiber Optic Engineers Conference," (2011), pp. 1–3.
9. I.-C. Lu, J.-W. Shi, H.-Y. Chen, C.-C. Wei, S.-F. Tsai, D.-Z. Hsu, Z.-R. Wei, J.-M. Wun, and J. Chen, "Ultra low power VCSEL for 35-Gbps 500-m OM4 MMF transmissions employing FFE/DFE equalization for optical interconnects," in "Optical Fiber Communication Conference and Exposition and the National Fiber Optic Engineers Conference (OFC/NFOEC), 2013," (2013), pp. 1–3.
10. D. M. Kuchta, A. V. Rylyakov, C. L. Schow, J. E. Proesel, C. W. Baks, P. Westbergh, J. S. Gustavsson, and A. Larsson, "A 50 Gb/s NRZ Modulated 850 nm VCSEL Transmitter Operating Error Free to 90^oC," Journal of Lightwave Technology **33**, 802–810 (2015).
11. J. M. Castro, R. Pimpinella, B. Kose, Y. Huang, B. lane, adrian Amezcua-Correa, M. Bigot, denis molin, and P. Sillard, "200m 2x50Gbps PAM-4 SWDM transmission over WideBand Multimode Fiber using VCSELs and pre-distortion signal," in "Optical Fiber Communication Conference," (Optical Society of America, 2016), p. Tu2G.2.
12. I. Lyubomirsky, R. Motaghian, H. Daghighian, D. McMahon, S. Nelson, C. Kocot, J. A. Tatum, F. Achten, P. Sillard, D. Molin, and A. Amezcua-Correa, "100G SWDM4 transmission over 300m wideband MMF," in "Optical Communication (ECOC), 2015 European Conference on," (2015), pp. 1–3.
13. B. Cimoli, J. Estaran, G. A. Rodes, A. Tatarczak, J. J. V. Olmos, and I. T. Monroy, "100G WDM Transmission over 100 meter Multimode Fiber," in "Asia Communications and Photonics Conference 2015," (Optical Society of America, 2015), p. ASu2A.89.
14. Y. Sun, R. Lingle, roman shubochkin, K. balemarthy, D. braganza, timo gray, wenjuan fan, kent wade, deepa gazula, and J. Tatum, "51.56 Gb/s SWDM PAM4 Transmission over Next Generation Wide Band Multimode Optical Fiber," in "Optical Fiber Communication Conference," (Optical Society of America, 2016), p. Tu2G.3.
15. I.-C. Lu, C.-C. Wei, H.-Y. Chen, K.-Z. Chen, C.-H. Huang, K.-L. Chi, J.-W. Shi, F.-I. Lai, D.-H. Hsieh, H.-C. Kuo, W. Lin, S.-W. Chiu, and J. Chen, "Very High Bit-Rate Distance Product Using High-Power Single-Mode 850-nm VCSEL With Discrete Multitone Modulation Formats Through OM4 Multimode Fiber," Selected Topics in Quantum Electronics, IEEE Journal of **21**, 444–452 (2015).
16. R. Motaghian, I. Lyubomirsky, H. Daghighian, and C. Kocot, "45Gb/s PAM4 VCSEL 850/940nm Transmission over OM3 and OM4 Multimode Fibers," in "Frontiers in Optics 2015," (Optical Society of America, 2015), p. FM2E.3.
17. C. Caspar, J.-R. Kropp, V. A. Shchukin, N. N. Ledentsov, V. Jungnickel, and R. Freund, "High speed transmission over Multimode Fiber with direct modulated single-mode VCSEL," in "Broadband Coverage in Germany. 9th ITG Symposium. Proceedings," (2015), pp. 1–4.
18. G. Stepniak, J.-R. Kropp, N. N. Ledentsov, V. A. Shchukin, N. Ledentsov, G. Schaefer, and J. P. Turkiewicz, "54 Gbps OOK Transmission Using Single Mode VCSEL up to 1 km OM4 MMF," in "Optical Fiber Communication Conference," (Optical Society of America, 2016), p. Th4D.5.
19. A. Tatarczak, M. A. Usuga, and I. Tafur Monroy, "OAM-enhanced transmission for multimode short-range links," Proc. SPIE **9390** (2015).
20. J. Carpenter and T. Wilkinson, "Characterization of Multimode Fiber by Selective Mode Excitation," Lightwave Technology, Journal of **30**, 1386–1392 (2012).

Paper 2: Reach Extension and Capacity Enhancement of VCSEL based Transmission over Single Lane MMF Links

Tatarczak, A.; Reza Motaghiannezam, S. M.; Kocot, C.; Hallstein, S.; Lyubomirsky, I.; Askarov, D.; Daghighian, H.M.; Nelson, S.; Tafur Monroy, I.; Tatum, J.A., "Reach Extension and Capacity Enhancement of VCSEL based Transmission over Single Lane MMF Links," submitted to *Journal of Lightwave Technology*, 2016.

This article has been accepted for publication in a future issue of this journal, but has not been fully edited. Content may change prior to final publication. Citation information: DOI 10.1109/JLT.2016.2615815, Journal of Lightwave Technology

Reach Extension and Capacity Enhancement of VCSEL-based Transmission over Single Lane MMF Links

Anna Tatarczak, S. M. Reza Motaghiannezam, Chris Kocot, Sascha Hallstein, Ilya Lyubomirsky, Daulet Askarov, Henry M. Daghighian, *Senior Member, IEEE*, Stephen Nelson, Idelfonso Tafur Monroy, *Senior Member, IEEE*, and Jim A. Tatum, *Member, IEEE*

***Abstract* — This paper reviews and examines several techniques for expanding the carrying capacity of multimode fiber (MMF) using vertical cavity surface emitting lasers (VCSELs). The first approach utilizes short wavelength division multiplexing (SWDM) in combination with MMF optimized for operation between 850 and 950 nm. Both non-return to zero (NRZ) and four level pulse amplitude modulation (PAM4) signaling are measured and demonstrate up to 170 Gbps post-forward error correction (FEC) transmission over 300 m. For single wavelength transmission the use of selective modal launch to increase the optical bandwidth of a standard OM3 MMF to more than 2.1 GHz•km for standard MMF is presented. A statistical model is used to predict the bandwidth enhancement of installed MMF and indicates that significant link extension can be achieved using selective modal launch techniques. These results demonstrate the continued effectiveness of VCSEL based MMF links in current and future data center environments.**

***Index Terms*—Data center, interconnects, vertical cavity surface emitting laser (VCSEL), fiber optics.**

I. Introduction

OPTICAL data links based on an 850 nm VCSELs and MMF have served as cost-effective data center interconnects for more than two decades. It is estimated that more than 500M VCSEL based links have been deployed. Over this time, the signaling rate defined by standards such as IEEE 802.3 (Ethernet) and ANSI X3.T11 (Fibre Channel) has increased from 1 Gbps to more than 25 Gbps today. To support higher speed operation, MMF has been standardized by the Telecommunications Industry Association (TIA) by effective modal bandwidth (EMB) at 850 nm, including OM3 (2000 MHz•km) and OM4 (4700 MHz•km) [1]. To address the need for higher density interconnects, multilane parallel optical transceivers and fibers have been developed. However, this represents additional fiber and transceiver costs, has limited scalability, and does not address the installed base of single channel OM3 and OM4 fiber. The need for higher bandwidth density has led to investigation of the limits of current VCSEL and MMF technologies. For example, a 43 Gbps link operating error-free without FEC up to 100 m on OM4 fiber (57 Gbps at 1 m) has recently been demonstrated using NRZ signaling [2]. To further push the VCSEL capacity, other signaling protocols such as PAM4, signal processing such as Forward Error Correction (FEC), and other digital signal processing techniques are being investigated [3,4,5]. For example, a two-tap feed-forward equalizer (FFE) on the transmitter (TX) side enabled error-free NRZ transmission without FEC up to 71 Gbps over 7 m OM4 [6], and 60 Gbps over 107 m OM4 [7]. With the addition of PAM4 signaling, a 148.6 Gbps transmission over 5 m MMF was reported in [8] and 100 Gbps PAM4 transmission over 100 m OM4 fibers was reported in [9]. In these measurements, the equalization was implemented in the receiver and the reported rates are after removal of the FEC overhead. Using an optimized OM4 a 200 m 48.7 Gbps link was achieved in [10] and a 150 m 50 Gbps link in [11]. Using OM3 and discrete multitone (DMT) signaling, links operating up to 66 Gbps at 100 m and up to 42 Gbps at 300 m have been reported [4].

Another method to increase the capacity of a single MMF is to utilize SWDM [12]. In this approach, the capacity of a single MMF scales with the number of wavelengths. Using a combination of signaling, equalization and SWDM, 200 m OM4 links operating at 42.5 Gbps [13], and 48.8 Gbps [14] per wavelength have been reported. SWDM technology is currently under IEEE 802.3 standardization process [15]. One limitation to its deployment is that traditional MMF has not been specified for operation outside of the 840 to 860 nm range. In response, the TIA has recently developed a new fiber standard TR-42.12 for MMF to include operation up to 950 nm. This MMF is referred to as wide band OM4 (WB-OM4) in this paper. To achieve operation over the wider wavelength the minimum effective bandwidth (the combination of modal and chromatic dispersion) is specified

A. Tatarczak, S. M. R. Motaghiannezam, C. Kocot, S. Hallstein, D. Askarov, H. Daghighian, S. Nelson and J. Tatum are with Finisar Corp., 1389 Moffett Park Dr., Sunnyvale, CA, 94089, USA (e-mail: Anna.Tatarczak@finisar.com, Reza.Motaghian@finisar.com, Chris.Kocot@finisar.com, Sascha.Hallstein@finisar.com, Daulet.Askarov@finisar.com, Henry.Daghighian@finisar.com, Stephen.Nelson@finisar.com, Jim.Tatum@finisar.com). I. Lyubomirsky is with Facebook, 1 Hacker Way, Menlo Park, California 94025, USA (email: Ilya.Lyubomirsky@facebook.com). A. Tatarczak and I. Tafur Monroy are with DTU Fotonik, Technical University of Denmark, 2800, Denmark (email: atat@fotonik.dtu.dk, idtm@fotonik.dtu.dk) Manuscript received June 2, 2016.

This article has been accepted for publication in a future issue of this journal, but has not been fully edited. Content may change prior to final publication. Citation information: DOI 10.1109/JLT.2016.2615815, Journal of Lightwave Technology

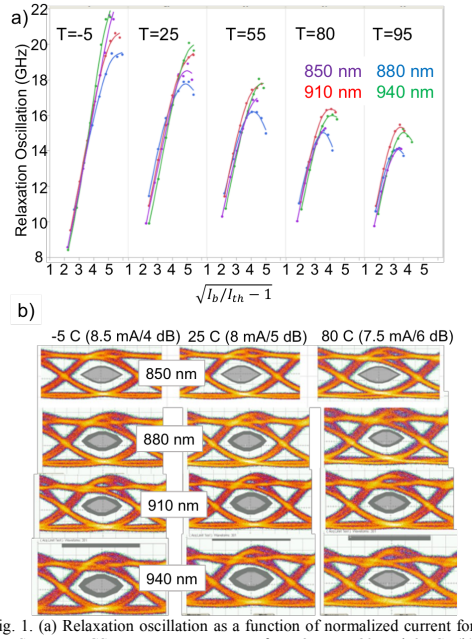

Fig. 1. (a) Relaxation oscillation as a function of normalized current for the SWDM VCSELs at temperatures of -5, 25, 55, 80 and 95 C. (b) Optical eye diagrams at 25 Gbps for each of the SWDM VCSELs at -5, 25 and 80 C. The bias current and the measured extinction ratio are given in the parenthesis for each temperature.

as 2000 MHz•km from 840 to 950 nm. A performance comparison for OM4 and WB-OM4 for this range of wavelengths was presented in [16]. In this paper we will expand on the previous set of results and combine the several techniques described earlier to achieve 170 Gbps on a single optical fiber at distances up to 300 m. Carrying capacity of MMF is limited by both the effective bandwidth (EB) and the total fiber link length. As the speed of optical communication standards has increased, the operating length has been reduced. For example, 10 Gbps lengths could be deployed up to 300 m and this was sufficient for many data centers. As the speed increased to 25 Gbps, the specified link length has been reduced to 100 m. This has limited the infrastructure cabling deployment in some data centers and has not allowed full utilization of the installed base of OM3 and OM4 at 25 Gbps. Selective modal launch (SML) is one technique that can be used to increase the bandwidth of MMF, and has been demonstrated at 1550 nm [17], 1310 nm [18] and 664 nm [19]. These schemes employed a single-mode source and a spatial light modulator (SLM) to selectively launch light into to the MMF. In this paper we utilize a simple phase plate to increase the measured effective bandwidth of an OM3 fiber from 1800 MHz•km to 2100 MHz•km and demonstrate 25 Gbps transmission over 300 m.

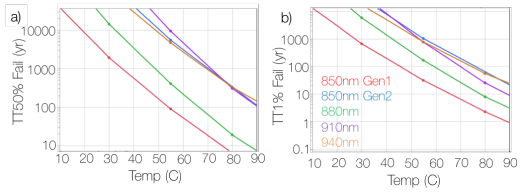

Fig. 2. (a) Years to 50% fail and (b) 1% fail as a function of VCSEL heat sink temperature.

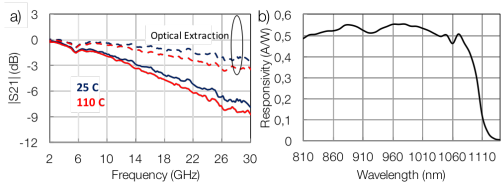

Fig. 3. (a) Frequency response (S21) of the SWDM photodiode as measured and with the electrical parasitics extracted (b) Responsivity of the SWDM PD as a function of wavelength.

II. VCSELs and PDs for SWDM Technology

The basic SWDM VCSEL structure is derived from the commercialized 850 nm 25 Gbps design which was previously discussed in [20]. A 30 nm wavelength grid (850, 880, 910 and 940 nm) was chosen to fit into the WB-OM4 specifications defined in TIA TR-42.12 standard and allows for uncooled operation over the anticipated temperature range with the use of relatively low cost optical filters. The longer wavelengths are designed by scaling the mirror thickness and active region composition. Extending the SWDM grid towards longer wavelengths (970, 1000, 1030 and 1060 nm for example) is relatively simple in terms of epitaxial growth and device fabrication, allowing for future bandwidth expansion on a single MMF. Fig. 1(a) is a plot of the relaxation oscillation as a function of current normalized to threshold at temperatures from -5 to 95 C. At 25 C all four wavelengths achieve ROF>18 GHz, and more than 14 GHz at 95 C. Fig. 1(b) depicts eye diagrams captured for each SWDM wavelength at three different temperatures. Almost identical eye openings were captured using the same NRZ electrical drive signal. The uniformity of device performance greatly simplifies the laser driver design. Fig 2 shows the reliability prediction (time to 50% fail, TT50%, and time to 1% fail, TT1%) for each of the VCSELs based on extrapolation from accelerated aging tests similar to those described in [21]. The time to 1% failure is more than 10 years of continuous operation at 80 C. These VCSELs are currently used in production transceivers. Note the 10x reliability improvement realized in the 850 nm VCSEL (GEN2) from previous reports of GEN 1 devices [21].

A single photodiode (PD) was designed to operate over the entire SWDM band. The InGaAs active region is grown on a GaAs substrate. Fig 3(a) shows the PD frequency response

This article has been accepted for publication in a future issue of this journal, but has not been fully edited. Content may change prior to final publication. Citation information: DOI 10.1109/JLT.2016.2615815, Journal of Lightwave Technology

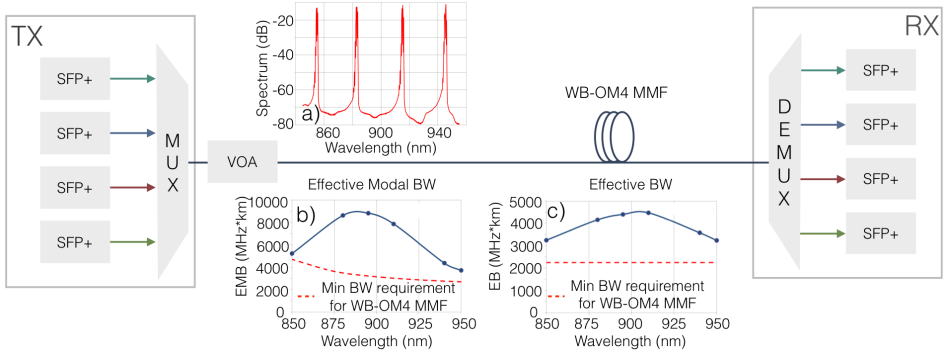

Fig. 4. SWDM experimental setup, each of the VCSELs is packaged in an SFP+ transceiver. The optical signal is combined in a MUX and then passes through a VOA, the WB-OM4 MMF (supplied by Prysmian), a DEMUX, and is received by a PD packaged in an SFP+ transceiver. Inset (a) shows the measured optical spectra measured after the MUX, inset (b) is the measured EMB WB-OM4 (solid dark blue line) and WB-OM4 minimum EMB requirement (red dashed line) as a function of wavelength. Inset (c) is the measured EB of the WB-OM4 (solid dark blue line) and a minimum WB-OM4 EB requirement (red dashed line) as a function of wavelength.

and Fig. 3(b) is the responsivity as a function of wavelength. Responsivity >0.5 A/W was achieved for wavelengths from 820 nm to 1060 nm. The series resistance of the PD is 11 Ω, total capacitance is approximately 160 fF. When the electrical parasitic is removed, the optical bandwidth of the device is >25 GHz. The optical bandwidth is determined to be limited by the transit time of photo-excited carriers in the active region by studying several active region thicknesses. Further increases in the total bandwidth of the PD can be increased by reducing the device pad capacitance and reducing the active region diameter. For this PD, the active region diameter was chosen to be 35 μm and represents the tradeoffs between total PD bandwidth and ease of optical alignment.

III. SWDM TRANSMISSION OVER WB-OM4

In this section we present measured results of a NRZ 100 Gbps and a PAM4 170 Gbps SWDM link on WB-OM4. The VCSELs and PDs described in section II are used in these measurements.

A. NRZ transmission

Fig. 4 is a schematic diagram of the experimental setup used in the NRZ transmission experiments. Each of the lasers was packaged in a small form factor pluggable (SFP+) transceiver. Inside each SFP+ is a laser driver and a clock and data recovery (CDR) circuit. There is no dispersion compensation included in the laser drive circuitry. The SFP+ transceivers were driven with a 2^{31}-1 pseudorandom binary sequence (PRBS) at 25.78 Gbps. The four wavelengths (855 nm, 883 nm, 915 nm, and 945 nm) were combined using an external optical multiplexer (MUX). The external MUX has a 2 dB insertion loss and 20 nm pass band to account for wavelength fluctuations over temperature (the VCSELs and transceivers are uncooled). The measured optical spectrum after MUX is presented in the inset (a) of Fig. 4. The root mean square (RMS) spectral bandwidths of the sources range from 0.34 nm to 0.41 nm. The optical signal was passed through a variable optical attenuator (VOA) and then coupled to a WB-OM4 fiber provided by Prysmian. The solid dark blue line in the inset (b) of Fig. 4 displays the measured EMB of the WB-OM4 fiber as a function of wavelength. The red curve presents the minimum bandwidth requirement of a WB-OM4 fiber, which was defined for wavelength window of 850 nm to 950 nm in [22]. The EMB of the WB-OM4 fiber measured at 850 nm is above the minimum OM4 requirement and increases for higher wavelengths, peaking at 880 nm. Since the chromatic dispersion for longer wavelengths is lower, the combined effect of the modal and chromatic dispersion results in the shift of the EB peak towards longer wavelengths [23]. The inset (c) of Fig. 4 displays the peak shifted towards 905 nm. At the end of the fiber, the optical wavelengths are separated with an external de-multiplexer (DEMUX) with an insertion loss of 1.5 dB. The receivers were also assembled into SFP+ transceivers using the PD described earlier, a transimpedance amplifier (TIA) and a CDR.

The experimental results are summarized in Fig. 5 and described in further detail in [24]. Fig. 5(a) shows the average optical power (AOP) received at a bit error rate (BER) of 1e-12 for each of the wavelengths for three transmission cases; a 2 m patch cord, 200 m of WB-OM4 and 300 m of WB-OM4. The optical extinction ratio was approximately 3.3 to 3.5 dB for each of the wavelengths. In this experiment error-free transmission (BER<1e-12) was achieved up to 200 m for all four wavelengths. At 300 m, the 940 nm channel was able to achieve BER<1e-9. There are a few options to improve the 940 nm channel performance, such as a lower spectral width VCSEL, higher bandwidth MMF, transmitter equalization or FEC. The Ethernet standards 100GBASE-KP4 and 100GBASE-SR4 adopted Reed Solomon (RS) code RS (528,514) for FEC. By applying this coding scheme, a signal can be recovered to a BER less than 1e-12 from an input signal with BER less than 2e-4 (KP4 FEC threshold) [25]. The KP4 level was used to allow straightforward comparison of

This article has been accepted for publication in a future issue of this journal, but has not been fully edited. Content may change prior to final publication. Citation information: DOI 10.1109/JLT.2016.2615815, Journal of Lightwave Technology

AOP receiver sensitivities for NRZ and PAM4 signaling to be presented in subsection IIIB.

Figure 5(b) shows the received AOP at the KP4 FEC threshold for each of the wavelengths. For the 2 m patch cord, the AOP was approximately -13.7 dBm for all four wavelengths. The AOP penalty increased from 0.65 dB at 850 nm to 1.6 dB at 940 nm for 200 m transmission. For the 300 m link, the power penalty increased to 2.2 dB and 4.25 dB for the 850 nm and 940 nm channel respectively. With the KP4 FEC, a recovered BER<1e-12 was achieved for all four channels up to 300 m on the WB-OM4 fiber. Fig. 7(a) and (c) present the NRZ optical eye diagrams received after propagating through 200 m and 300 m of WB-OM4 fibers, respectively, for each of the wavelengths.

The results presented here demonstrate that SWDM transceivers operating on WB-OM4 optical fiber can achieve BER<1e-12 up to 200 m without FEC, and up to 300 m using KP4 FEC. This further indicates that these transceivers could be used with existing 25GBASE-SR and 100GBASE-SR4 (parallel fiber) channels.

The results demonstrate a) an error-free 103.12 Gbps transmission through a 200 m WB-OM4 fiber on an SWDM grid and b) 100 Gbps SWDM realization over a 300 m WB-OM4 fiber requires using FEC. Thus, the SWDM solution is applicable for 100 Gbps Ethernet utilizing the same multiplexing and demultiplexing technologies used in the existing 40 G SR SWDM product [20].

B. PAM4 transmission

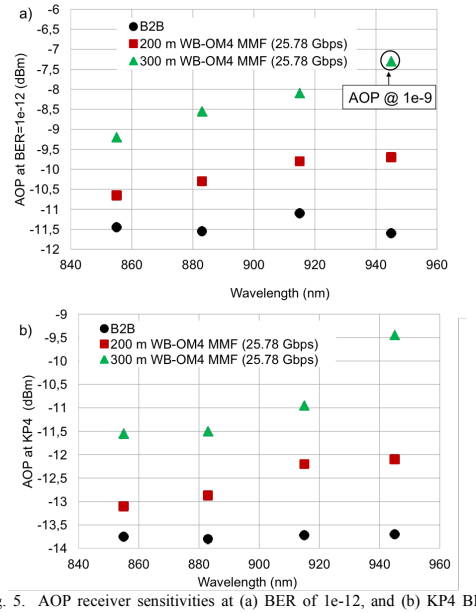

Fig. 5. AOP receiver sensitivities at (a) BER of 1e-12, and (b) KP4 BER threshold of 2e-4 for the four NRZ SWDM channels transmitted over WB-OM4 supplied by Prysmian. The black arrow in Fig. 5 a) shows the receiver sensitivity at 1e-9 for 945 nm NRZ channel over 300 m WB-OM4 fiber. The measured ER for each wavelength is approximately 3.3 to 3.5 dB.

Advanced modulation formats can be coupled with the SWDM technology to further increase the capacity of the VCSEL MMF link. A combination of SWDM and PAM4 provides a promising solution for 200 Gbps transmission through a single optical lane. Fig. 6 summaries the experimental results described in further detail in [13]. AOP receiver sensitivities at the KP4 BER threshold of 2e-4 are plotted for all four wavelengths (851.9 nm, 888.0 nm, 912.1 nm, and 942.4 nm) and two edge wavelengths through WB-OM4 fibers and/or OM4 fibers at 45 Gbps and 51.6 Gbps, respectively. Two experiments were performed with different commercially available PAM4 physical layer integrated circuits (PHY), two WB-OM4 fiber types from separate vendors and an OM4 MMF. The availability of PHYs limited our study of different fiber types and lengths. The first PHY chip had a symbol rate of 22.5 Gbaud, provided pulse shaping and CDR functionalities, and enabled equalization for chromatic and modal dispersion compensation. In the first experiment, a 45 Gbps PAM4 signal was transmitted over 100 m and 300 m of the WB-OM4 supplied by Prysmian (the same fiber type as in the NRZ experiment), as well as 200 m of the OM4 fiber. For a 2 m patch cord, the AOP receiver sensitivity at the KP4 BER threshold ranged from -9.6 dBm to -9.3 dBm for all four SWDM wavelengths. An AOP penalty of 0.2 dB was measured for PAM4 transmission over a 100 m WB-OM4 fiber for all four channels. PAM4 transmission over 200 m of the OM4 fiber resulted in AOP penalties ranging from 0.7 dB at 851.9 nm to 2.7 dB at 942.4 nm. Lower AOP penalties were captured for two long wavelengths (912.1 nm and 942.4 nm) at a 300 m WB-OM4 versus a 200 m standard OM4 fiber, indicating that an OM4 fiber is optimized for 850 nm wavelength while a WB-OM4 fiber covers a wider

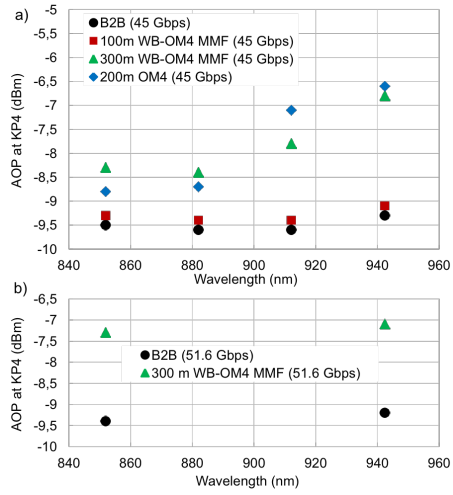

Fig. 6. (a) AOP receiver sensitivities at KP4 BER threshold of 2e-4 for PAM4 SWDM channels transmitted through WB-OM4 fibers using the 45 Gbps PHY and WB-OM4 supplied by Prysmian. (b) AOP sensitivity at KP4 FEC threshold for the 51.6 Gbps PHY and the WB-OM4 fiber supplied by OFS. The measured ER for each of the wavelengths was 3.0 dB and 4.0 dB for a) 45 and b) 51.6 Gbps PAM4 signals respectively.

This article has been accepted for publication in a future issue of this journal, but has not been fully edited. Content may change prior to final publication. Citation information: DOI 10.1109/JLT.2016.2615815, Journal of Lightwave Technology

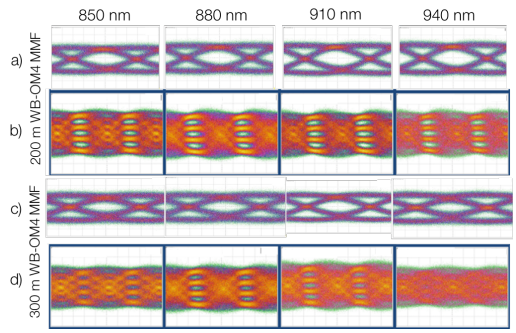

Fig. 7. Received optical eye diagrams for the SWDM wavelengths (a) 25.78 Gbps NRZ over 200 m WB-OM4, (b) 45 Gbps PAM4 over 200 m WB-OM4, (c) 25.78 Gbps NRZ over 300 m WB-OM4, and (d) 45 Gbps PAM4 over 300 m WB-OM4. WB-OM4 fiber was supplied by Prysmian.

wavelength range and is more suitable for SWDM systems. The same experiment was repeated with another PAM4 PHY chip, which had a 25.8 Gbaud data rate and capabilities equivalent to the first PHY chip. Two 51.6 Gbps PAM4 signals were transmitted at the shortest and longest SWDM grid wavelengths (851.9 nm and 942.4 nm) over a 300 m WB-OM4 fiber supplied by OFS. AOP penalties (2.2 dB) were captured for both wavelengths, which imply that the transmission at net rate 195.2 Gbps is possible over 300 m of this WB-OM4 fiber. The results for this measurement are summarized in Fig. 6(b).

Fig. 7(b) and (d) show the received eye diagrams for 45 Gbps PAM4 signaling over 200 m and 300 m WB-OM4 MMFs at four SWDM wavelengths. The columns and rows correspond to four different wavelengths and two fiber lengths, respectively.

C. *Discussion*

The results presented show that the combination of SWDM and WB-OM4 fiber technologies may provide a promising solution for improving both link capacity and reach. The WB-OM4 fiber type may also serve as a suitable option for extending the reach in the newly built data centers. Our results show that a) the specified reach using the IEEE KP4 standard (100 m OM4 at 25 Gbps) is extended to 300 m OM4 and b) 100 Gbps transmission is possible by combining either four wavelengths carrying NRZ signals or two wavelengths carrying PAM4 signals.

NRZ signaling allows for simple and energy-efficient implementation. In scenarios where an additional parallel lane can be added, NRZ transmission is a cost-effective option that provides the same capacity as PAM4 in two parallel lanes instead of one. No equalization is required to enable a net rate after FEC of 25 Gbps per wavelength in transmission over 300 m WB-OM4 fiber, as presented in Section III.A. Standard NRZ off-the-shelf electronic solutions, such as CDR circuits, may be used. On the contrary, commercially available PAM4 solutions are equipped with the energy-consuming equalizers in the TX for signal shaping and in the RX for the dispersion compensation. The PHY chips used in our experiments also include CDR. Combination of these functionalities allows for a high-capacity density of 50 Gbps per wavelength transmission over a 300 m WB-OM4 fiber. Another aspect is FEC, which has been standardized at the IEEE KP4 BER threshold of 2e-4. While FEC is required for PAM4 signaling, it is not necessary for NRZ signaling over shorter transmission distances. As presented in Section III.A, the 200 m transmission over a WB-OM4 fiber was error-free at 25.78 Gbps for all four NRZ SWDM channels with margin of approximately 3 dB. For this reason, there was no need to account for the FEC overhead. Currently, PAM4 electronics are improving in power consumption, but they will always exceed that of NRZ links. The presented results also show that AOP receiver sensitivity (at KP4 BER threshold) for the un-equalized 25.78 Gbps NRZ scheme is 4.5 dB lower than the one required in the equalized 51.6 Gbps PAM4 scheme. Due to this inherent penalty resulting from the lower optical modulation amplitude, the NRZ scheme supports applications that require higher link power budgets. The transmission penalties cannot be directly compared because the PAM4 PHY chip uses an equalizer for dispersion compensation and the NRZ module does not.

IV. Reach Extension for Standard MMF

The previous results indicate that WB-OM4 MMF is a good choice for the new data center fiber infrastructure. However, new data centers are just a portion of the market. In existing data centers the fiber infrastructure cabling is rarely exchanged due to the high cost of replacement. In this section, we discuss solutions for improving the reach of the standard MMF links, such as those using OM3.

A. *Selective mode launch*

One way to improve the bandwidth of the existing OM3 MMF links is to use a selective modal launch. Utilizing the selective launch and an offset launch was proposed in order to improve bandwidth and fiber characterization in the 1550 nm [17], 1310 nm [18] and 664 nm [19] regimes. These schemes employed a single-mode source and a spatial light modulator (SLM) to selectively launch light into specific mode groups of the MMF. In this section, we present the experimental and simulation results for a selective launch in the 850 nm wavelength regime. The experiment was performed using an optical phase mask designed for 850 nm. The transmitter includes the multimode VCSEL structure described in Section II and an optical phase mask to enable SML into a MMF. The SML excites fewer mode groups in the MMF and the modal dispersion effect is mitigated as a result.

Fig. 8(a) shows the measured frequency responses of a 300 m OM3 MMF with a selective modal launch (blue line) and a standard central launch (black line). The fiber frequency response of the 305 m OM3 spool was measured by subtracting the optical response measured with a 2 m patch cord from the full-system response. In the standard central laser launch configuration the fiber bandwidth is 1800 MHz•km at 6 dB. With the optical phase plate in place for the SML, the fiber bandwidth is increased to

This article has been accepted for publication in a future issue of this journal, but has not been fully edited. Content may change prior to final publication. Citation information: DOI 10.1109/JLT.2016.2615815, Journal of Lightwave Technology

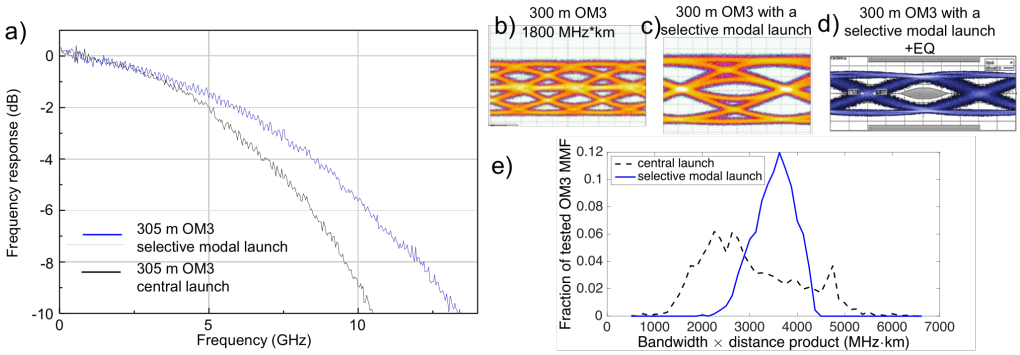

Fig. 8. (a) Bandwidth measured with and without selective modal launch in a 300m OM3 fiber (b) optical eye diagrams captured after 300 m OM3 fiber transmission without SML, (c) optical eye diagrams captured after the 300 m OM3 with SML, d) electrical eye diagrams after the 300 m OM3 fiber with SML and equalization, (e) Histogram of the calculated bandwidth-distance product of the TIA sample of OM3 fiber with (solid line) and without (dashed line) SML.

2100 MHz•km. The NRZ eye diagrams at 25.78 Gbps shown in Fig.s 8 (b)-(d) were captured after propagating through 300 m of the OM3 MMF. Fig. 8(b) is the optical eye diagram without SML, and Fig. 8(c) is with the SML. Clear improvement in the optical eye diagram is demonstrated. Fig. 8(d) is the analog electrical output from the receiver which does include equalization. With the SML and equalization, error-free transmission over 300 m of OM3 fiber was obtained.

To determine if an SML could be used with a wide range of OM3 fibers, we have calculated the EMB of a statistically representative sample of fiber bandwidths. The OM3 fiber set used was a subset of the TIA 5000 fiber set described in [26], which lists modal delays for 19 mode groups of 5000 multimode fibers without specifically describing index profile perturbations. The OM3 subset was chosen by simulating offset SMF launch procedure, using differential mode delay (DMD) weightings from TIA-455-220A to calculate impulse response, frequency responses and minimum modal bandwidth, which were filtered to >2000 MHz·km and <4700 MHz·km. This filtering left 2300 fiber profiles in the data set. Because there is a large variance within OM3 fiber group, we use the bandwidth criterion to assess if the specific fiber sample can support a 300 m 25 Gbps transmission. Fig. 8(e) is a histogram of the bandwidth-distance product of the 300 m OM3 links from the data set using a central laser launch (dashed line) and the SML profile (solid line). The phase plate design has been optimized to improve the worse tail of the OM3 fiber distribution. The simulation results indicate that by using an SML the variance of the bandwidth-distance product distribution of OM3 MMF is reduced, and the bandwidth improvement is possible for more than 80 percent of OM3 fiber samples. More importantly, the minimum bandwidth of a 300 m OM3 MMF link can be improved to more than 2000 MHz·km.

B. Quasi-single mode VCSELs

The previous results relied on addressing the modal dispersion in the MMF. Another method to increase the MMF bandwidth is to reduce the contribution of chromatic dispersion to the total bandwidth. In one example, an 850 nm VCSEL with an integrated mode filter supported 25 Gbps NRZ transmission over 1.3 km of MMF [27], and in another example a NRZ net rate after FEC of 50 Gbps was transmitted over 2.4 km of MMF [28]. In a third example, an equalized 25 Gbps transmission over 1 km OM4 was shown by utilizing a Zn-diffusion and oxide-relief VCSEL structure [29]. In addition, the Zn-diffusion VCSEL structure enabled a 72 Gbps DMT transmission over 300 m of OM4 fiber [30]. The disadvantage of using single mode lasers is that they are often limited in optical power and may require more complex optical alignment to minimize feedback to the laser. Still this is a promising approach to increasing the optical link length in some installed fiber. However, if the modal bandwidth of the fiber is low, a SML may also be needed to realize the full benefit.

C. Discussion

The experimental results presented in this section indicate the possibility of enhanced performance of an existing MMF infrastructure when SML is used to improve the modal bandwidth and/or a low SBW source is used to minimize the chromatic dispersion. The link capacity may be further increased if both strategies are combined with SWDM and advanced modulation formats. More experimental confirmation of the bandwidth improvement from the SML across a broad sample of OM3 is required before this technique could be widely deployed. SML techniques have been previously standardized using an offset launch from a single mode fiber for 1310 nm links operating on MMF in IEEE 10GGASE-LR. The proposed SML solution can be applied to the other SWDM VCSELs by adjusting the phase mask design to the specific wavelength.

V. Conclusion

We reviewed and suggested several methods for enhancing the capacity and extending the reach for VCSEL based MMF links. We showed that four wavelength SWDM can support 100 Gbps NRZ and 200 Gbps PAM4 transmissions. Our results demonstrated that an error-free transmission at

100 Gbps is possible for all four wavelengths with NRZ signaling over a 200 m WB-OM4 fiber, and with the addition of KP4 FEC 300 m links are possible. With PAM4 signaling and FEC the SWDM link on WB-OM4 fiber achieved 170 Gbps. Further improvements to these link speeds and distance could be realized with the addition of SML or possibly quasi-single mode VCSELs.

ACKNOWLEDGMENT

The authors would like to thank Dr. Julie Eng at Finisar for her support of this research, and both Prysmian and OFS for supplying samples of the WB-OM4 fibers.

REFERENCES

[1] *TIA Specification for 850 nm Laser Optimized OM4 MMF* TIA-492ADDD, Sept. 2009.

[2] P. Westbergh, E. P. Haglund, E. Haglund, R. Safaisini, J. S. Gustavsso, and A. Larsson, "High-speed 850 nm VCSELs operating error free up to 57 Gbit/s," *Electronics Letters*, vol. 49, no. 16, pp. 1021–1023, Aug 2013.

[3] J. Castro, R. Pimpinella, B. Kose, Y. Huang, B. Lane, K. Szczerba, P. Westbergh, T. Lengyel, J. Gustavsson, A. Larsson, and P. Andrekson, "Investigation of 60 Gb/s 4-PAM using an 850 nm VCSEL and multi-mode fiber," *Journal of Lightwave Technology*, vol. PP, no. 99, pp. 1–1, 2016.

[4] W.A. Ling, I. Lyubomirsky, R. Rodes, H. M. Daghighian, and C. Kocot, "Single-channel 50G and 100G discrete multitone transmission with 25G VCSEL technology," *J. Lightwave Technol.,* vol. 33, no. 4, pp. 761–767, Feb 2015.

[5] I. Lyubomirsky and W. A. Ling, "Digital QAM modulation and equalization for high performance 400 GbE data center modules," in *Optical Fiber Communications Conference and Exhibition (OFC)*, 2014, March 2014, pp. 1–3.

[6] D. M. Kuchta *et al*., "A 71-Gb/s NRZ Modulated 850-nm VCSEL-Based Optical Link," in *IEEE Photonics Technology Letters*, vol. 27, no. 6, pp. 577-580, March15, 15 2015.

[7] D. M. Kuchta *et al*., "64Gb/s transmission over 57m MMF using an NRZ modulated 850nm VCSEL," *Optical Fiber Communications Conference and Exhibition (OFC), 2014*, San Francisco, CA, 2014, pp. 1-3.

[8] T. Zuo, L. Zhang, J. Zhou, Q. Zhang, E. Zhou, and G. Ning Liu, "Single Lane 150-Gb/s, 100-Gb/s and 70-Gb/s 4-PAM Transmission over 100-m, 300-m and 500-m MMF Using 25-G Class 850nm VCSEL," *2016 The European Conference on Optical Communication (ECOC)*, Dusseldorf, 2016, paper Th.1.C.2, pp. 1-3.

[9] J. Lavrencik, S. J Varughese, V. A. Thomas, G. Landry, Y. Sun, R. Shubochkin, K. Balemarthy, J. Tatum, and S. Ralph, "100 Gbps PAM-4 Transmission over 100m OM4 and Wide-band Fiber using 850nm VCSELs," *2016 The European Conference on Optical Communication (ECOC)*, Dusseldorf, 2016, paper Th.1.C.5, pp. 1-3.

[10] J. M. Castro, R. Pimpinella, B. Kose, Y. Huang, B. Lane, K. Szczerba, P. Westbergh, T. Lengyel, J. S. Gustavsson, A. Larsson, and P. A. Andrekson, "48.7-Gb/s 4-PAM transmission over 200 m of high bandwidth MMF using an 850-nm VCSEL," *IEEE Photonics Technology Letters*, vol. 27, no. 17, pp. 1799–1801, Sept 2015.

[11] Y. Sun, R. Lingle, R. Shubochkin, K. Balemarthy, D. Braganza, T. Gray, W. Fan, K. Wade, D. Gazula, and J. Tatum, "51.56 Gb/s SWDM PAM4 Transmission over Next Generation Wide Band Multimode Optical Fiber," in Optical Fiber Communication Conference, OSA Technical Digest (online) (Optical Society of America, 2016), paper Tu2G.3.

[12] D. M. Kuchta *et al*., "A 4-λ, 40Gb/s/λ bandwidth extension of multimode fiber in the 850nm range," *Optical Fiber Communications Conference and Exhibition (OFC), 2015*, Los Angeles, CA, 2015, pp. 1-3.

[13] R. Motaghian, I. Lyubomirsky, H. Daghighian, C. Kocot, T. Gray, J. Tatum, Adrian Amezcua-Correa, M. Astruc, Denis Molin, F. Achten, and P. Sillard, "180 Gbps PAM4 VCSEL transmission over 300m wideband OM4 fibre," in *Optical Fiber Communication Conference*. Optical Society of America, 2016, p. Th3G.2.

[14] R. Motaghian and C. Kocot, "104 Gbps PAM4 transmission over OM3 and OM4 fibers using 850 and 880 nm VCSELs," in *Lasers and Electro-Optics Conference*. Optical Society of America Technical Digest, 2016, p. SW4F.8.

[15] *Wideband MMF Standardization and S-WDM technology*, IEEE 802.3 50G & NGOATH Study Groups, January 2016, Atlanta GA.

[16] R. Motaghiannezam, I. Lyubomirsky, H. Daghighian, C. Kocot, T. Gray, J. Tatum, A. Amezcua-Correa, M. Bigot-Astruc, D. Molin, F. Achten, and P. Sillard, "Four 45 Gbps PAM4 VCSEL based transmission through 300 m wideband OM4 fiber over SWDM4 wavelength grid," Opt. Express 24, 17193-17199 (2016).

[17] J. Carpenter and T. Wilkinson, "Characterization of multimode fiber by selective mode excitation," *Lightwave Technology, Journal of*, vol. 30, no. 10, pp. 1386–1392, May 2012.

[18] L. Geng, S. Lee, K. William, R. Penty, I. White, and D. Cunningham, "Symmetrical 2-D Hermite-Gaussian square launch for high bit rate transmission in multimode fiber links," in *Optical Fiber Communication Conference and Exposition (OFC/NFOEC)*, 2011 and the National Fiber Optic Engineers Conference, March 2011, pp. 1–3.

[19] G. Stepniak, L. Maksymiuk, and J. Siuzdak, "Binary-phase spatial light filters for mode-selective excitation of multimode fibers," *Lightwave Technology, Journal of*, vol. 29, no. 13, pp. 1980–1987, July 2011.

[20] J. A. Tatum, D. Gazula, L. A. Graham, J. K. Guenter, R. H. Johnson, J. King, C. Kocot, G. D. Landry, I. Lyubomirsky, A. N. MacInnes, E. M. Shaw, K. Balemarthy, R. Shubochkin, D. Vaidya, M. Yan, and F. Tang, "VCSEL-based interconnects for current and future data centers," *Journal of Lightwave Technology*, vol. 33, no. 4, pp. 727–732, Feb 2015.

[21] J. Guenter, B. Hawkins, R. Hawthorne, and G. Landry, "Reliability of VCSELs for >25Gb/s," in *Optical Fiber Communication Conference*, OSA Technical Digest (online) (Optical Society of America, 2014), paper M3G.2.

[22] D. Molin, F. Achten, M. Bigot, A. Amezcua-Correa and P. Sillard, "WideBand OM4 multi-mode fiber for next-generation 400Gbps data communications," *2014 The European Conference on Optical Communication (ECOC)*, Cannes, 2014, pp. 1-3.

[23] D. Molin, M. Bigot, F. Achten, A. Amezcua-Correa, and P. Sillard, "850-950nm wideband OM4 multimode fiber for next-generation WDM systems," in *Optical Fiber Communications Conference and Exhibition (OFC)*, 2015, March 2015, pp. 1–3.

[24] I. Lyubomirsky, R. Motaghian, H. Daghighian, D. McMahon, S. Nelson, C. Kocot, J. A. Tatum, F. Achten, P. Sillard, D. Molin, and A. Amezcua-Correa, "100G SWDM transmission over 300m wideband MMF," in *Optical Communication (ECOC)*, 2015 European Conference on, Sept 2015, pp. 1–3.

[25] *IEEE 40/100Gb/s Ethernet Standard Task Force*, IEEE Standard 802.3.bm, Mar. 2014. Available: http://www.t11.org/ftp/t11/pub/fc/pi-6p/15-057v4.pdf

[26] P. Pepeljugoski *et al*., "Development of system specification for laser-optimized 50-µm multimode fiber for multigigabit short-wavelength LANs," in *Journal of Lightwave Technology*, vol. 21, no. 5, pp. 1256-1275, May 2003.

[27] R. Safaisini, E. Haglund, P. Westbergh, J.S. Gustavsson, and A. Larsson, "20 Gbit/s data transmission over 2 km multimode fibre using 850 nm mode filter VCSEL," *Electronics Letters*, vol. 50, no. 1, pp. 40–42, January 2014.

[28] G. Stepniak *et al*., "54 Gbit/s OOK transmission using single-mode VCSEL up to 2.2 km MMF," in *Electronics Letters*, vol. 52, no. 8, pp. 633-635, 4 14 2016.

[29] I.-C.Lu,J.-W.Shi,H.-Y.Chen,C.-C.Wei,S.-F.Tsai,D.Hsu,Z.-R.Wei, J.-M. Wun, and J. Chen, "Ultra low power VCSEL for 35-Gbps 500-m OM4 MMF transmissions employing FFE/DFE equalization for optical interconnects," in *Optical Fiber Communication Conference/National Fiber Optic Engineers Conference 2013*. Optical Society of America, 2013, p. JTh2A.75.

[30] B. Wu, X. Zhou, N. Ledentsov, and J. Luo, "Towards 100 Gb/s serial optical links over 300m of multimode fibre using single transverse mode 850nm VCSEL," in *Asia Communications and Photonics Conference* 2015. Optical Society of America, 2015, p. ASu4C.3.

Paper 3: Enabling 4- Lane Based 400 G Client-Side Transmission Links with MultiCAP Modulation

Tatarczak, A.; Iglesias Olmedo, M.; Zuo, T.; Estaran, J.; Bevensee Jensen, J.; Xu, X.; Tafur Monroy, I., "Enabling 4- Lane Based 400 G Client-Side Transmission Links with MultiCAP Modulation," Advances in Optical Technologies, vol. 2015, Article ID 935309, 2015.

Hindawi Publishing Corporation
Advances in Optical Technologies
Volume 2015, Article ID 935309, 9 pages
http://dx.doi.org/10.1155/2015/935309

Review Article

Enabling 4-Lane Based 400 G Client-Side Transmission Links with MultiCAP Modulation

Anna Tatarczak,[1] Miguel Iglesias Olmedo,[1,2] Tianjian Zuo,[3] Jose Estaran,[1] Jesper Bevensee Jensen,[1] Xiaogeng Xu,[3] and Idelfonso Tafur Monroy[1]

[1]*DTU Fotonik, Technical University of Denmark, Building 343, 2800 Kongens Lyngby, Denmark*
[2]*Optics Division, Royal Institute of Technology, Electrum 229, 164 40 Kista, Sweden*
[3]*Transmission Technology Research Department, Huawei Technologies Co., Ltd., Shenzhen 518129, China*

Correspondence should be addressed to Anna Tatarczak; atat@fotonik.dtu.dk

Received 9 May 2015; Revised 15 July 2015; Accepted 22 July 2015

Academic Editor: José Luís Santos

We propose a uniform solution for a future client-side 400 G Ethernet standard based on MultiCAP advanced modulation format, intensity modulation, and direct detection. It employs 4 local area networks-wavelength division multiplexing (LAN-WDM) lanes in 1300 nm wavelength band and parallel optics links based on vertical cavity surface emitting lasers (VCSELs) in 850 nm wavelength band. Total bit rate of 432 Gbps is transmitted over unamplified 20 km standard single mode fiber link and over 40 km link with semiconductor optical amplifier. 70.4 Gb/s transmission over 100 m of OM3 multimode fiber using off-the-shelf 850 nm VCSEL with 10.1 GHz 3 dB bandwidth is demonstrated indicating the feasibility of achieving 100 Gb/s per lane with a single 25 GHz VCSEL. In this review paper we introduce and present in one place the benefits of MultiCAP as versatile scheme for use in a number of client-side scenarios: short range, long range, and extended range.

1. Introduction

Ever growing video-rich Ethernet traffic on the client-side optical networks calls for high-speed, cost-effective optical transport data links. Standardization of client-side optical data links is critical to ensure compatibility and interoperability of telecom and datacom equipment from different vendors. As depicted in Figure 1, the IEEE standardization body classifies the client-side links in three categories: short range (SR), long range (LR), and extended range (ER). SR links, which cover up to 100 m, are usually employed in data centers and central offices. LR links cover up to 20 km and are typically used to privately connect buildings of the same company or institution. ER links cover up to 40 km and are typically used to provide connectivity to customer-premises equipment (CPE) and for metro applications. The current work of the 400 Gbps Ethernet Study Group [1] and the wider research community focuses on these three scenarios [2]. An optical intensity modulation/direct detection (IM/DD) link offering 400 Gbps capacity with use of advanced modulation formats is an attractive and easily adaptable solution for client-side links, such as inter- and intradata center interconnects.

The client-side links presented in this work are based on the multiband and multilevel approach to carrierless amplitude phase (CAP) modulation, MultiCAP [3]. In this review paper we demonstrate the flexibility of the IM/DD MultiCAP based solutions for a SR 100 m link [4], a LR 20 km link, and an ER 40 km link [5]. A SR client-side link that achieves error-free 65.7 Gbps over a 100 m multimode fiber (MMF) OM3 using an 850 nm vertical cavity surface-emitting laser (VCSEL) is presented. Furthermore, two IM/DD LAN-WDM 432 Gbps links are described: an unamplified 20 km link for the LR scenario and semiconductor optical amplifier (SOA) based 40 km link for the ER scenario. Four-lane LAN-WDM with 108 Gbps per lane is obtained using 4 externally modulated lasers (EMLs) in the O-band.

Figure 2 summarizes the capacity per lane reported at the considered transmission distances for several modulation formats. The short range (SR) area of Figure 2 shows the highest error-free bit rates achieved for 850 nm vertical cavity surface-emitting laser (VCSEL) based links. Bit rate of

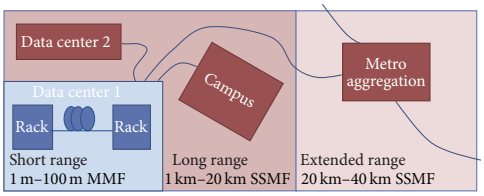

Figure 1: Scenario of client-side optical transmission links for short range (SR), long range (LR), and extended range (ER).

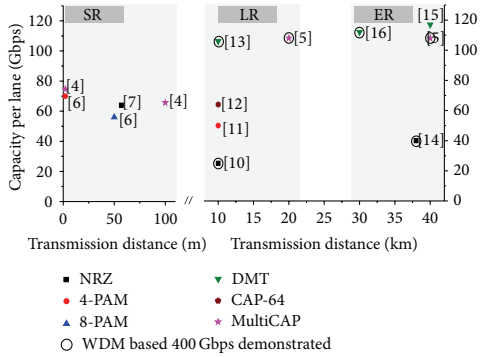

Figure 2: State-of-the-art summary; capacity per lane versus transmitted distance for the following modulation formats: Nonreturn to Zero (NRZ), pulse amplitude modulation (PAM), discrete multitone (DMT), carrierless amplitude phase (CAP), and multiband carrierless amplitude phase (MultiCAP), demonstrated in literature approaches to 400 Gbps systems based on IM/DD WDM are indicated by the black circle.

70 Gbps over 2 m OM4 MMF was achieved using 4-level pulse amplitude modulation (4-PAM) [6], 64 Gbps over 57 m OM2 using Nonreturn to Zero (NRZ) [7], and 56 Gbps over 50 m OM4 using 8-PAM [6]. All of these require very fast electrical interfaces and suffer from low tolerance to modal dispersion compared to pass-band modulation formats [8]. Using discrete multitone (DMT) at an 850 nm window enabled a high transmission distance of 500 m MMF with a bit rate of 30-Gbps [9].

The MultiCAP solution presented in this paper achieves error-free 65.7 Gbps over 100 m and 74.7 Gbps over 1 m using an 850 nm VCSEL with a bandwidth of 10.1 GHz. This solution has the prospect of achieving 100 Gbps over 100 m MMF with emerging 25 GHz 850 nm VCSELs. It overcomes both electrical and optical bandwidth limitations towards single lane 100 Gbps active optical cable (AOC) and employs cost efficient 850 nm MMF technologies. The 400 GE standard requirement can thus be met by employing parallel optical lanes.

The client-side links of long range (LR) and extended range (ER) are expected to meet the 400 Gbps capacity by using advanced modulation formats in combination with wavelength division multiplexing (WDM) [1]. The higher the capacity per lane, the lower the number of WDM lanes and therefore the number of transceivers. The LR and ER areas in Figure 2 show the highest capacities per lane reported in O-band for different modulation formats. In the LR of 10 km, NRZ coding enables 25 Gbps [10], 4-PAM 50 Gbps [11], CAP-64QAM 60 Gbps [12], and DMT 106 Gbps [13]. MultiCAP achieves 108 Gbps per lane with 20 km reach [5]. In the ER of 40 km, NRZ coding allows 40 Gbps per lane [14]. Beyond 100 Gbit/s per lane for ER is reached by DMT modulation [15] and MultiCAP [5]. The DD/IM WDM-based 400 Gbps systems were demonstrated as feasible in several of the cited works (indicated in Figure 2). Eight lanes × 40 Gbps [14] or 16 lanes × 25-Gbps [10] were used to reach 400 Gbps with NRZ coding. A four-lane LAN-WDM 400 Gbps solution was demonstrated using DMT over 30 km [16] and MultiCAP over 40 km standard single mode fiber (SSMF) [5]. Both of them assume the 7% FEC overhead.

The main contribution of this paper is the overview of a uniform MultiCAP based solution for short, long, and extended range client-side links. In all of these scenarios the same implementation scheme can be used. We review the previously presented experimental results focusing on the implementation similarities for different client-side scenarios. We include detailed description of the performed experiments. Moreover, we present the first full description of the used equalizer that was used in previous reported experiments. Having a uniform modulation format in different links types, lengths, and different wavelength bands will not only allow for interoperability between kinds of equipment from different vendors but also reduce the cost and complexity for the clients. In this way a newly developed client's link can leverage the already existing implementation of different link type. We show that using the same transceiver's structure and equalization technique allows satisfying the 400 GE capacity requirement in SR, LR, and ER. MultiCAP advanced modulation format is combined with parallel optics in SR and with WDM in LR and ER. This easily applicable solution enables a simple upgrade from 100 Gbps to 400 Gbps in both 850 nm MM links and 1310 nm SM links. In the context of 400 Gbps Ethernet standardization we demonstrate that a MultiCAP based solution is feasible and worth considering for SR, LR, and ER.

2. Methods

Figure 3 depicts the experimental setup for all of the considered transmission scenarios. At the transmitter side, 5 effective number of bits (ENOB) 64 GSa/s digital-to-analog converter (DAC) is used to generate MultiCAP signal. The transmitter consists of a linear amplifier and a laser. 850 nm VCSEL is used and in SR EMLs are used in LR and ER scenarios. The channel consists of 100 m MMF for SR and 20 km of SSMF for LR. ER scenario consists of 40 km SSMF and an SOA at the receiver. The receiver consists of a photodiode, transimpedance amplifiers (TIAs), and a digital storage oscilloscope (DSO). The 400 Gbps standard requirement in the SR multimode scenario is expected to be fulfilled by parallel optics. Therefore, for the SR scenario we verify only one lane. In the LR and ER scenarios the expected solution to reach 400 Gbps is WDM. Hence, in the experimental

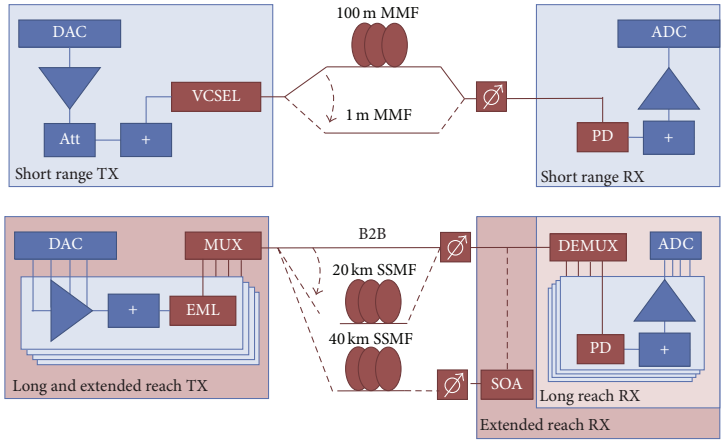

Figure 3: Experimental setup of the short range (SR) scenario employs digital-to-analog converter (DAC), attenuator (Att), vertical cavity surface-emitting laser (VCSEL), multimode fiber (MMF), photodiode (PD), and analog-to-digital converter (ADC); setups for long range (LR) and extended range (ER) additionally employ externally modulated laser (EML), multiplexer (MUX), standard single mode fiber (SSMF), semiconductor optical amplifier (SOA), and demultiplexer (DEMUX).

Table 1: Modulation order per band for different bit rates.

Number	Scenario	Bit rate	Baud rate per band	B1	B2	B3	B4	B5	B6
1	SR	70.4 Gbps	3.4 Gbaud	32	32	16	8	8	4
2	SR	80 Gbps	3.4 Gbaud	64	32	32	16	8	4
3	LR and ER	108 Gbps	4 Gbaud	64	64	32	16	16	4

verification of the LR and ER setup, four independent channels of DAC are used to drive four parallel lanes of WDM transmitter. Additionally, a WDM transmitter includes the WDM multiplexer and the receiver a WDM demultiplexer.

2.1. Signal Generation. The signals are generated by a 4-output 64 GSa/s digital-to-analog converter (DAC) with 5 ENOB. For signal generation, we choose a 6-band configuration of MultiCAP [3] with different modulation orders per band which result in different bit rates. Table 1 presents three configurations and Figures 4(c)–4(e) depict the corresponding electrical spectra. Each MultiCAP band is constructed from a pseudorandom bit sequence (PRBS) of $2^{13} - 1$ bits and delivers a baud rate as described in Table 1. The total number of transmitted symbols is 49146. MultiCAP symbols are generated by upsampling to 16 samples per symbol and subsequent CAP filtering. Upsampling factor is an integer multiple of baud rate of each subband. The upsampling procedure is explained in detail in [3]. The CAP filters are realized as finite impulse response (FIR) with a length of 20 symbols for SR scenario and 30 symbols for LR and ER scenarios. A roll-off coefficient of 0.05 was used at the transmitter. At the receiver, time inverted versions of the CAP filters (roll off = 0.09) are used to recover the symbol constellations. We use the MultiCAP features of power and bit loading. The constellation and power level for each band differs and is chosen empirically to best fit the signal-to-noise ratio (SNR) of the specific frequency band. The bands' configuration and power choice depend on the frequency response of the overall system.

The frequency response of SR system is presented in Figure 4(a). A 3 dB bandwidth of 10.1 GHz, a 10 dB bandwidth of 17 GHz, and a 20 dB bandwidth of 20.1 GHz are measured. This frequency response allows for the first and the second MultiCAP bands configurations presented in Table 1. First configuration shown in Table 1 and in Figure 4(c) enables a total throughput of 70.4 Gbps (65.7 Gbps after 7% overhead forward error correction (FEC) decoding), whereas the second configuration shown in Figure 4(d) enables 80 Gbps (74.7 Gbps after 7% FEC). In these two cases, 6 MultiCAP bands occupied the bandwidth of 21 GHz. The frequency response of optical back-to-back for both LR and ER systems is presented in Figure 4(b). A 3-dB bandwidth of 8.90 GHz, a 10-dB bandwidth of 17.35 GHz, and a 20-dB bandwidth of 24 GHz are observed. The bandwidth in this case is effectively limited by the bandwidth of the DAC used. This response allowed for implementing the last band configuration from Table 1 presented in Figure 4(e). This configuration enabled throughput of 108 Gbps (100.9 Gbps after 7% FEC). Bandwidth of 26 GHz has been used for MultiCAP bands.

2.2. Short Range. A commercially available 850 nm VCSEL is used in the SR scenario. Figure 5 shows the LIV curves and the optical spectrum measured for the VCSEL. The center

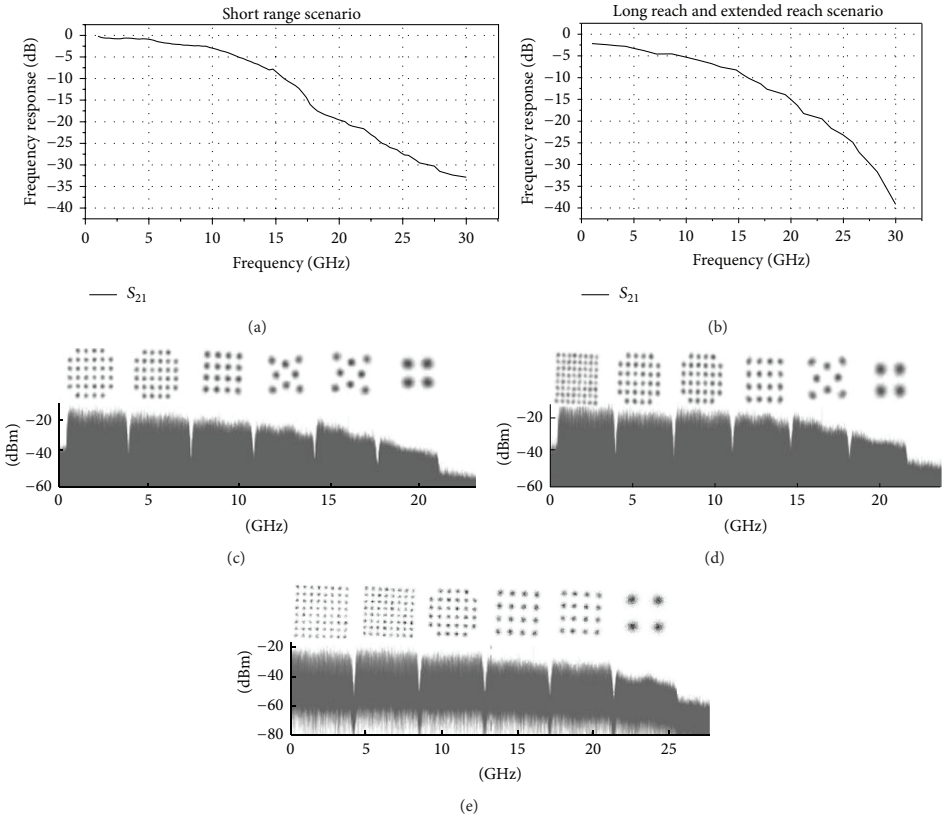

Figure 4: (a) Frequency response measured for short range (SR) scenario end-to-end link; (b) frequency response measured for the optical back-to-back of long range (LR) and extended range (ER) scenarios. Received electrical MultiCAP spectrum and corresponding constellations transmitted in each MultiCAP band for (c) short range (SR) scenario with total bit rate 70.4 Gbps; (d) short range (SR) scenario with total bit rate 80 Gbps; (e) long range (LR) and extended range (ER) scenarios with total bit rate 108 Gbps.

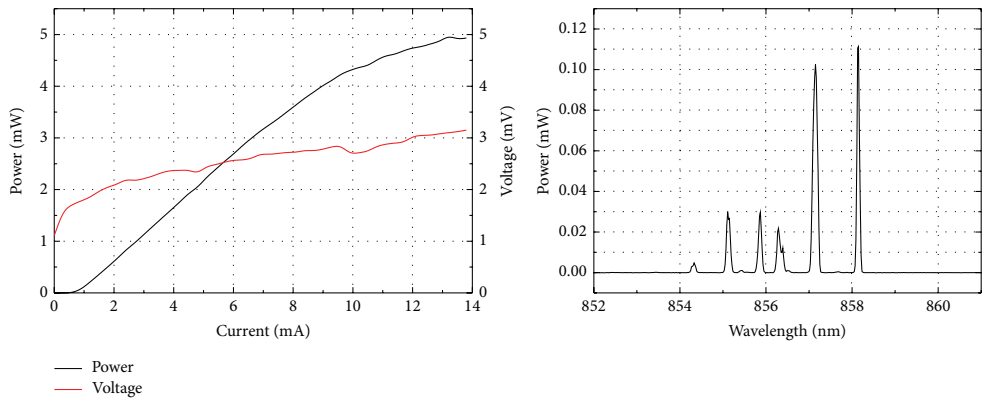

Figure 5: Characterization of the VCSEL used in the short range scenario; LIV curve measured at the room temperature; optical spectrum measured at bias current of 8 mA.

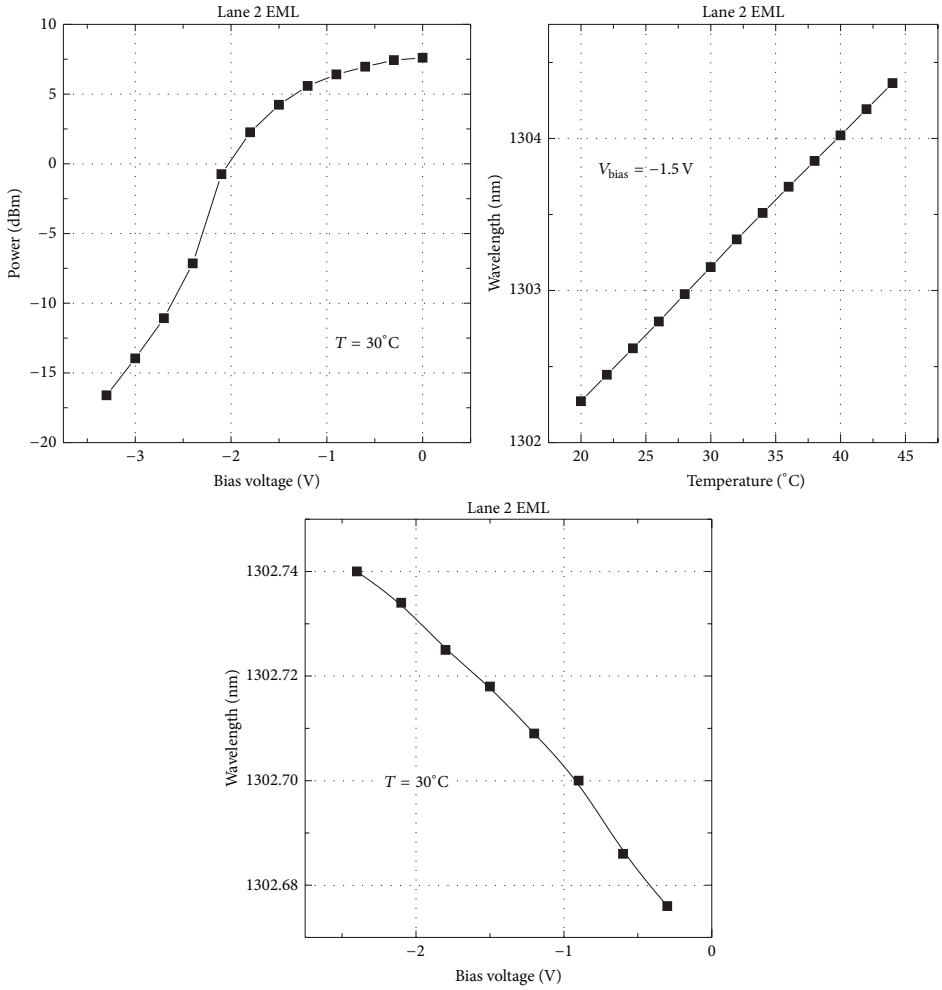

Figure 6: Characterization of the EML of Lane 2; power versus bias current measured at $T = 30^{\circ}$; wavelength versus temperature measured at bias voltage of –1.5 V; wavelength versus bias voltage measured at $T = 30^{\circ}$.

frequency of the VCSELs' spectrum at 8 mA bias is 857.2 nm. The DAC output is amplified to a 1.2 Vp-p signal that is used to drive the VCSEL biased at 8 mA. An optical power of 6 dBm is launched into 100 m of OM3 compliant MMF, with a total link loss of 0.5 dB. The signal is photodetected with an 850 nm photodiode reverse biased at 4 V. The signal is then amplified to a Vp-p of 1 V and digitally stored with an 80 GSa/s DSO with a resolution of 8 bits.

2.3. Long Range and Extended Range. The signals generated by a 4-output DAC are decorrelated with delay lines. The laser source used in these scenarios is EML. The bias voltage and temperature characteristics of the EML employed in Lane 2 are presented in Figure 6. The EML's bias voltage is −1.5 V and the MultiCAP signal has a CMOS compatible peak-to-peak voltage of 2.5 Vp-p. The center wavelengths of the EMLs in Lanes 0 to 3 are 1294 nm, 1299 nm, 1303 nm, and 1308 nm. In order to keep the wavelengths stable, temperature control is applied. The output power of the EML in the tested lane is 6 dBm. Average output power of the EMLs ranges from 4 dBm to 6 dBm.

The optical signals are combined in a LAN-WDM multiplexer (MUX) with a channel spacing of 800 GHz (G.694.1 compliant) and transmitted over 20 km or 40 km (G.652 compliant) SSMF links. MUX introduces 0.6 dB of insertion loss. The span losses are 7 dB and 14 dB, respectively. For the

Table 2: Equalizer's performance in terms of BER as compared to the nonequalized system measured for three different signal-to-noise ratio (SNR) settings; compared systems: nonequalized system with a standard multimodulus algorithm (MMA) equalization and with decision directed (DD) K-means equalizer.

SNR (dB)	BER nonequalized system	BER MMA equalizer	BER DD K-means equalizer
20.6	$1.89 \cdot 10^{-2}$	$3.83 \cdot 10^{-3}$	$8.67 \cdot 10^{-4}$
19.5	$2.23 \cdot 10^{-2}$	$7.66 \cdot 10^{-3}$	$3.9 \cdot 10^{-3}$
18.2	$3.67 \cdot 10^{-2}$	$1.96 \cdot 10^{-2}$	$1.48 \cdot 10^{-2}$

40 km transmission case, a semiconductor optical amplifier (SOA) with a noise figure (NF) of 6.5 dB is employed at the receiver, before demultiplexing. At the receiver side the signal is demultiplexed by a LAN-WDM demultiplexer (DEMUX), received by a photodiode (PD), and amplified by a transimpedance amplifier (TIA). DEMUX introduces 0.9 dB of insertion loss. All of the components are 100GBASE-LR4 and ER4 compatible.

2.4. Demodulation and Equalization. The receiver consists of several digital signal processing (DSP) blocks which are implemented in Matlab environment. CAP filtering, signal downsampling, phase offset removal, and signal normalization are performed as explained in [3]. Additionally, we implement an adaptive frequency domain equalization to mitigate linear impairments. The described adaptive decision directed (DD) equalization algorithm minimizes the received constellation cluster size and quantization noise.

We define the reference constellation by the centroids found using K-means algorithm which groups the received data in the clusters [17]. This reference constellation initializes the described DD equalization algorithm. Clusters' means are the points of reference (starting decision).

We use an iterative equalizer where in every iteration the following steps are performed: first, the error is calculated based on the Euclidean distance from the closest centroid as in a least mean square (LMS) equalizer:

$$\varepsilon(n) = \min \left\| \mathbb{C} - y(n) \right\|, \tag{1}$$

where $\mathbb{C}$ denotes all centroids of the reference constellation and $y(n)$ is the received signal sample. For equalization we use $T/2$ fractionally spaced FIR filter with 12 taps determined empirically. The taps coefficients of the DD equalizer are updated according to the following equation:

$$h(n+1) = h(n) + \mu(n) \cdot \varepsilon(n) \cdot y(n)^*, \tag{2}$$

where $h(n)$ is the equalizer coefficient, $\mu(n)$ is the step size initialized as $7.5 \cdot 10^{-4}$, and $y(n)^*$ is the complex conjugate $y(n)$. Secondly, the received signal is passed through the equalizer. Finally, the iterative process reestimates the centroids of the equalized constellation and the described steps are repeated. It was experimentally determined that 2 iterations result in satisfactory equalization and further iterations do not show the performance improvement. To assure a faster convergence we implement the variable step in DD. The step size is updated in the following manner [18]:

$$\mu(n+1) = \frac{\mu(n)}{1 + \lambda \mu(n) \left|\varepsilon(n)\right|^2},$$
$$\lambda = \begin{cases} 1, & \text{if } n = 0 \\ 0, & \text{if } \operatorname{sgn}(\operatorname{Re}\{\varepsilon(n)\}) = \operatorname{sgn}(\operatorname{Re}\{\varepsilon(n-1)\}),\ \operatorname{sgn}(\operatorname{Im}\{\varepsilon(n)\}) = \operatorname{sgn}(\operatorname{Im}\{\varepsilon(n-1)\}) \\ 1, & \text{otherwise,} \end{cases} \tag{3}$$

where sgn denotes a sign function.

In order to quantify the improvement due to using an equalizer, we calculate BER for the equalized and nonequalized system for three different SNR values. Moreover, we present BER calculated for the system with a standard frequency domain equalizer, namely, multimodulus algorithm (MMA). Table 2 summarizes the BERs for all equalization and SNR scenarios. Decision directed (DD) K-means equalizer improves the performance in terms of BER in all three SNR scenarios. At SNR of 20.6 dB using an equalizer allows for the improvement of 0.0181 in terms of BER. In the following sections all of the presented results are equalized using DD K-means algorithm.

After the signal is equalized, the EVM is calculated and BER is computed. In order to calculate bit error rate (BER), the received demodulated signal is cross-correlated with the transmitted signal and the errors are counted.

3. Experimental Results

Figure 7 shows the measured BER curves for SR scenario. We define the sensitivity at a BER of the hard decision FEC code at 7% overhead. For the reported system it is $4.5 \cdot 10^{-3}$ [19]. Thereby, we can observe sensitivities of 2.1, 4.7, and 5.4 dBm for experimentally obtained 70.4 Gbps over 1 m, 70.4 Gbps over 100 m, and 80 Gbps over 1 m, respectively. The measured transmission penalty after 100 m MMF is 2.5 dB.

For LR scenario, per lane received bit error ratio (BER) back-to-back (B2B) and after 20 km SSMF transmission (no SOA) of the received signal is plotted in Figure 8(a). The

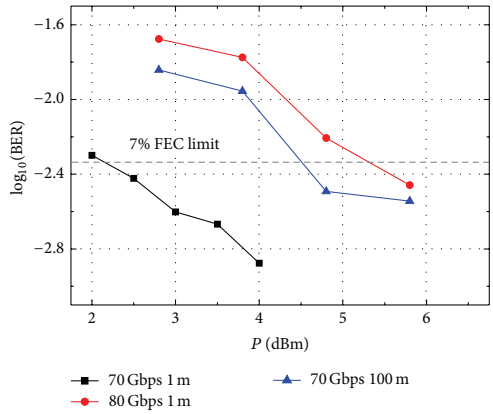

Figure 7: BER versus received optical power (ROP) for B2B and 100 m transmission for 70 Gbps MultiCAP configuration and B2B for 80 Gbps configuration.

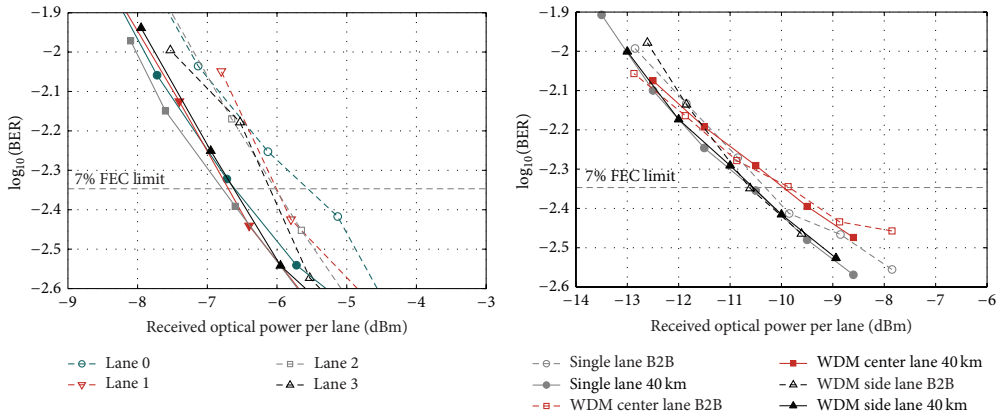

(a) (b)

Figure 8: (a) BER versus received optical power (ROP) for B2B and 20 km transmission for 4 lanes; (b) BER versus ROP for the data transmitted in the single lane (Lane 2) and for the data transmitted in all lines (BER curves for center lane, Lane 2, and side lane, Lane 3); ROP measured before SOA; the total bitrate of WDM system is 432 Gbps.

received optical power is measured before the MUX. For all LAN-WDM lanes, BERs are below the 7% hard decision FEC limit, and no error floor is observed within the tested power range. Receiver sensitivity at the FEC limit is −6.0 dBm B2B and −6.6 dBm after transmission. No transmission power penalty is observed. The results for ER scenario are presented in Figure 8(b). Received BER of a center lane and a side lane is plotted B2B and after 40 km SSMF transmission with all 4 LAN-WDM lanes simultaneously amplified by a single SOA before demultiplexing. Received optical power per channel is measured before the SOA. For comparison, the BER of a single lane (remaining three lanes switched off) is included in the graph. All LAN-WDM lanes were received with a BER below the FEC limit after 40 km SSMF transmission with a worst-case receiver sensitivity of −9.9 dBm. Presence of neighboring channels in the link does not introduce penalty in the 20 km scenario. In case of 40 km scenario, we observe a 0.5 dB power penalty for the center lanes in the 4-lane case due to interlane modulation in the SOA. In both scenarios no penalty is observed in the side lanes.

In the results presented, BER is an average of the BERs in all MultiCAP bands.

Finally, the power budget calculation is evaluated in Table 3. For the SR scenario, the optical output power measured at the output of the VCSEL is 6 dBm. The sensitivity at 7% FEC limit for 70 Gbps 1 m transmissions is equal to 2.4 dBm. Therefore power budget for this scenario is equal to 3.6 dB. In the LR and ER scenarios, the optical output power

Table 3: System power budget.

Transmission link type	Output power	Sensitivity @ FEC limit	System power budget
sr 70 Gbps	6 dBm	2.4 dBm	**3.6 dB**
LR 20 km unamplified	5.4 dBm	−6.6 dBm	**12.6 dB**
ER 40 km SOA amplified	5.4 dBm	−9.9 dBm	**15.9 dB**

per lane is equal to 5.4 dBm. It is measured after transmitter and hence after MUX. The worst receiver sensitivity is −6.6 dBm at FEC limit in case of 20 km transmission link with no amplification. Therefore the power budget of this link is 12.6 dB. In case of 40 km transmission with SOA based amplification, the worst receiver sensitivity is −9.9 dBm at the FEC limit. Therefore for the amplified 40 km link, the power budget is 15.9 dB. The given receiver sensitivity is based on ROP measured before receiver: before PD in SR case, before DEMUX in LR case, and before SOA in ER case.

The SR scenario represents a solution for an active optical cable for data centers. In terms of power budget, the margin is necessary only for the components heating up and aging. In case of LR and ER, the calculated margin of 5.6 dB and 1.9 dB is sufficient for client-side links.

4. Discussion

In the results presented for SR, a steep roll-off of the VCSEL's frequency response reduces the achievable capacity. We use the bit loading and power loading features of MultiCAP to overcome those limitations, at the cost of worse sensitivity. As a consequence, increasing the capacity from 70 Gbps to 80 Gbps introduces the 3.1 dB penalty in sensitivity as shown in Figure 7. The bandwidth of the existing VCSELs is not sufficient to support 100 Gbps per lane. With the proposed MultiCAP scheme, the emerging 25 Gbps VCSELs are expected to satisfy the bandwidth requirement.

The performance of the EMLs used in LR and ER is satisfactory to obtain 100 Gbps after FEC per lane. Moreover, the local area network-wavelength division multiplexing (LAN-WDM) is proved to introduce negligible penalty both for 20 km and for 40 km link. The power budget calculation indicates the maturity of the solution, which allows for link losses of 12.6 dB and 15.9 dB in LR and ER, respectively.

The clear difference in performance and achievable capacity between SR and LR, ER scenarios is attributed to the system bandwidth. Even though the 3 dB and 10 dB bandwidths are similar for both systems, the 20 dB bandwidth varies by 5 dB. For this reason, the MultiCAP in SR is recoverable when it occupies up to 21 GHz while the LR and ER signal is possible to recover when it occupies 26 GHz (Figure 4). The last band in all three scenarios is highly suppressed, but thanks to the power loading and bit loading features of MultiCAP, the information in the last band is also possible to recover if it carries QPSK.

The proposed approach for 400 Gbit/s client-side transmission links using MultiCAP modulation format represents an easily applicable solution that is robust, simple, and flexible in upgrading from 100 Gbit/s to 400 Gbit/s while operating at the O-band LAN-WDM wavelengths. Moreover, we present applicability of the MultiCAP solution in the SR multimode (MM) links. We expect that with higher bandwidth of the upcoming 850 nm VCSELs this solution will enable 100 Gbps per lane and 400 Gbps using parallel optics. This technology potentially provides a bridge for gray optics approach to client-side, inter- and intradata centers, access, and metro segments.

5. Conclusions

We present a uniform MultiCAP based solution for short range (SR) MM links, long range (LR) 20 km single mode (SM) links, and extended range (ER) 40 km SM links. The advantageous feature of MultiCAP approach of being able to assign parallel electrical interfaces of smaller bandwidth into different frequency bands overcomes both electrical and optical bandwidth limitations and eases the DSP pipelining. Its pass-band nature and multiband structure allow optimal usage of the available bandwidth maximizing obtainable capacity. In the SR scenario, we have achieved record below-FEC bit rate transmission of 65.7 Gbps over 100 m and 74.7 Gbps over 1 m for 850 nm MMF data links. For upcoming 400 GE standard long range and extended range criteria, we present a MultiCAP LAN-WDM 400 Gbps solution which uses only commercial optical components from 100GBASE-LR4 and ER4. 432 Gbit/s MultiCAP signals are transmitted over 20 km SSMF without amplification and over 40 km SSMF with SOA. Interchannel mixing in the 40 km link and in SOA is proven to be negligible for a MultiCAP IM/DD LAN-WDM system. The proposed MultiCAP approach is a robust and flexible scheme, which can cover most of the client-side scenarios, including inter- and intradata centers and up to 40 km client-side links.

Conflict of Interests

The authors declare that there is no conflict of interests regarding the publication of this paper.

References

[1] IEEE 400 Gb/s Ethernet Study Group Meeting Materials, 2014.

[2] J. D'Ambrosia and P. Mooney, "400 Gb/s ethernet: why now?" Whitepaper of Ethernet Alliance, 2013.

[3] M. I. Olmedo, T. Zuo, J. B. Jensen et al., "Multiband carrierless amplitude phase modulation for high capacity optical data links," *Journal of Lightwave Technology*, vol. 32, no. 4, pp. 798–804, 2014.

[4] M. I. Olmedo, A. Tatarczak, T. Zuo, J. Estaran, X. Xu, and I. T. Monroy, "Towards 100 Gbps over 100 m MMF using a 850 nm VCSEL," in *Proceedings of the Optical Fiber Communications Conference and Exhibition (OFC '14)*, pp. 1–4, March 2014.

[5] T. Zuo, A. Tatarczak, M. Olmedo et al., "O-band 400 Gbit/s client side optical transmission link," in *Proceedings of the*

Optical Fiber Communications Conference and Exhibition (OFC '14), pp. 1–3, San Francisco, Calif, USA, March 2014.

[6] K. Szczerba, P. Westbergh, M. Karlsson, P. A. Andrekson, and A. Larsson, "70 Gbps 4-PAM and 56 Gbps 8-PAM using an 850 nm VCSEL," in *Proceedings of the European Conference on Optical Communication (ECOC '14)*, September 2014.

[7] D. Kuchta, A. V. Rylyakov, C. L. Schow et al., "64 Gb/s transmission over 57 m MMF using an NRZ modulated 850 nm VCSEL," in *Proceedings of the Optical Fiber Communications Conference and Exhibition (OFC '14)*, pp. 1–3, Optical Society of America, March 2014.

[8] L. Raddatz and I. H. White, "Overcoming the modal bandwidth limitation of multimode fiber by using passband modulation," *IEEE Photonics Technology Letters*, vol. 11, no. 2, pp. 266–268, 1999.

[9] S. Lee, F. Breyer, S. Randel, D. Cardenas, H. van den Boom, and A. Koonen, "Discrete multitone modulation for high-speed data transmission over multimode fibers using 850-nm VCSEL," in *Proceedings of the Conference on Optical Fiber Communication—Incudes Post Deadline Papers (OFC '09)*, pp. 1–3, IEEE, San Diego, Calif, USA, March 2009.

[10] Y. Doi, T. Ohyama, T. Yoshimatsu, S. Soma, and M. Oguma, "400GbE demonstration utilizing 100GbE optical sub-assemblies and cyclic arrayed waveguide gratings," in *Proceedings of the Optical Fiber Communications Conference and Exhibition (OFC '14)*, pp. 1–3, San Francisco, Calif, USA, March 2014.

[11] W. Kobayashi, T. Fujisawa, S. Kanazawa, and H. Sanjoh, "25 Gbaud/s 4-PAM (50 Gbit/s) modulation and 10 km SMF transmission with 1.3 μm InGaAlAs-based DML," *Electronics Letters*, vol. 50, no. 4, pp. 299–300, 2014.

[12] J. Zhang, X. Li, Y. Xia et al., "60-Gb/s CAP-64QAM Transmission using DML with direct detection and digital equalization," in *Proceedings of the Optical Fiber Communication Conference and Exposition and the National Fiber Optic Engineers Conference (OFC/NFOEC '14)*, IEEE, March 2014.

[13] T. Chan, I.-C. Lu, J. Chen, W. Way, and T. Chan, "400-Gb/s transmission over 10-km SSMF using discrete multitone and 1.3-mm EMLs," *IEEE Photonics Technology Letters*, vol. 26, no. 16, pp. 1657–1660, 2014.

[14] J. P. Turkiewicz and H. de Waardt, "Low complexity up to 400-Gb/s transmission in the 1310-nm wavelength domain," *IEEE Photonics Technology Letters*, vol. 24, no. 11, pp. 942–944, 2012.

[15] W. Yan, L. Li, B. Liu et al., "80 km IMDD transmission for 100 Gb/s per lane enabled by DMT and nonlinearity management," in *Proceedings of the Optical Fiber Communication Conference*, p. M2I.4, Optical Society of America, San Francisco, Calif, USA, March 2014.

[16] T. Tanaka, M. Nishihara, T. Takahara et al., "Experimental demonstration of 448-Gbps+ DMT transmission over 30-km SMF," in *Proceedings of the Optical Fiber Communications Conference and Exhibition (OFC '14)*, pp. 1–3, March 2014.

[17] N. G. Gonzalez, D. Zibar, X. Yu, and I. T. Monroy, "Optical phase-modulated radio-over-fiber links with K-means algorithm for digital demodulation of 8PSK subcarrier multiplexed signals," in *Proceedings of the Conference on Optical Fiber Communication, Collocated National Fiber Optic Engineers Conference (OFC/NFOEC '10)*, pp. 1–3, March 2010.

[18] D. Ashmawy, K. Banovic, E. Abdel-Raheem, M. Youssif, H. Mansour, and M. Mohanna, "Joint MCMA and DD blind equalization algorithm with variable-step size," in *Proceedings of the IEEE International Conference on Electro/Information Technology (EIT '09)*, pp. 174–177, June 2009.

[19] F. Chang, K. Onohara, and T. Mizuochi, "Forward error correction for 100 G transport networks," *IEEE Communications Magazine*, vol. 48, no. 3, pp. S48–S55, 2010.

Paper 4: Eight Dimensional Optimized Modulation for IM-DD 56 Gbit/s Optical Interconnections Using 850 nm VCSELs

Lu, X.; Tatarczak, A.; Tafur Monroy, I., "Eight Dimensional Optimized Modulation for IM-DD 56 Gbit/s Optical Interconnections Using 850 nm VCSELs," Optical Communication (ECOC), 2014 European Conference on, pp. , September 2016.

Eight Dimensional Optimized Modulation for IM-DD 56 Gbit/s Optical Interconnections Using 850 nm VCSELs

Xiaofeng Lu, Anna Tatarczak, Idelfonso Tafur Monroy

DTU Fotonik, Technical University of Denmark, DK2800, Kgs. Lyngby, Denmark, xilu@fotonik.dtu.dk

Abstract *A novel 8-dimensional optimized modulation format is designed and compared with PAM-n in a 28-GBd 850 nm VCSEL based IM-DD system, enabling the transmission on 100GBASE-SR4 FEC threshold over various 100 m MMF links.*

Introduction

Multi-dimensional (MD) modulation formats have been investigated in coherent systems[1-5]. MD modulations can be also implemented in an intensity modulation and direct detection (IM/DD) system by combining temporally adjacent symbols into super-symbols. Additionally, standard 4-lane quad small form-factor pluggable (QFSP) links are inherently 4-dimensional (4D), as 4 independent parallel fiber links form a 4D basis in signal space. With two consecutive symbols in each channel, an 8-dimensional (8D) signal space can be found to accommodate 8D optimized formats. A specially designed 8D format for IM-DD system has been proposed and discussed numerically[6].

In the following we proposed an alternative Block-Based 8-dimsional/8-level format, namely BB8, which carries 2 bits per symbol, i.e. the same spectral efficiency with a four-level pulse amplitude modulation (PAM-4). A corresponding simplified bit-mapping/de-mapping algorithm was designed with a specific bit-to-symbol mapping considering the trade-off between performance and computational simplicity. A hyper-space based hard-decision was designed for the application scenario of vertical-cavity surface-emitting laser (VCSEL) and multi-mode fiber (MMF) based data links, where low latencies are critical. In a 28-GBd lab setup the proposed 8D format was compared with PAM-n by the bit-to-error ratio (BER) performance in back-to-back (BTB) measurements and in measurements in different types of 100 m MMF.

8-Dimensional Modulation Format

BB8 is an 8D densest lattice optimizing format, in which each super-symbol is visualized as one 8D point. The orthogonal projections of points in each dimension correspond to individual symbols in the transmitted sequence. The points are selected from the E8 lattice, following the trade-off between optimal performance and modulation convenience. Each projection (or symbol) of BB8 super-symbols has 8 levels with equal transmission probability.

The set of super-symbols can be divided into 4 subsets. The subsets can be further divided into two independent groups, i.e. even and odd subsets. As an illustration, a 2D projection in an arbitrary direction is shown in Fig.1. (a), The subsets are displayed in different colours. The signal is arbitrarily mapped into points in the same subset, or conditionally between either two odd subsets or two even ones. The BER sensitivity is determined by the minimum mutual Euclidean distance between closest points in 8D space. Theoretically, relative to PAM-n counterparts having the same maximum peak-to-peak modulation amplitude, E8 grid brings BB8 a 1.5-dB asymptotic BER benefit. The histogram of an individual symbol and an illustration of the 2D projection constellation of the odd and even symbols are shown in Fig. 1. (b). To maintain the orthogonality of signal space, i.e. the independence of symbols under inter-symbol interference, block-wise interleaved sequences were used in the experiment as an analogy of the independent channels in real QSFP links. Each block only contains the symbols with the same position in a specific super-symbol.

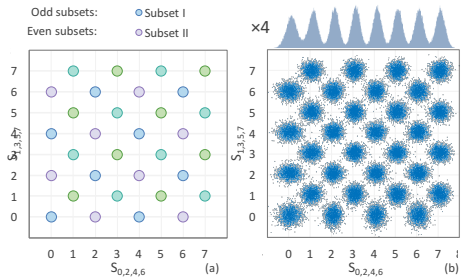

Fig. 1: (a) Designed formats with aids of 2D projection in constellation diagram. (b) Experiment measured histogram of each symbol and 2D projection.

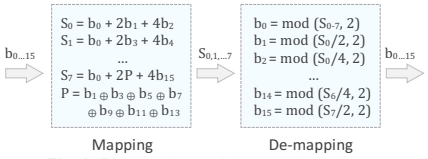

Fig. 2: Bit-mapping and de-mapping rules.

Bit-mapping, De-mapping and Decision

The principle of the bit-to-symbol mapping is shown in Fig. 2. 16 bits are mapped into one 8-symbol super-symbol, with eight levels per symbol. The first bit (b_0) is used for selecting candidate points from the even/ odd subset. Bits b_1-b_{14} are simply mapped into PAM-4. The last symbol is generated from bits b_0, b_{15} and a parity bit (P); P is calculated from b_1-b_{14}. The benefits of such bit-mapping include: (i) minimum change from conventional PAM-4; (ii) minimum extra computational resources; (iii) real-time solution with low latency. The de-mapping algorithm is implemented by decoding b_0 with the subset parity of the received super-symbol and the rest bits with PAM-4 decoding.

65536 possible super-symbol states of BB8 make the maximum likelihood (ML) soft-decision unrealistic in real systems. Hence, a hyper-space hard-decision (HS-HD) algorithm was used in this work. Generally, a hard decision threshold is determined by n-1 dimensional boundaries of cells in n-dimensional signal space. Therefore, 7-dimensional hyper-planes ($H = \{x \in \mathbb{R}^n | \boldsymbol{a}^T x = d\}, \boldsymbol{a} = (a_1, a_2, \dots a_8)^T$) can divide the whole 8D signal space into cells of symbols, with the normal direction determined by the closest neighbouring symbols. The difference with the conventional decision is extra linear transforms required before the decision. Compared to the ML algorithm, the HS-HD is 1600 times faster. For further enhancing the performance, a hybrid scheme combining ML and HS-HD can also be used if computational efficiency is not a priority.

Experimental Setup

Fig. 3. (a) shows the experimental setup. The optical signal was directly modulated by an 850 nm multimode VCSEL with a 520 mV peak-to-peak differential electrical signal. A power versus current and voltage versus current (LIV curve), a frequency response and an optical spectrum of the VCSEL used are presented in Fig. 3. (b), (c) and (d). The electrical signal was generated from 28 GBaud sequences of 256K symbols by a 65 GSa/s 8-bit arbitrary waveform generator (AWG). The sequences were pre-calculated with a raised cosine (roll-off =0.5) pulse shaping and repeatedly transmitted. An pre-equalization on the electrical signal was included to mitigate the spectral roll-off of AWG.

The signal was received with the commercially available VI-Systems photodiode package with trans-impedance amplifier (TIA). Traces were captured with a 33 GHz, 80GSa/s dynamic signal analyser (DSA). The received signal was processed offline with a T/2 fractional IIR filter. The taps were trained during the initialization and fixed in measurements.

100 traces with 2M points (25 μs) for each transmission condition in critical regime and 10 traces with 1M (12.5 μs) in the remaining regimes were stored. The each point was given by the mean value of 90% confidence.

Performance

A back-to-back sensitivity measurement was taken for a primary characterization. Then link measurements were performed with two spools of 100 m MMF, i.e. OM3 and OM4.

Fig. 2. (e) shows the BTB BER sensitivity of BB8, PAM-4, and PAM-8. BB8 and PAM-4 perform similarly with respect to the 7% overhead (OH) FEC limit with required BER=3.8×10^{-3}. With the increase in received optical power, BB8 outperforms PAM-4 by an asymptotic gain around 1.5 dB. An apparent error floor due to laser nonlinearities and a limited bandwidth can be observed for PAM-4, while its new counterpart, BB8, provides a potential to reach BER=10^{-12} before reaching the maximum laser optical output power (can be seen by fitting the trend), or conceals the error

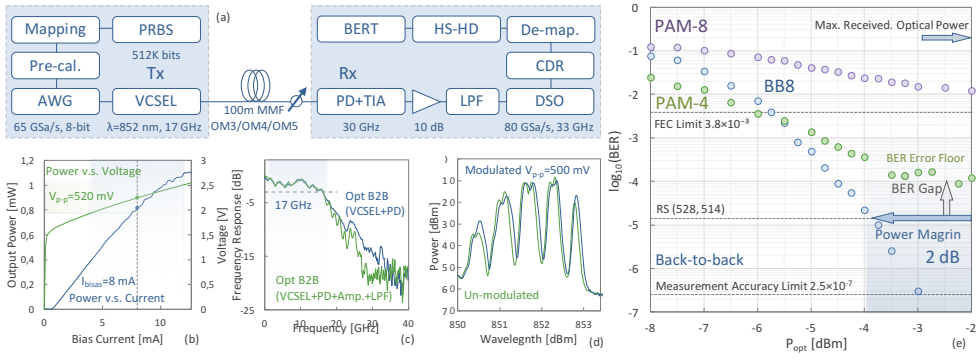

Fig. 3: (a) Experiment setup of performance measurements between PAM-4 and BB8. (b) LIV curves. (c) S21 curve. (d) Spectrum of VCSEL. (e) Comparison on back-to-back BER sensitivity between BB8 (azure), PAM-4 (lemon grass) and PAM-8 (lavender) in 28GBaud/s data-links.

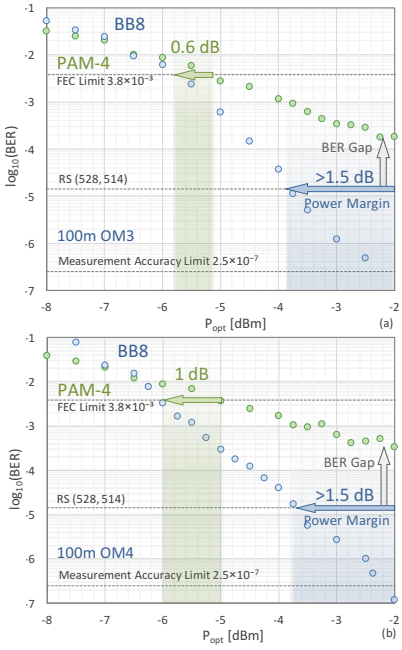

Fig. 4: BER performances of BB8 and PAM-4 with varying received optical power over 100m (a) OM3 MMF; (b) OM4 MMF; (c) OM5 MMF, with evaluation criteria of 7% OH standard FEC limit, RS (528, 514) and measurement accuracy limit at 2.5×10^{-7}.

floor below the detection limit at BER=10^{-7}. PAM-8 displays an unsuccessful transmission using 7% FEC. Recently 2.7% OH FEC of Reed-Solomon (528, 514) has been adopted in IEEE 802.3 bm, 100GBASE-SR4[7,8]. BB8 gives a 2dB power margin (maximum optical power -2dBm) on such limit, which gives the output BER<10^{-12}, whereas PAM-4 has a major BER gap of larger than an order of magnitude.

As shown above, BB8 transmitted over two 100 m MMF links (OM3 in Fig. 4. (a) and OM4 in Fig. 4. (b) performs similarly in BTB measurements by <1 dB degradation with respect to 7% FEC limit. Yet, PAM-4 experiences a 0.5 dB degradation from OM3 to OM4. Unlike the ideal simulation, the gap between two formats is enlarged to 1 dB. In both cases BB8 has a successful transmission at the lower FEC threshold, but with reduced power margin; error floor close to VCSEL's maximum output power makes 56 Gbit/s PAM-4 unsuccessful. Since 100 m links are typical in commercial product, these results imply the potential of BB8 in application of MMF based data links.

Conclusions

An 8D modulation format based on E8 lattice was proposed for short-reach data links. The experimental performance shows a 2 dB power margin in BTB and ~1.5 dB over 100 m OM3/OM4 MMF links with respect to 2.7% 100BASE SR4 FEC. It implies the potential advantages of BB8 in intra-datacentre and other short-reach applications. Due to better asymptotic BER performance, BB8 relieves the requirement on maximum laser output power. Potential non-FEC transmission of BB8 down to BER=10^{-12} without extra redundancy reduces latency and complexity of the transceivers. Moreover, it is inherently compatible to the 4-lane QSFP links. BB8 has also a potential in future modulation flexible transceivers as the simplified mapping and de-mapping offer a smooth transition between BB8 and PAM-n. Considering the requirements on spectral efficiency, power efficiency, latency, reliability and flexibility, BB8 is a possible candidate for next generation IM/DD optical interconnections.

Acknowledgements

This work is partly financed by the HOT project of the Danish Innovation Fund. We would like to specially thank Dr. Henning Bülow from Bell Labs, Nokia for the constructive discussion and Finisar U.S. for the support with VCSELs. We also thank Keysight for providing AWG and DSA.

References

[1] E. Agrell et al., "Power-Efficient Modulation Formats in Coherent Transmission Systems," J. Lightwave Technol., Vol. **27**, p. 5115 (2009).

[2] M. Karlsson et al., "Spectrally Efficient Four-Dimensional Modulation," Proc. OFC, OTu2C.1, Los Angeles (2012).

[3] David S. Millar, et al., "High-dimensional modulation for coherent optical communications systems," Opt. Express, Vol 22, p. 8798 (2014).

[4] J. K. Fischer et al., "Bandwidth-Variable Transceivers based on Four-Dimensional Modulation Formats," J. Lightwave Technol., Vol 32, p. 2886 (2014).

[5] H. Buelow et al., "Experimental Performance of 4D Optimized Constellation Alternatives for PM-8QAM and PM-16QAM," Proc. OFC, M2A.6, San Francisco (2014).

[6] X. Lu et al., "8-dimensional Lattice Optimized Formats in 25-GBaud/s VCSEL based IM/DD Optical Interconnections" Proc. ACP, AS4D.3, Hong Kong (2015).

[7] IEEE Standard for Ethernet - Amendment 3: Physical Layer Specifications and Management Parameters for 40 Gb/s and 100 Gb/s Operation over Fiber Optic Cables," in IEEE Std 802.3bm-2015, March 27 2015

[8] "100G SR4 & RS (528, 514, 7, 10) FEC," IEEE 802.3, September 2012. [Online]. Available: http://www.ieee802.org/3/bm/public/sep12/petrilla_02a_0912_optx.pdf. [Accessed 06 March 2016].

Paper 5: 30 Gbps bottom-emitting 1060 nm VCSEL

Tatarczak, A.; Zheng, Y.; Rodes, G.A.; Estaran, J.; Lin, Chin- Han; Barve, A.V.; Honore, R.; Larsen, N.; Coldren, L.A.; Tafur Monroy, I., "30 Gbps bottom-emitting 1060 nm VCSEL," *Optical Communication (ECOC), 2014 European Conference on*, pp. 1, 3, September 2014.

30 Gbps Bottom-Emitting 1060 nm VCSEL

A. Tatarczak[(1)], Y. Zheng[(2)], G. A. Rodes[(1)], J. Estaran[(1)], Chin-Han Lin[(2)], A. V. Barve[(2)], R. Honoré[(1)], N. Larsen[(1)], L. A. Coldren[(2)], I. Tafur Monroy[(1)]

[(1)] DTU Fotonik, Department of Photonics Engineering, Technical University of Denmark, DK2800 Kgs. Lyngby, Denmark, atat@fotonik.dtu.dk
[(2)] Departments of Electrical and Computer Engineering and Materials, University of California, Santa Barbara, CA 93106, USA

Abstract *1060 nm VCSEL-based data transmission over 50 m OM3 MMF at 30 Gbit/s is experimentally demonstrated. A highly-strained bottom-emitting QW VCSEL with p-type modulation doping is used with 3.77 mA bias and 0.55 V data amplitude.*

Introduction

Vertical cavity surface emitting lasers (VCSELs) have long been recognized as key components for optical interconnects due to their small size, high speed and low power consumption. The most common operating wavelength for VCSELs used for data transmission, using multimode fibers (MMF), is 850 nm. Other VCSELs wavelengths explored are 980 nm, 1010 nm, 1060 nm, 1090 nm and 1310 nm. Moving to higher wavelengths allows taking advantage of e.g. lower fiber attenuation.

VCSELs operating in the wavelength region around 1060 nm are particularly attractive due to very high energy efficiency[1,2] and good reliability[3]. An interesting feature of the presented 1060 nm VCSEL is the possibility of emitting the light through the bottom of the VCSEL rather than through top as it is usually done[4]. This offers significant benefits in terms of optical coupling, packaging and heat management, since the wirebonding can be placed opposite the optical aperture[5]. As previously mentioned, the 1060 nm wavelength region has the advantage over 850 nm region in terms of lower fiber attenuation (1.5 dB/km@1060 nm compared to 3.5 dB/km @850 nm), lower power consumption (threshold currents below 1 mA) and of existence of high sensitivity indium-gallium-arsenide (InGaAs) photodiodes. Unfortunately, the most common multi-mode fibers OM3 and OM4 have higher modal dispersion at 1060 nm than at 850 nm; a factor that makes high-speed transmission challenging. Even so, in this paper we present the FEC-conformed performance over 50 m of OM3 multimode fiber.

A transmission over 200 m OM3 MMF has been recently reported using a top emitting 1060 nm VCSEL operating at 25 Gbaud[4]. In this contribution we present a 30 Gbps transmission over 50 m of OM3 MMF. This result is realized with a bottom-emitting 1060 nm VCSEL using only 3.77 mA bias and 0.55 V peak-to-peak data amplitude.

1060 nm VCSEL design

The employed light source is a bottom emitting, highly-strained 1060 nm QW VCSEL with p-type modulation doping. It has previously been presented and described in the referenced work[1]. Fig. 1 shows the schematic diagram of the device.

The VCSEL is grown on a semi-insulating GaAs substrate using molecular beam epitaxy (MBE). The bottom mirror consists of GaAs/AlAs and Si doped GaAs. The top mirror consists of GaAs/AlGaAs. The active region is surrounded by an asymmetric $Al_{0.3}Ga_{0.7}As$ separate

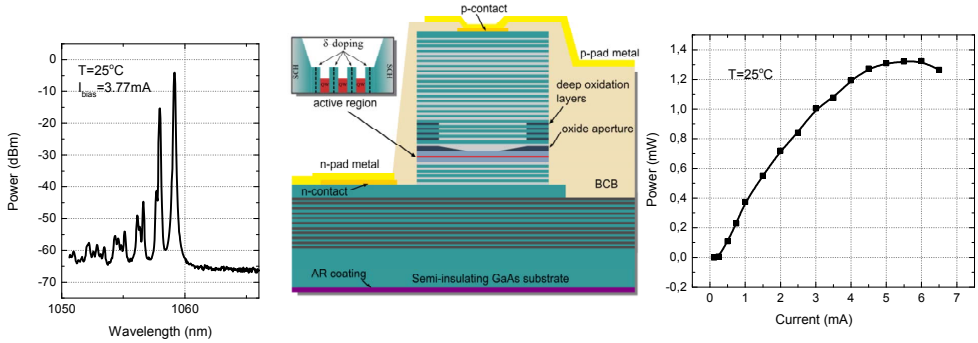

Fig. 1: Optical spectrum; VCSEL structure[1]; Power versus current curve.

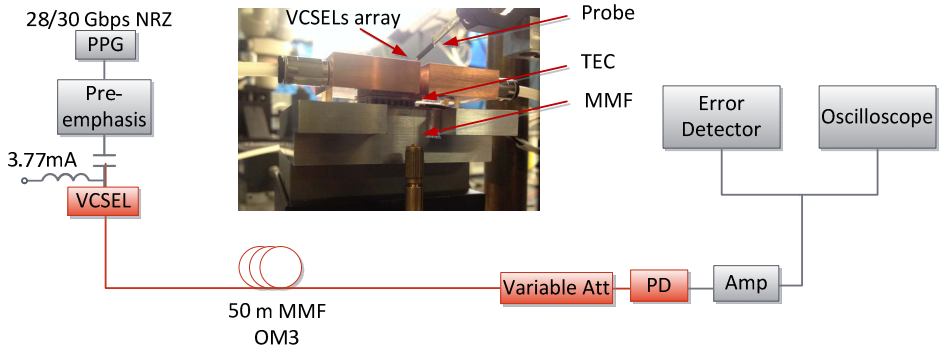

Fig. 2: Experimental setup for high speed transmission with 1060 nm VCSEL.

confinement heterostructure (SCH) that is parabolically graded down to GaAs spacers. Three 8 nm thick highly-strained $In_{0.3}Ga_{0.7}As$ quantum wells (QWs) are separated by 8 nm GaAs barriers. Growth is stopped halfway into the barrier and the surface is δ-doped with carbon using a carbon tetrabromide (CBr_4) precursor. The high differential gain of the 1060 nm laser comes at the price of increasing the nonlinear gain compression. Modulation p-type doping was used to suppress nonlinear gain compression which resulted in increasing the K-factor compared to stained QWs alone.

Fig. 1 shows the power versus current curve measured at T=25°C for the VCSEL used in the transmission experiment. A very low threshold current of 0.15 mA is observed. The corresponding optical spectrum measured at a bias current of 3.77 mA is presented in an inset of Fig.1. Further information on the presented 1060 nm VCSEL design are described in referenced work[1] and the details on analogous device design at 980 nm is presented in the Chapter 7 of 'VCSELs'[6].

Experimental setup

Fig. 2 shows the setup used in the transmission experiment. Electrical pseudo-random binary (PRBS 2^{15}-1) data signals at 28 Gbps (0.682 V peak-peak) or 30 Gbps (0.548 V peak-to-peak) generated by a pulse pattern generator (PPG) is combined with a 3.77 mA bias current in a bias-Tee and applied to the VCSEL using a 40 GHz electrical probe. The temperature is stabilized at 25°C using a temperature controller. The modulation format used is non-return-to-zero (NRZ). In the transmitter the 1 post/1 pre-cursor pre-emphasis configuration is used, as shown in Fig. 3. The pre-emphasis parameters (Cursor 1, 2 and Vpp in inset Table in Fig. 3) are optimized for the transmission scenario and the same settings are used for measuring the B2B case. The light from the VCSEL is coupled into a 50 m OM3 compliant multimode 50 µm core diameter fiber. Fiber launch power is 0.7 dBm and the attenuation of the used 50 m fiber link is 0.9 dB. The optical signal is received by a VI Systems photodiode with a wavelength range of 900-1350 nm and a 30 GHz 3-dB bandwidth. The

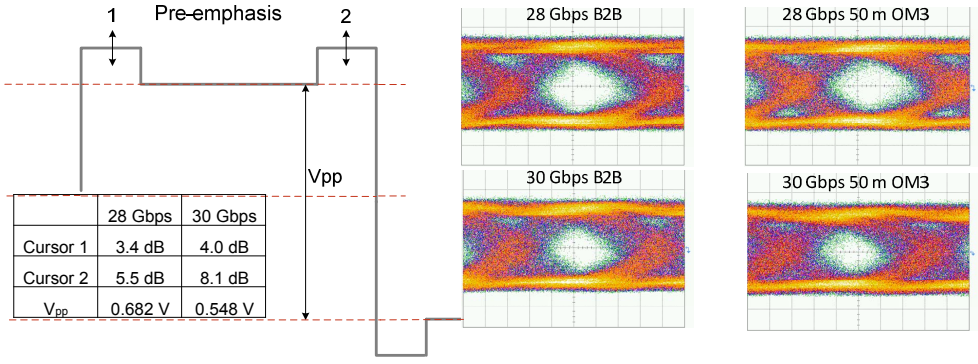

	28 Gbps	30 Gbps
Cursor 1	3.4 dB	4.0 dB
Cursor 2	5.5 dB	8.1 dB
V_{pp}	0.682 V	0.548 V

Fig. 3: Pre-emphasis module settings; Eye diagrams for B2B and transmission over 50 m OM3 MMF at 28 Gbps and 30 Gbps.

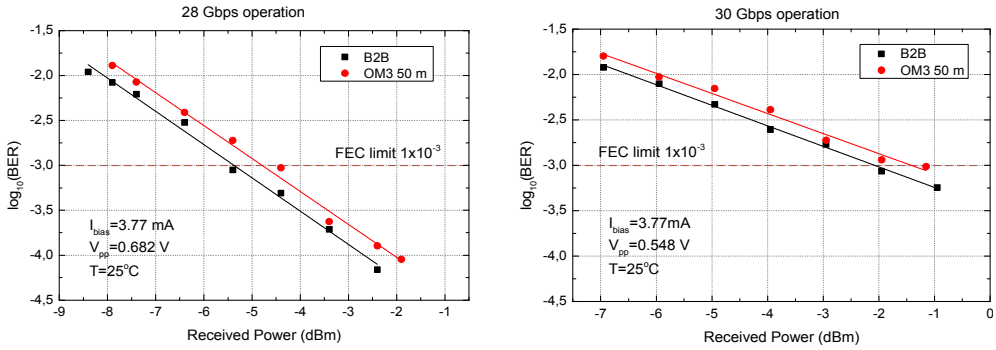

Fig. 4: Bit error rate curves for B2B and Transmission at 28 Gbps and 30 Gbps with 1060 nm VCSEL.

received signal is then amplified to 1 V peak-to-peak and analyzed in real time by an error detector.

Results and Discussions

Fig. 3 shows the measured eye diagrams and Fig. 4 bit error ratio (BER) as a function of the received optical power back-to-back (B2B) and after 50 m MMF transmission for the two considered bit rates. Receiver sensitivity at the 7%-overhead forward error correction (FEC) limit of $1x10^{-3}$ for B2B is -5.4 dBm at 28 Gbps and -2.05 dBm at 30 Gbps. In both cases a penalty of 0.8 dB is observed after fiber transmission.

The optimal setting of pre-emphasis (Fig. 3) improves the transmission BER by 1 order of magnitude allowing BER to be below the FEC limit.

Further work on pre-emphasis is required to maximize the achievable distance. Moreover, the transmission reach can be imcreased by employing OM4 MMF or fibers designed and optimized for 1060 nm range. The 1060 nm VCSEL is proven to be a potential candidate for the optical interconnects which use the benefits of direct intensity modulation and direct detection. The advantage of 1060 nm VCSELs for interconnect links include the ability to balance energy efficiency and reliability.

Conclusions

A high speed 28 Gbps and 30 Gbps transmission employing 1060 nm bottom-emitting VCSEL has been demonstrated with transmission over 50 m of OM3 MMF resulting in a bit rate-distance product of 1.5 Tbpsxm. In the reported experiment, the bias of only 3.77 mA and 0.55 V peak-to-peak data amplitude confirms energy efficiency of the VCSEL based system. The optimized pre-emphasis module at the transmitter allows a FEC-conformed BER values to be achieved.

Our reported results have encouraging prospects in relation to bottom emitting devices for packaging and heat management when incorporating these light sources into modules for interconnects and short range links.

Acknowledgements

We would like to acknowledge VI Systems Germany for supporting this work with the VIS Photoreceiver.

References

[1] Y. Zheng et al., "P-type δ-doping of highly-strained VCSELs for 25 Gbps operation," Photonics Conference (IPC), 2012 IEEE, pp.131,132, 23-27 Sept. (2012).

[2] T. Suzuki et al., "Reliability study of 1060nm 25Gbps VCSEL in terms of high speed modulation," Proc. SPIE 8276, Vertical-Cavity Surface-Emitting Lasers XVI, 827604 Feb. (2012).

[3] S. Imai et al., "Recorded Low Power Dissipation in Highly Reliable 1060-nm VCSELs for "Green" Optical Interconnection," Selected Topics in Quantum Electronics, IEEE Journal of, vol. **17**, no. 6, pp. 1614 - 1620 (2011).

[4] S. K. Pavan et al., "50Gbit/s PAM-4 MMF Transmission Using 1060nm VCSELs with Reach beyond 200m," Proc. OFC, W1F.5, San Francisco (2014).

[5] M. Johnson et al., "In-Phase Bottom-Emitting Vertical Cavity Laser Array," in CLEO: 2013, OSA Technical Digest (online) (Optical Society of America, 2013), paper CF2F.2.F. (2013).

[6] Y. C. Chang, L. A. Coldren, *Design and Performance of High-Speed VCSELs*, In: R. Michalzik *VCSELs*, Springer Series in Optical Sciences, Vol. **166**, Berlin, (2013).

Paper 6: 100G WDM Transmission over 100 meter Multimode Fiber

B. Cimoli, J. Estaran, G. A. Rodes, A. Tatarczak, J. J. Vegas Olmos, and I. Tafur Monroy, "100G WDM Transmission over 100 meter Multimode Fiber," in *Asia Communications and Photonics Conference 2015*, OSA Technical Digest, paper ASu2A.89, 2015.

100G WDM Transmission over 100 meter Multimode Fiber

B. Cimoli, J. Estaran, G. Arturo Rodes, A. Tatarczak, J. J. Vegas Olmos, and I. Tafur Monroy
(1) Technical University of Denmark, Department of Photonics Engineering, Ørsted Plads, Building 343, Kgs. Lyngby, 2800, Denmark, idtm@fotonik.dtu.dk

Abstract: We present a comparative performance analysis for wavelength-grid selection in WDM short-range multimode-fibers. We study 100Gbps links over OM2, OM3 and OM4 fibers and show it is feasible to reach over 100 m transmission distances.

1. Introduction

Cisco analysis forecasts that as much as 76% of the traffic increase over the next 4 years will remain within data centers [1], where currently more than 80% of the existing data links are shorter than 100m [2]. In order to tackle the upcoming need for high capacity in data center links, 100G standards have already been made available and a task force is finalizing the 400G standards. 100GBASE-SR10 and 100GBASE-SR4 standards propose parallel 10-lanes of 10G and 4-lanes of 25G links using 850 nm vertical-cavity surface-emitting lasers (VCSELs) and multimode fibers (MMF) technologies [3]. In this paper, we study links that migrate from the standard multiple-fiber-lane approach to a single-fiber-lane link by employing wavelength division multiplexing (WDM) of 4x25G channels.

The main benefit of using WDM is the reduction of the number of fibers per link while keeping the same capacity and reducing footprint [4]. As to reported experimental work, a total capacity of 10 Gbps over 100 m and 20 Gbps back-to-back transmission was reported by Hewlett-Packard Laboratories and Agilent, respectively [5,6]. Considering that both cost and simplicity are mandatory for such WDM MMF links, it is relevant to study which wavelength grid in combination with the OM fiber types fulfills both requirements on capacity, reach and simplicity. Our study shows that WDM data links over 100 m of MMF is achievable with capacity of 100G even with OM2 fiber types for properly selected WDM grids.

2. WDM short-wavelength over multimode-fiber data link

Figure 1 depicts the generic multimode WDM transmission link for which we perform a comparative performance analysis. Three WDM grids of four wavelengths, which cover the entire short-wave band, are considered in this paper. The interchannel spectral separation is fixed to 30 nm according to the standard for Coarse WDM (CWDM): ITU_T Rec. G.694.2 Appendix I. The modal bandwidth B_m of the fiber is one of the key limiting factors in transmission over MMF [7]. Modal bandwidth stems from the modal dispersion, which depends significantly on the nominal wavelength of the transmitted signal.

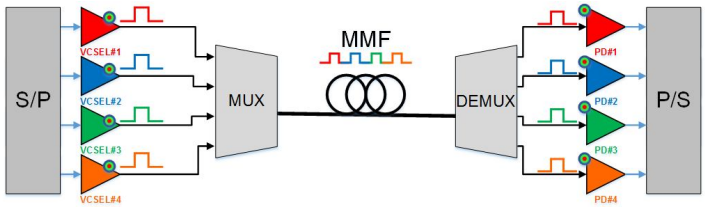

Fig 1: Schematic diagram of 100G WDM data transmission over MMF. PD: Photodiode.

3. Computer simulation of data transmission performance

Computer simulations were performed using the commercially available software Optsim™ version 5.2 of Rsoft. The VCSEL modules at the transmitter side adopt parameters from reported realized devices as follows. The 850 nm and 880 nm are based on [8], the 910 nm, 940 nm, 970 nm and 1000 nm on [9], the 1030 nm and 1060 nm on [10], and the 1090 nm and 1120 nm are based on [11]. In all cases considered, the MUX/DEMUX has a 3-dB bandwidth of 20 nm and a minimum band isolation of –14 dB. For comparison reasons we use three types of fibers: OM4, OM3 and OM2. As we present in Table 1, OM4 and OM3 fibers grant the best performance in terms of modal bandwidth for the standard wavelength 850 nm; instead OM2 fibers are not optimized for 850 nm and their lowest dispersion wavelength is close to 1060 nm [12].

At the receiver side, simple PIN photodiodes (PDs) are used and variable power attenuators control the received optical power level. We assume a maximum received optical power tolerated by the PDs of 3 dBm.

Table 1: WDM grids and their modal bandwidth

WDM Grid	Wavelength (nm)		OM4 B_m (MHz·km)	OM3 B_m (MHz·km)	OM2 B_m (MHz·km)
A	CH#1	850	4500	2000	700
	CH#2	880	3300	1750	800
	CH#3	910	2325	1500	870
	CH#4	940	2000	1250	1030
B	CH#1	970	1625	1100	1160
	CH#2	1000	1350	875	1345
	CH#3	1030	1200	780	1530
	CH#4	1060	1000	700	1625
C	CH#1	1030	1200	780	1530
	CH#2	1060	1000	700	1625
	CH#3	1090	750	625	1630
	CH#4	1120	625	575	1570

Electrical outputs of the PDs are amplified before being processed by the bit error rate tester (BERT) for error counting.

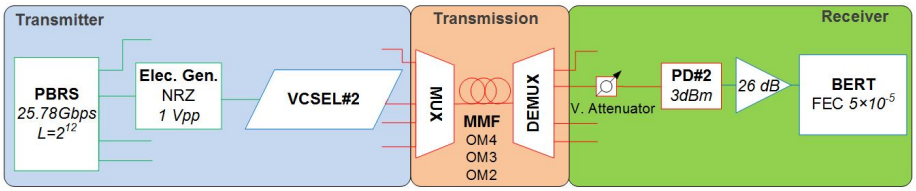

Fig 2: Generic setup for experimental channel testing.

4. Simulation results

Simulation results are presented as BER curves: *Log(-Log(BER))* versus the received optical power by the PDs. The BER are calculated through the overlap integration of the noise distributions per symbol, which were estimated with Monte Carlo (MC) technique of OptSim™. The forward error correction (FEC) threshold adopted is $5x10^{-5}$ [13], and the receiver BER operating limit is set to 10^{-9}.

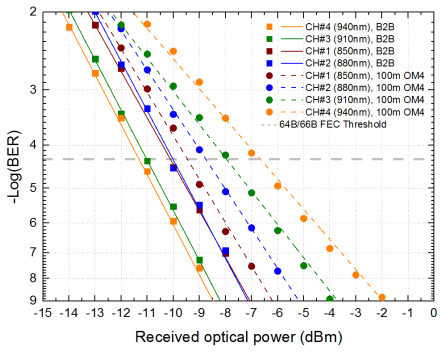

Fig 3: WDM grid A BER curves

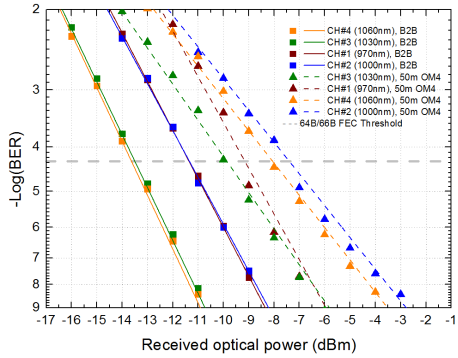

Fig 4: WDM grid B BER curves

Fig 3 show that transmission over 100 m of OM4 with BER<10^{-9} is achievable for all the channels of the WDM grid A. CH#4 (940 nm) has the worst performance due to its higher modal dispersion. Results shown in Fig 4 confirm that transmission over 50 m of OM4 with BER<10^{-9} is still achievable in the WDM grid B, whose wavelengths are located above 100 nm higher than the standard 850 nm wavelengths.

BER curves presented in Fig 5 show that data transmission over 100 m of OM2 is achievable for all the channels of WDM grid C. CH#1 (1030 nm) has the narrowest modal bandwidth of 1530 MHz·km, however CH#3 and CH#4 have worse performance because of the narrower bandwidths of the employed VCSELs [10,11]. BER floors appear when the

modal bandwidth, which decreases with the distance, is too narrow. Then the signal is deteriorated resulting in considerable eye aperture closure.

The curves in Fig 6 represent the power penalty introduced by the MMF, in particular by the modal dispersion, at the FEC threshold; the red line depicts the maximum power tolerated by the PDs (3 dBm). In Fig 6 we consider the worst channel for each grid, hence the one with the highest modal dispersion for the tested types of MMF.

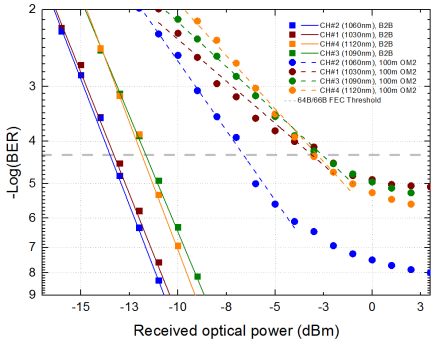

Fig 5: WDM grid A BER curves

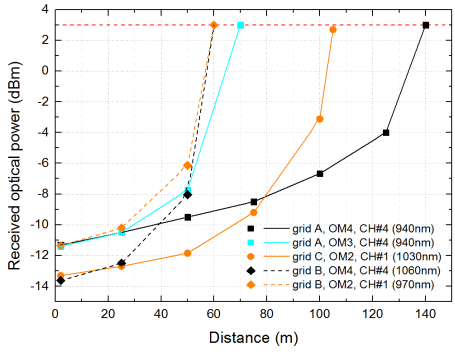

Fig 6: WDM grid A BER curves

Table 2 reports the maximum fiber length, which grants the FEC BER threshold performance over OM4, OM3 or OM2 at 25.78 Gbps per channel for each WDM grid. Grid A and C grant 100 m transmissions over OM4 and OM2 respectively.

Table 2: Reach limitations of the three WDM grids

Grid	Fiber	Worst channel	FEC max reach (*m*)	BER<10^{-9} max reach (*m*)
A	OM4	CH#4 (*940nm*)	140	115
	OM3	CH#4 (*940nm*)	70	50
B	OM4	CH#4 (*1060nm*)	60	50
	OM2	CH#1 (*970nm*)	60	50
C	OM2	CH#1 (*1030nm*)	105	80

5. Conclusion

Computer simulations perform 100G transmissions over a single MMF data link using short-wavelength WDM. WDM grids ranging from 850 nm to 1120 nm and using OM2,3,4 MMF fibers are tested in order to study the limitations due to modal dispersion on the achievable transmission distance. Simulation results confirm that grid A, which is close to 850 nm is a valid solution for OM4 and OM3 data center links. Moreover, WDM grid C allows transmission over 100 m of OM2. This result rehabilitates existing OM2 links and 1100 nm VCSELs technologies for 100G data center solutions.

6. References

[1] Cisco, "Cisco Global Cloud Index : Forecast and Methodology , 2012 – 2017," *white paper*, 2013. [Online]. Available: http://www.cisco.com/c/en/us/solutions/collateral/service-provider/global-cloud-index-gci/Cloud_Index_White_Paper.pdf.

[2] J. Jewell, P. Kolesar, J. King, C. Cole, R. J. Lingle, and J. Petrilla, "MMF Objective for 400GbE," no. November, 2013.

[3] C. Cole, "Beyond 100G client optics," *IEEE Commun. Mag.*, vol. 50, 2012.

[4] J. Manuel and E. Tolosa, "Long-Term Evolution of Optical Avionic Networks," DTU, 2012.

[5] L. B. Aronson, B. E. Lemoff, L. A. Buckman, and D. W. Dolfi, "Low-cost multimode WDM for local area networks up to 10 Gb/s," *IEEE Photonics Technol. Lett.*, vol. 10, pp. 1489–1491, 1998.

[6] B. E. Lemoff, M. E. Ali, G. Panotopoulos, E. de Groot, G. M. Flower, G. H. Rankin, A. J. Schmit, K. D. Djordjev, M. R. T. Tan, A. Tandon, W. Gong, R. P. Tella, B. Law, L. K. Chia, and D. W. Dolfi, "Demonstration of a compact low-power 250-Gb/s parallel-WDM optical interconnect," *IEEE Photonics Technol. Lett.*, vol. 17, pp. 220–222, 2005.

[7] P. Agrawal Govind, *Fiber-Optic communication systems*, 3rd ed. Wiley India Pvt Ltd, 2007.

[8] VIS systems, "Datasheet: Up to 40 Gbit/s VCSEL Multi-Mode Fiber-Coupled Module (850 nm)," 2012.

[9] A. Mutig, J. a. Lott, S. a. Blokhin, P. Wolf, P. Moser, W. Hofmann, A. M. Nadtochiy, A. Payusov, and D. Bimberg, "Highly temperature-stable modulation characteristics of multioxide-aperture high-speed 980 nm vertical cavity surface emitting lasers," *Appl. Phys. Lett.*, vol. 97, 2010.

[10] T. Suzuki, M. Funabashi, H. Shimizu, K. Nagashima, S. Kamiya, and A. Kasukawa, "1060nm 28-Gbps VCSEL developed at Furukawa," vol. 9001, p. 900104, Feb. 2014.

[11] T. Anan, N. Suzuki, K. Yashiki, K. Fukatsu, H. Hatakeyama, T. Akagawa, K. Tokutome, and M. Tsuji, "High-speed 1.1-μm-range InGaAs VCSELs," *OFC/NFOEC 2008 - 2008 Conf. Opt. Fiber Commun. Fiber Opt. Eng. Conf.*, pp. 1–3, Feb. 2008.

[12] H. Nasu, Y. Ishikawa, Y. Nekado, M. Yoshihara, and A. Izawa, "1060-nm VCSEL-based parallel-optical modules for short link application," *OSA / OFC/NFOEC*, vol. 1, pp. 3–5, 2010.

[13] P. Anslow, "BER and FER for 100GBASE-SR4," *IEEE P802. 3bm™ MMF ad hoc Meet.*, no. November, pp. 1–13, 2012.

Paper 7: OAM - enhanced Transmission for Multimode Short-Range Links

Tatarczak, A.; Usuga Castaneda, M.; Tafur Monroy, I., "OAM - enhanced Transmission for Multimode Short-Range Links," Proc. SPIE 9390, Next-Generation Optical Networks for Data Centers and Short-Reach Links II, 93900E, March 2015.

OAM-enhanced transmission for multimode short-range links

Anna Tatarczak, Mario A. Usuga, and Idelfonso Tafur Monroy

DTU Fotonik, Technical University of Denmark, 2800 Kgs. Lyngby, Denmark

ABSTRACT

We propose, experimentally demonstrate, and evaluate the performance of a multimode (MM) transmission fiber data link which is based on orbital angular momentum (OAM) modes. The proposed scheme uses OAM modes to increase capacity or reach without recurring to mode division multiplexing (MDM) or special fibers: we first excite an OAM mode and couple it to a 50 m, 100 m, 200 m and 400 m MM fibers. We compare three OAM modes and a conventional optical multimode under the same launch and received optical power conditions. The proposed OAM based solution is a promising candidate for the data centers interconnects and short range links that employ the existing multimode fiber infrastructure.

Keywords: Optical Communication, Data Center Interconnects, OAM

1. INTRODUCTION

Vertical cavity surface emitting lasers (VCSELs) are the dominant optical sources in the data center's interconnects due to their low power consumption and a small footprint. In particular, 850 nm VCSELs together with OM3 multi mode fiber (MMF) or OM4 MMF are the base of the short-range links, widely employed in the existing data center infrastructures. The main restraint in this type of links is the intermodal dispersion, which limits the transmission distance to a few hundred meters for bitrates of 10 Gbps. IEEE 802.3ae 10G Ethernet standard specifies 300 m as the multimode span length for 10 Gbps transmission and IEEE 802.3ba 40G/100G Ethernet gives 75 m as the maximum transmission length required at 40 Gbps. Due to the increasing lengths of connections between buildings in data centers there is a need for longer reach multimode interconnects supporting high bit-rates.[1] Several ways of achieving further distances with 850 nm VCSELs have been presented in the literature. First approach involves mode filtering of a multi-mode VCSEL. This results in a VCSEL that emits single or quasi-single fundamental transverse mode with a high side-mode suppression ratio of e.g. 16 dB,[2] 22 dB,[3] or 30 dB.[4] The mode-filtering is performed within the VCSEL structure. Error-free transmission with the single mode 850 nm VCSEL is achieved over 1 km OM4 MMF at 25 Gbps,[5] over 1.1 km OM4 MMF at 20 Gbps,[6] over 600 m OM3+ MMF at 25 Gbps[7] and over 50 m OM3+ MMF at 40 Gbps. A second approach is to couple the light from a multimode VCSEL to a standard single mode fiber (SSMF). Adding a mode filter to remove LP_{11} mode allows transmission distance of 1 km SSMF at 10 Gbps.[8] The third approach involves using special 850 nm optimized singlemode fiber, e.g. photonic crystal fiber (PCF). The core region of PCF is surrounded by multiple air holes, thus assuring single mode operation. Transmission over 3 km PCF has been presented at 10 Gbps.[9] For the multimode VCSELs over multimode fiber, error free transmission over 200 m has been achieved at 25 Gbps.[10] All these approaches require substantial modifications of the existing data center infrastructure: replacement of the multimode sources in the first approach, or the fibers in the second and third approaches. Therefore, an alternative solution that employs the existing fibers and VCSELs is of interest.

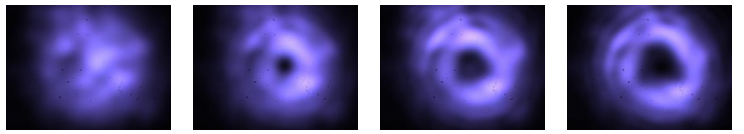

Figure 1. Orbital angular momentum (OAM) modes captured with the camera after spatial light modulator (SLM): M0 (left), M1, M2 and M3 (right); M0 is a standard optical mode.

Next-Generation Optical Networks for Data Centers and Short-Reach Links II, edited by Atul K. Srivastava,
Proc. of SPIE Vol. 9390, 93900E · © 2015 SPIE · CCC code: 0277-786X/15/$18 · doi: 10.1117/12.2079795

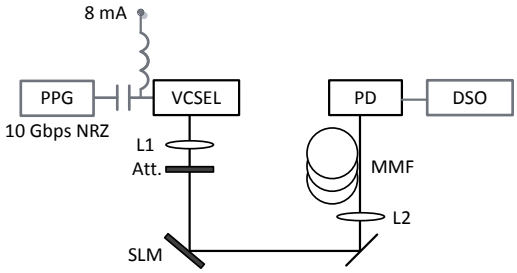

Figure 2. Experimental setup for the transmission of the orbital angular momentum (OAM) modes over multi mode fiber (MMF); Signal from pulse pattern generator (PPG) directly modulates vertical cavity surface-emitting laser (VCSEL) biased at 8 mA; the VCSEL beam is collimated at lens L1 and in free-space passes through the attenuator to the spatial light modulator (SLM), where the beam is shaped to the OAM mode; the shaped beam is coupled to the 3 m OM3 MMF patchcord; Lens L2 is used for the coupling; The signal is then transmitted through the multi mode fiber (MMF): 3 m back to back (B2B), 50 m OM3, 50 m OM4, 100 m OM3, 200 m OM3, 400 m OM3, 400 m OM4 and 400 m customized OM4 by Draka; the signal is then received with photodiode (PD) with the inbuilt transimpedance amplifier (TIA) and the data is stored at digital storage oscilloscope (DSO).

In this paper we propose an approach to increase the obtainable transmission distance for the multi-mode sources over multi-mode fibers. Shaping a multimode VCSEL beam as an orbital angular momentum (OAM) mode (Fig. 1) enabled achieving performance below forward error correction (FEC) threshold during transmissions at 10 Gbps over 400 m MMF. We provide a comparison between transmission of OAM modes M1, M2, and M3 and standard optical mode M0. The modes are transmitted over: 50 m OM3, 50 m OM4, 100 m OM3, 200 m OM3, 400 m OM3, 400 m OM3, and 400 m Draka OM4. The last mentioned fiber is a Max-CAP-OM4 fiber designed by Prysmian Group Draka. It will be further referred to as Draka OM4 fiber.

2. SETUP

The experimental setup is shown in Fig. 2. The 850 nm multimode commercially available VCSEL is biased at 8 mA and directly modulated with 10 Gbps or 11 Gbps pseudo-random bit sequence (PRBS). The sequence length is $2^{15} - 1$ and the amplitude is 800 Vpp. The LIV curves and optical spectrum of the VCSEL used are presented in Fig. 3 and Fig. 4, respectively. The modulated optical beam from the pigtailed VCSEL is collimated and passed through the variable attenuator to the spatial light modulator (SLM) in the free-space part of the setup. The optical power level is controlled by the variable attenuator. The SLM is used to shape the multimode beam to the OAM mode. We verify the transmission performance with OAM modes M1 to M3 and a conventional multimode M0. For M0, SLM behaves as a mirror. The 4 modes under investigation are captured with the camera after SLM and presented in Fig. 1. The full length of the free-space link is 1.5 m. At the end of the free-space link the beam is coupled into the 1 m long MMF OM3 patchcord. The coupling after free-space is aligned to obtain maximum output power and is readjusted for each OAM mode.

The OM3 patchcord used for coupling is connected to the multimode fiber spool via the fiber connector. Several MMFs are tested: 50 m OM3, 50 m OM4, 100 m OM3, 200 m OM3, 400 m OM3, 400 m OM4 and 400 m OM4 special fiber by Draka. The loss in 50 m, 100 m and 200 m is below 0.5 dB. For 400 m spools the measured loss is: 0.98 dB for OM3, 0.95 for OM4, and 0.97 dB for Draka OM4. After transmission the signal is received by the 850 nm commercially available photodiode (PD) with 25 GHz bandwidth. The signal is then stored at digital storage oscilloscope (DSO) with 14 GHz bandwidth. For each BER point 10^7 symbols are saved and errors are counted. No additional equalization is used.

The optical system frequency response is characterized with the vector network analyzer (VNA) before the transmission is performed. For the S_{21} measurement the output of pulse pattern generator (PPG) is replaced

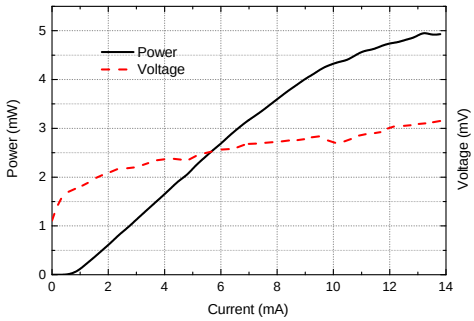

Figure 3. Static characteristics of the VCSEL: Power versus current and voltage versus current (LIV curves).

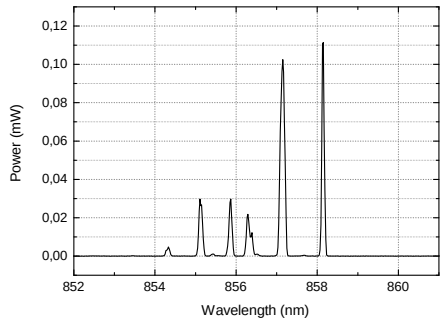

Figure 4. Optical spectrum of the VCSEL captured after 400 m of MMF; two major modes are around 858 nm.

with the VNA output and input to DSO is instead received by the VNA input. The optical path, from VCSEL to PD included, is kept the same.

3. RESULTS

We compare a transmission performance for different OAM modes (M1, M2, M3) and for a conventional multimode M0. Firstly, the modes M0 – M2 are transmitted at 11 Gbps over 100 m OM3 and 200 m OM3. Secondly, the modes M0 – M2 are transmitted over two 50 m long MMFs, OM3 and OM4, at 11 Gbps. Finally, modes M0 – M3 are transmitted over 3 types of 400 m MMF. The performance is compared in terms of the bit-error-ratio (BER) relative to the received average power measured before PD. Transmission over 1 m of OM3 MMF is referred to as back to back (B2B) transmission. Additionally, the S_{21} is measured for each optical system.

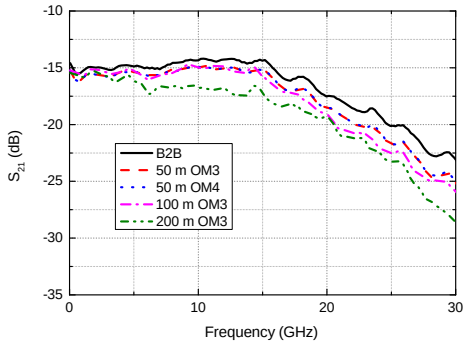

Figure 5. S_{21} measured for the optical system with back to back (B2B) and four different multi mode fiber (MMF): 50 m OM3, 50 m OM4, 100 m OM3 and 200 m OM3; All curves are measured with a conventional multimode M0.

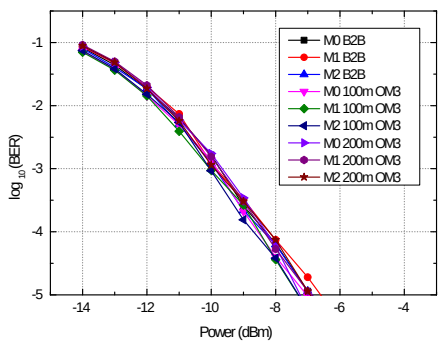

Figure 6. BER versus received optical power (ROP) measured for back to back (B2B), 100 m OM3 and 200 m OM3 for 2 different orbital angular momentum (OAM) modes: M1 and M2 and a conventional multimode M0.

3.1 Transmission over B2B, 100 m OM3, and 200 m OM3

Fig. 5 presents S_{21} measured for the optical system with back to back (B2B), 50 m MMF, 100 m and 200 m. All of the S_{21} are measured for a conventional multimode M0. 3-dB bandwidth of the system ranges from 16 GHz for 200 m to 22 GHz for B2B. The measured analog bandwidths for all presented cases are sufficient for the 11 Gbps transmission. The bit error rate (BER) curves measured at 11 Gbps for B2B and all the fibers are presented in Fig. 6. No penalty is observed, neither for different fiber lengths nor for the different modes. The power measurement error due to the procedure is equal to -/+ 0.25 dB. Receiver sensitivity at BER of 10^{-3} is equal to -10 dBm.

3.2 OM3 vs. OM4

In Fig. 7 the comparison between 11 Gbps transmission over 50 m links, OM3 and OM4 MMF, is presented. As apparent from Fig.5, the bandwidth for both fibers is the same. The measured 3-dB bandwidth is 20 GHz for the length under consideration. The sensitivity at BER 10^{-3} for OM4 fiber is up to 0.2 dB better than for OM3. The same is observed for all of the OAM modes. This difference in the sensitivity is within the power measurement error margin. The difference between OM3 and OM4 is expected to be more significant for longer fiber link.

3.3 400 m

A link of 400 m is used to evaluate the transmission performance with the OAM modes. We use three different 400 m long links in which the intermodal dispersion is dominant. S_{21} curves measured for the optical system with each of the three links are shown in Fig. 8. The S_{21} curves are measured with for M0 OAM mode. The 3-dB bandwidth is only 4.9 GHz for MMF OM4 by Draka, 4.8 GHz for MMF OM3 and 4 GHz for 400 m MMF OM4.

The impact of the OAM modes on the S_{21} of the system is presented in Fig. 9. The frequency response is measured for OM4 Draka fiber with OAM modes from M1 to M3 and with the conventional multimode M0. The measured responses are the same for modes M0 and M1, while responses of modes M2 and M3 have ∼2dB less power for frequencies above 15 GHz. For each of the modes the coupling is realigned to reach the highest coupled power. The coupling efficiency is a ratio between the power coupled to the MMF OM3 patchcord and the input power to the lens. Fig. 10 presents the coupling efficiency measured for modes M0 to M3. It shows that there is no difference in coupling efficiency for M0 and M1, however for M2 and M3 the coupling efficiency

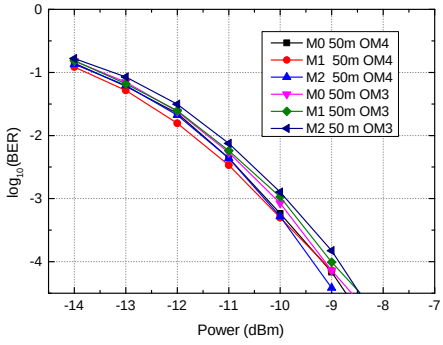

Figure 7. BER versus received optical power (ROP) measured for 2 OAM modes (M1 and M2) and a conventional multimode M0 for two types of 50 m MMF: OM4 and OM3.

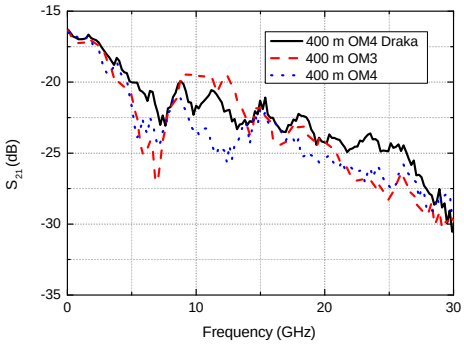

Figure 8. S_{21} measured for the optical system with three 400 m spools: OM3, OM4 and OM4 fiber by Draka; All curves are measured with a conventional M0 mode.

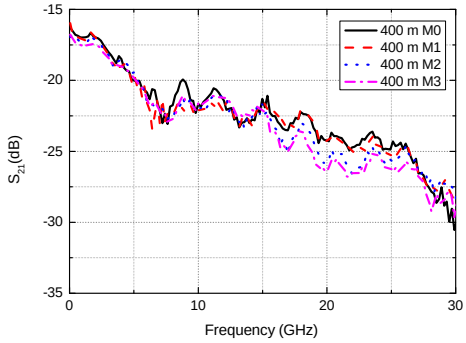

Figure 9. S_{21} measured for the optical system with 400 m OM4 by Draka with 4 OAM modes: M0, M1, M2 and M3.

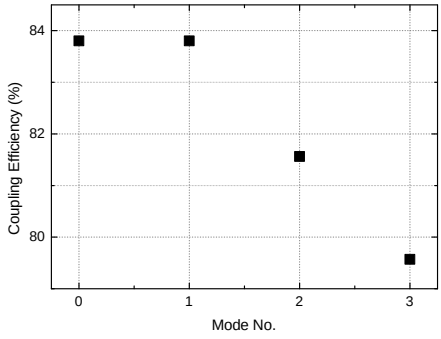

Figure 10. Coupling efficiency measured in the system as $P_{coupled}/P_{IN}$ for 4 modes.

decreases. Higher order modes suffer from larger loss, as the power is distributed outside of the beam center and the coupling is imperfect.

Fig. 11, Fig. 12 and Fig. 13 depict the BER curves measured at 10 Gbps for three 400 m links. For all of the curves the same tendency is observed: the higher the order of OAM mode, the lower amount of errors is counted. During the measurement the coupling from the free-space through the second lens L2 is realigned for each mode to reach the highest coupling efficiency. The BER below FEC threshold is obtained by transmitting the beam shaped in OAM mode. The error floor observed at $log(BER)$ of -1.8 for 400 m OM3 link is moved down to -2.1 with M1 and M2 and down to -2.8 with M3. OM4 fiber has the lowest 3-dB bandwidth out of the three links under consideration, as shown in Fig.8. The error floor for this fiber is measured at $log(BER)$ of -1.3. Using OAM mode M1 allows to move the error floor down to $log(BER)$ of -1.5, M2 to -2.3 and M3 to -3.3. In case of Draka 400 m OM4 fiber, the 3-dB bandwidth is the highest of the three links (Fig.8). Therefore, the error floor

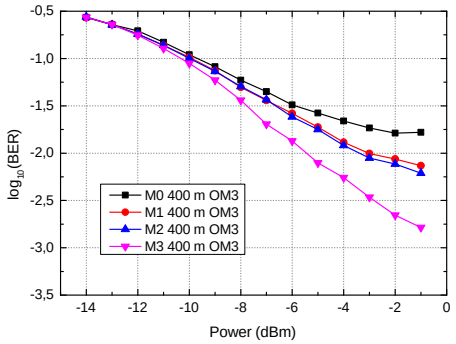

Figure 11. Bit error rate (BER) versus received optical power (ROP) measured at 10 Gbps for 400 m OM3 multi mode fiber (MMF) for 3 OAM modes (M1, M2, and M3) and a conventional multi mode M0.

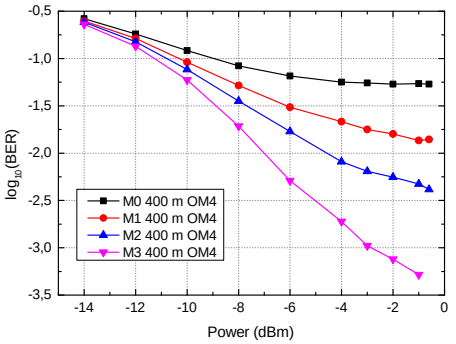

Figure 12. Bit error rate (BER) versus received optical power (ROP) measured at 10 Gbps for 400 m OM4 multi mode fiber (MMF) for 3 OAM modes (M1, M2, and M3) and a conventional multi mode M0.

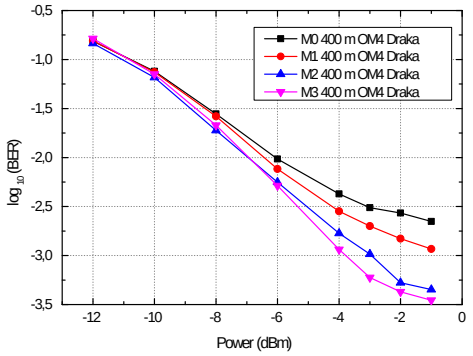

Figure 13. Bit error rate (BER) versus received optical power (ROP) measured at 10 Gbps for 400 m OM4 multi mode fiber (MMF) by Draka for 3 OAM modes (M1, M2, and M3) and a conventional multi mode M0.

for M0 is the lowest, at $log(BER)$ of -2.6. Usage of M3 allows reaching -3.45.

4. DISCUSSION

As shown in Fig. 6, using the OAM modes M1 and M2 over 100 m OM3 and 200 m OM3 results in the same performance in terms of BER as using a conventional multimode M0. The same transmission performance within the tested BER range indicates a potential for simultaneous use of several OAM modes in the future spatial division multiplexing (SDM) systems.

For 400 m transmission, 3-dB system bandwidth becomes a limiting factor, as presented in Fig. 8. The 'dip' in the frequency response occurs due to the interaction between several modes in the fiber. It is the most pronounced for the OM3 fiber and the least for the Draka's OM4 fiber. The 3-dB bandwidth of 4 GHz measured for 400 m OM4 fiber results in the error floor measured at $log(BER)$ of -1.3 for 10 Gbps transmission. Using OAM modes introduces the most significant performance improvement for 400 m OM4 fiber. Using OAM mode M3 allows to reach error floor below FEC threshold, at $log(BER)$ of -3.3. For Draka OM4 fiber, the measured 3-dB bandwidth was 4.9 GHz. It allows for the error floor below $log(BER)$ of -2.6. Using OAM mode M3 enables $log(BER)$ of -3.45. An improvement in the transmission performance while using higher order OAM modes is measured for all 400 m fiber types with the best performance of OAM mode M3 transmitted over Draka OM4 MMF.

5. FUTURE WORK

The presented results provide an interesting solution for improving performance in terms of BER in the multimode transmission scenarios. A further study is required to define the optimal launching and transmission conditions. The next step is to create an all fiber coupled OAM-enhanced transmission, with no free-space link. Secondly, higher order modes M4 – M6 are expected to result in further performance improvement, hence need to be tested. Additionally, checking the behavior of the OAM enhanced transmission with a single mode source should be verified and compared with the presented results.

6. CONCLUSION

In this work we present a novel OAM-enhanced transmission over multi mode fiber (MMF) which can be applied in the short-range optical interconnects. OAM modes M1 and M2 perform the same as conventional multi mode

M0 within the tested BER range for transmission over 50 m OM3, 50 m OM4, 100 m OM3, 200 m OM3. For a further distance of 400 m, the higher order modes perform better than the conventional M0 mode, enabling BER below FEC threshold at 10 Gbps in the system with 3-dB bandwidth of 4 GHz.

REFERENCES

1. C. Lam, H. Liu, B. Koley, X. Zhao, V. Kamalov, and V. Gill, "Fiber optic communication technologies: What's needed for datacenter network operations," *Communications Magazine, IEEE* **48**, pp. 32–39, July 2010.
2. P. Moser, J. Lott, P. Wolf, G. Larisch, H. Li, N. Ledentsov, and D. Bimberg, "56 fJ dissipated energy per bit of oxide-confined 850 nm VCSELs operating at 25 Gbit/s," *Electronics Letters* **48**, pp. 1292–1294, September 2012.
3. P. Wolf, P. Moser, G. Larisch, H. Li, J. Lott, and D. Bimberg, "119 fJ of Dissipated energy per bit for error-free 40 Gbit/s transmission across 50 m of multimode optical fiber using energy efficient 850 nm VCSELs," in *Lasers and Electro-Optics (CLEO), 2013 Conference on*, pp. 1–2, June 2013.
4. F. Mederer, C. Jung, R. Jager, M. Kicherer, R. Michalzik, P. Schnitzer, D. Wiedenmann, and K. Ebeling, "12.5 Gbit/s data rate fiber transmission using single-mode selectively oxidized GaAs VCSELs at λ=850 nm," in *LEOS '99. IEEE Lasers and Electro-Optics Society 1999 12th Annual Meeting*, **2**, pp. 697–698 vol.2, 1999.
5. M. P. Tan, S. Fryslie, J. Lott, N. Ledentsov, D. Bimberg, and K. Choquette, "Error-Free Transmission Over 1-km OM4 Multimode Fiber at 25 Gb/s Using a Single Mode Photonic Crystal Vertical-Cavity Surface-Emitting Laser," *Photonics Technology Letters, IEEE* **25**, pp. 1823–1825, Sept 2013.
6. R. Safaisini, K. Szczerba, E. Haglund, P. Westbergh, J. Gustavsson, A. Larsson, and P. Andrekson, "20 Gbit/s error-free operation of 850 nm oxide-confined VCSELs beyond 1 km of multimode fibre," *Electronics Letters* **48**, pp. 1225–1227, September 2012.
7. P. Moser, J. Lott, P. Wolf, G. Larisch, A. Payusov, N. Ledentsov, and D. Bimberg, "Energy-Efficient Oxide-Confined 850-nm VCSELs for Long-Distance Multimode Fiber Optical Interconnects," *Selected Topics in Quantum Electronics, IEEE Journal of* **19**, pp. 7900406–7900406, March 2013.
8. Z. Tian, C. Chen, and D. Plant, "850-nm VCSEL Transmission Over Standard Single-Mode Fiber Using Fiber Mode Filter," *Photonics Technology Letters, IEEE* **24**, pp. 368–370, March 2012.
9. H. Hasegawa, Y. Oikawa, T. Hirooka, M. Yoshida, and M. Nakazawa, "10 Gb/s transmission over 3 km at 850 nm using single-mode photonic crystal fiber, single-mode VCSEL, and Si-APD," in *Optical Fiber Communication Conference, 2006 and the 2006 National Fiber Optic Engineers Conference. OFC 2006*, pp. 3 pp.–, March 2006.
10. J. Kropp, J. Lott, N. Ledentsov, P. Otruba, C. Knochenhauer, and F. Ellinger, "25 Gb/s transmission at 850 nm on multimode fiber with low cost optical component assemblies," in *Semiconductor Conference Dresden (SCD), 2011*, pp. 1–4, Sept 2011.

Paper 8: Radio-over-Fiber Transmission over 400m MMF

Tatarczak, A.; Lu, X.; Rommel, S.; Rodriguez, S.; Vegas Olmos, J.J.; Monroy, I.T., "Radio-over-Fiber Transmission over 400m MMF," submitted to *JOCN*.

Radio-over-Fiber Transmission over 400m MMF

Anna Tatarczak, Xiaofeng Lu, Simon Rommel, *Student Member, IEEE*,
Sebastian Rodriguez, *Student Member, IEEE*, Juan Jose Vegas Olmos, *Senior Member, IEEE*,
and Idelfonso Tafur Monroy, *Senior Member, IEEE*

***Abstract*—This paper experimentally demonstrates the distribution of radio-over-fiber signals over multimode fiber. We study four types of launches to the MMF and their impact on the RoF system performance. The carrier frequencies of the RoF signal range from 3.7GHz to 10GHz and bitrates up to 1.5Gbps. The selective launch enables higher achievable reach over MMF as compared to the standard launch, hence the fiber's capacity is improved. This approach can be applied in MMF antenna links and combined with free-space optics for easier access to the isolated cell stations. This work supports current developments towards 5G mobile backhaul systems.**

***Index Terms*—Radio frequency photonics, multimode fibers, selective modal launch.**

I. Introduction

THE growth and expansion of wireless networks is sustained thanks to parallel developments in wired transport networks operating underneath; these underlying networks, traditionally based on copper links, have migrated to optical fiber based links over the last years. However, fiber based links to feed antenna sites may not be a viable solution when the operator does not have access to the deployed fiber or the costs of deployment are deemed to be too high. Recently, radio-over-fiber (RoF) systems [1] and free space optics (FSO) [2] have been proposed and successfully demonstrated to provide large bandwidth to antenna sites, smoothly integrating the mobile fronthaul segment with the mobile backhaul segment.

The advantages of using RoF techniques to distribute wireless signals are multifold: it provides a scalable technology that allows seamless integration of the optical access network and the transmitting antenna by providing direct optical baseband to optical radio frequency (RF) up-conversion. The low transmission loss of optical fiber allows for antenna remoting, allowing centralizing wireless carrier generation and signal processing. Photonics is generally of advantage when generating and transmitting spectrally-broad and spectrally-efficient ultra-high capacity data signals. On the other hand, FSO has been proven to be a flexible tool to link short- to mid-range distances. Furthermore, the network planners and operators can skip fiber deployments in the last mile and utilize (largely) license-free RF bandwidth.

A selective modal launch is used to excite a single mode group or a fraction of fiber mode groups. Consequently, the propagation delay between different mode groups is decreased and the dispersion effect mitigated [3]. This approach has been presented with a single mode source and a multimode fiber in multiple works to study perfomance of the linearly polarized (LP) eigen modes of MMF [4]–[7]. The selective modal launch applied to multi mode fiber (MMF) links combined with a multimode vertical cavity surface-emitting laser (VCSEL) light source has been presented in [8]. In this approach the achievable distance is increased by launching a phase modulated beam to the MMF instead of a standard multi mode beam. A Liquid Crystal on Silicon – Spatial Light Modulator (LCOS-SLM) or a phase plate can be used to modulate the phase of the beam [9], [10]. Alternatively, a phase plate has also been proposed to be integrated within a light source, e.g. in the VCSEL structure [11]. The combination of FSO and cost effective MMF with a reach enhanced by a selective modal launch is a candidate for last mile RoF systems [12].

Fig. 1 shows a network scenario where the antenna is fed with the signal either through the MMF or through the combination of FSO and MMF. The selective mode launch can be performed at the cell cabinet or at the end of the FSO link (the phase information is preserved in free space [13]. The MMF links based on 850 nm VCSEL lasers meant for short distances up to 300 m have been demonstrated as a feasible solution for RoF applications [14]. In this work, we present RoF transmission over MMF as well as the potential of the selective launch to increase the length of the link carrying the RoF signal. We provide results for 850 nm VCSEL based intensity modulation/direct detection (IM/DD) links up to 400 m. The antenna link is used to support RoF signal distribution and serves as a range extension structure for mobile fronthaul systems.

We consider three different RoF signal configurations. Firstly, the LTE frequency band of 200 Mbps at 3.7 GHz carrier frequency is tested. Secondly, a bitrate of 1 Gbps is tested at the carrier frequency of 4 GHz. This scenario reveals an interesting property of higher order modes launched into the multimode fiber. With increasing order m of the phase

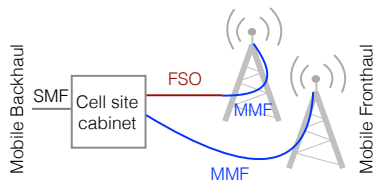

Fig. 1. Scenario of radio over fiber over a) MMF and b) FSO and MMF.

Manuscript received August ??, 2016; revised August ??, 2016; accepted August ??, 2016.

The authors are with the Department of Photonics Engineering, Technical University of Denmark, 2800 Kgs. Lyngby, Denmark. (e-mail: atat@fotonik.dtu.dk)

I. Tafur Monroy is further with ITMO University, St Petersburg, Russia.

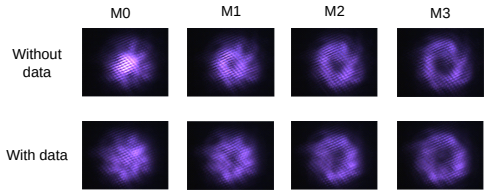

Fig. 2. Modes M0–M3 captured by the camera; continuous wave (CW) is compared with modes carrying 1.5 Gbps data on a 10 GHz carrier.

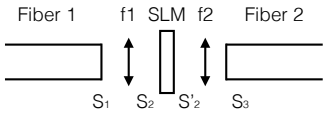

Fig. 3. Mode distribution transformation: the light from the multimode Fiber 1 is launched to free space, passes through the collimating lens f1, spatial light modulator (SLM), and lens f2 and is coupled to the second MMF Fiber 2. The mode densities S for the specific path's part are presented at the bottom of the Figure.

modulation, an improvement in terms of bit error rate (BER) is observed. Finally, the transmission of a 1.5 Gbps signal on a 10 GHz carrier is presented. This choice of frequencies is tested because higher carrier frequencies are proposed to be the next step for the RoF systems [15].

Four types of launches to MMF are tested. Fig. 2 presents the four modes modulated with the different phase information of order m. The modulated beams have been captured with the CCD/CMOS camera. M0 refers to a standard multimode beam without a phase information ($\varphi = 0$), modes with phase modulation orders from 1 to 3 are referred to as M1 to M3. The top row of Fig. 2 presents the beams without the RoF signal modulation (continuous wave (CW) light from a multimode VCSEL at 8 mA), while the bottom row presents the beams modulated with a 1.5 Gbps signal on a 10 GHz carrier.

II. Channel Description

The signal transformations which occur in the presented scenario are described in this section and depicted in Fig. 3. We cover the mode distribution in the pigtail of the multimode fiber (Fiber 1) where the light was launched form the multimode laser, the transformation to free space, through the lens f1, the phase modulation by the SLM, as well as the coupling through the lens f2 and a launch to the second fiber (Fiber 2).

The mode distribution S_1 at the end of the launch fiber (pigtail of the laser) can be decribed as the sum of the linearly polarized (LP) modes:

$$S_1 = \sum_{m,n} \alpha_{mn} LP_{mn}(\mathbf{x}) \tag{1}$$

where m, n is an index of the modes, α_{mn} is the mode coefficient, and LP_{mn} is a fiber Eigenmode. The spatial coordinates are described by $\mathbf{x} = (x, y)$. The phase information is assumed to be included in the LP_{mn} mode expression. At the fiber edge we need to transform LP mode combinationa to LG mode combinations to a free space description:

$$S_1 = \sum_{m',n'} \beta_{m'n'} LG_{m'n'}(\mathbf{x}) \tag{2}$$

m', n' are the indices of the modes in air, $\beta_{m'n'}$ is the coefficient of the Laguerre Gaussian (LG) modes that depends on α_{mn}. The signal distribution after transformation to free space, through the lens, and back to free space results in distribution S_2:

$$S_2 = \tilde{F}_1 \left\{ \tilde{P}_1 \left\{ S_1 \right\} \right\} \tag{3}$$

$\tilde{P}_1$ is a free space propagation transform, $\tilde{F}_1$ is a field transform of the lens f1. After being modulated on the SLM, the phase information is added to the distribution:

$$S_2' = \tilde{F}_1 \left\{ \tilde{P}_1 \left\{ S_1 \right\} \right\} e^{im\varphi} \tag{4}$$

where m is the phase modulation order, and φ is the azimuthal angle of the modulation. The phase modulation is dependent on the mode's wavelength. The distribution after launching back to the MMF Fiber 2 contains a different mode set than in Fiber 1, because they were spatially redistributed during the phase modulation and during other transformations:

$$S_3 = \tilde{P}_3 \left\{ \tilde{F}_2 \left\{ \tilde{P}_2 \left\{ S_2' \right\} \right\} \right\} \tag{5}$$

$\tilde{P}_2$ and $\tilde{P}_3$ are free space propagation transforms and $\tilde{F}_2$ is a field transform of the lens f2.

III. Experimental Setup

An experimental setup is presented in Fig. 4. The pseudo-random bit sequence (PRBS) signal of length 2^15-1, with an amplitude of 500 mVpp, is mixed with the carrier frequency in the Vector Signal Generator (VSG), producing a modulated RF carrier with a power of 0 dBm. Three configurations of data rate and carrier frequency are investigated and are summarized in Fig. 5. The corresponding electrical spectra are presented in Fig. 5(a)–(c).

The upconverted signal is used to directly modulate a multimode 850 nm VCSEL biased at 8 mA. The multimode beam from the fiber pigtailed VCSEL is launched to free space using a collimator. The beam passes through the polarizer and a single polarization is passed to the LCOS-SLM which phase modulates the beam. A second polarizer together with a polarization beam splitter are used as a variable attenuator to set the power required for BER measurement. The beam is then coupled into the MMF patchcord. The 1 m long patchcord is connected to the MMF spool. The fiber links considered in the scenarios are: 100 m OM4, 200 m OM3 and 400 OM4. An 850 nm reverse biased photodiode (PD) is used for direct detection of the signal. The received signal is then recorded with a digital storage oscilloscope (DSO) and downconverted in MATLAB.

The phase modulated beams presented in Fig. 2 are transmitted one by one in the multimode fiber and the transmission performance for each mode is evaluated in terms of BER. The BER is determined in MATLAB through bit error counting over a number of recorded sequences with a combined length of 5 Mbit.

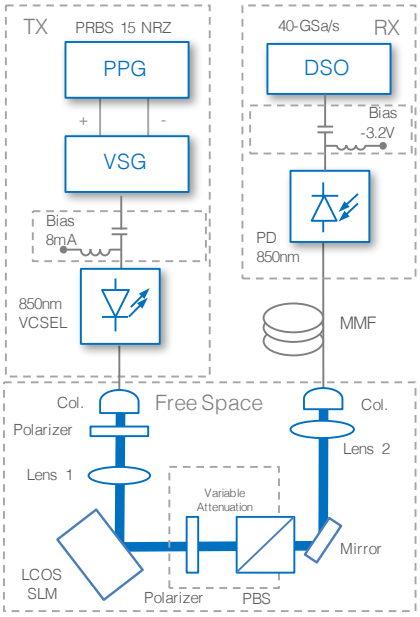

Fig. 4. Experimental setup. Pulse pattern generator (PPG), vector signal generator (VSG), vertical-cavity surface-emitting laser (VCSEL), liquid crystal on silicon spatial light modulator (LCOS SLM), polarization beam splitter (PBS), multimode fiber (MMF), photodiode (PD), digital sampling oscilloscope (DSO).

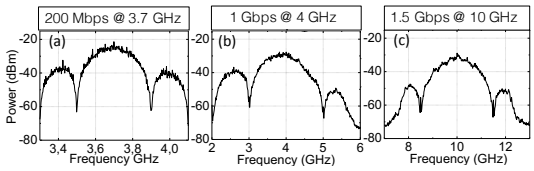

Fig. 5. Regarded data rates and carrier frequencies and their corresponding electrical spectra: (a) 200 Mbps signal on a 3.7 GHz carrier; (b) 1 Gbps signal on a 4 GHz carrier; (c) 1.5 Gbps signal on a 10 GHz carrier.

IV. Optical Channel Characterization

In this section, we present optical spectra captured without modulation and with modulation of a 1.5 Gbps signal on a 10 GHz carrier; the bias current of 8 mA is the same as used in the data transmission experiment. The optical spectra are presented in Fig. 6(a). The spectrum broadening due to modulation in the case of 1.5 Gbps on the 10 GHz carrier is negligible. For two other frequency scenarios with lower carrier frequency and bitrate no broadening is measured. Fig. 6(b) presents the measured static characteristics of the VCSEL used.

Additionally, as most of the signals driving RoF links are of small signal nature, we use small signal analysis to characterize the full channel. S_{21} curves measured with 100 m OM4 fiber and with 200 m OM3 fiber for modes M0 to M3 are

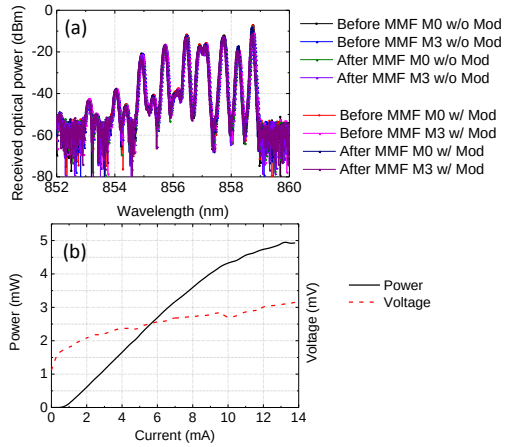

Fig. 6. (a) Optical spectra captured with and without modulation; (b) Light-current-voltage curves for the 850 nm VCSEL.

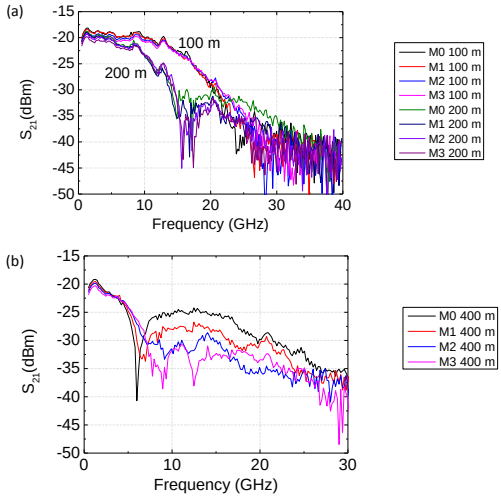

Fig. 7. (a) S_{21} captured for Modes M0–M3 for 100 m OM4 and 200 m OM3; (b) S_{21} captured for Modes M0–M3 for 400 m OM4.

presented in Fig. 7(a). The 3 dB bandwidth of the full optical link with 100 m OM4 fiber is 16 GHz for all tested modes; for the link with 200 m OM3 fiber the 3 dB bandwidth measured is 10 GHz for all modes. Fig. 7(b) presents S_{21} captured for the 4 modes with a 400 m OM4 fiber link. The S_{21} displays a discrepancy in the bandwidth below -3 dB between the 4 modes. 3 dB bandwidth is 4.4 GHz for all modes, but at −6 dB mode M3 has bandwidth of 2 GHz higher than mode M0.

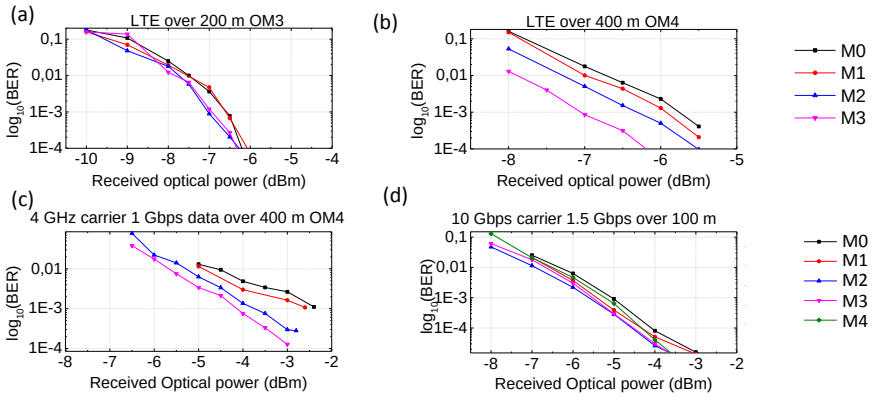

Fig. 8. (a) BER for LTE transmitted over 200 m OM3; (b) BER for LTE transmitted over 400 m OM4; (c) BER measured for a 1 Gbps signal on a 4 GHz carrier transmitted over 400 m OM4; (d) BER measured for a 1.5 Gbps signal on a 10 GHz carrier transmitted over 100 m OM4.

V. Results

A. LTE-like Signal

First, a signal in the 43rd LTE band is transmitted over 200 m of OM3 multimode fiber. The electrical and optical spectra for this scenario are presented in Fig. 5(a) and Fig. 6(a) respectively; the frequency response of the full optical link with 200 m OM3 fiber is presented in Fig. 7(a). The BER results for 4 different launched modes transmitted consecutively through the 200 m fiber are presented in Fig. 8(a). After 200 m transmission the performance of all tested modes is the same. The receiver sensitivity at a BER of 10^{-3} is -7 dBm. The observed differences of up to 0.5 dB between the modes' performance at a BER of 10^{-3} are within the error margin due to instabilities in the system including temperature variation impacting VCSEL and PD behavior.

Second, the LTE-like signal is transmitted over 400 m OM4 multimode fiber. The frequency response of the full optical link with 400 m OM4 fiber is presented in Fig. 7(b). The BER results are presented in Fig. 8(b). A performance improvement in terms of BER is observed for launched modes with higher order phase modulation. For a launched mode M3 a sensitivity improvement of 1.3 dB compared to M0 is observed at a BER of 10^{-3}.

B. 1 Gbps on a 4 GHz Carrier

In the previous section, the improvement in performance has been observed for phase modulated modes launched to MMF. They were modulated at low bitrates for a 400 m OM4 MMF link. Therefore, a higher data bitrate of 1 Gbps is tested on a 4 GHz carrier over the same distance of 400 m. Fig. 8(c) displays the results. The improvement in terms of BER for higher order phase modulation is more pronounced in this scenario and the difference in required received optical power between mode M3 and M0 is 1.8 dB at a BER of 10^{-3}.

C. 1.5 Gbps on a 10 GHz Carrier

The last scenario regarded includes a 1.5 Gbps signal on a 10 GHz carrier. The signal was transmitted over 100 m OM4 fiber. The electrical spectrum is presented in Fig. 5(c) and the frequency response of the full optical link with 100 m OM4 fiber is presented in Fig. 7(a). The BER results are presented in Fig. 8(d). All modes under test show the same performance within the tested BER range. The receiver sensitivity is -5.5 dBm at a BER of 10^{-3}. The differences in performance between modes in terms of BER are up to 0.5 dB and are related to the instability and thermal variations.

VI. Discussion

We show that launching a beam with a phase modulation supports carrying RoF signals in MMF both at the carrier frequencies and bandwidths specified by the LTE standard as well as at higher carrier frequencies and data rates (10 GHz, 1.5 Gbps). Four tested types of launches (modes M0–M3) yield the same performance in terms of BER when transmitted over 200 m (in case of LTE) and 100 m (in case of a 1.5 Gbps signal on a 10 GHz carrier) of MMF. The observed performance proves that the mobile fronthaul can be supported using MMF, where the multi mode links to the antennas are between 100 m and 400 m long.

An improvement in performance for higher order phase modulated modes was observed for a longer fiber link of 400 m. The selective modal launch technique enables the support of longer antenna links, or higher speeds on the existing links.

VII. Conclusions

Transmission of analog radio signals over conventional MMF fibers with enhanced robustness and enhanced capacity are a new prospect for low cost MMF RoF links. This paper presents different experiments on RoF distribution in MMF, using selective modal launch.

We demonstrate the stable performance of RoF signals with carriers varying from 3.7 GHz to 10 GHz. The transmitter is based on a multimode 850 nm VCSEL source, which is arguably a low-cost transmitter. The phase modulation of the beam is done using a SLM, although current developments in the area of devices indicate simple holographic masks enable selective on-chip mode generation [16].

Further work includes the assessment of transmission of more complex modulation formats; this aspect is critical to fully support radio signals for mobile communications and especially when considering turbulence effects, requiring the development of novel turbulent channel models to correctly parametrize the link including the MMF segment.

ACKNOWLEDGEMENTS

This work was partly supported by the Marie Skłodowska Curie Action FiWiN5G project, the HOT project of Innovation Fund Denmark, the Government of the Russian Federation (Grant 074-U01) through the ITMO Visiting Professorship scheme, and by the DFF FTP mmW-SPRAWL project.

REFERENCES

[1] J. J. Vegas Olmos, T. Kuri, T. Sono, K. Tamura, H. Toda, and K. Kitayama, "Wireless and optical-integrated access network with peer-to-peer connection capability," *IEEE Photonics Technology Letters*, vol. 13, no. 20, pp. 1127–1129, 2008.

[2] H. A. Willebrand and G. R. Clark, "Free space optics: a viable last-mile alternative," in *Proc. SPIE*, vol. 4586, 2001, pp. 11–21.

[3] R. A. Panicker and J. M. Kahn, "Algorithms for Compensation of Multimode Fiber Dispersion Using Adaptive Optics," *Journal of Lightwave Technology*, vol. 27, no. 24, pp. 5790–5799, Dec 2009.

[4] J. Carpenter and T. D. Wilkinson, "Characterization of Multimode Fiber by Selective Mode Excitation," *Journal of Lightwave Technology*, vol. 30, no. 10, pp. 1386–1392, May 2012.

[5] E. Alon, V. Stojanovic, J. M. Kahn, S. Boyd, and M. Horowitz, "Equalization of modal dispersion in multimode fiber using spatial light modulators," in *Global Telecommunications Conference, 2004. GLOBECOM '04. IEEE*, vol. 2, Nov 2004, pp. 1023–1029 Vol.2.

[6] F. Dubois, P. Emplit, and O. Hugon, "Selective mode excitation in graded-index multimode fiber by a computer-generated optical mask," *Opt. Lett.*, vol. 19, no. 7, pp. 433–435, Apr 1994. [Online]. Available: http://ol.osa.org/abstract.cfm?URI=ol-19-7-433

[7] G. Stepniak, L. Maksymiuk, and J. Siuzdak, "Binary-Phase Spatial Light Filters for Mode-Selective Excitation of Multimode Fibers," *Lightwave Technology, Journal of*, vol. 29, no. 13, pp. 1980–1987, July 2011.

[8] A. Tatarczak, M. A. Usuga, and I. Tafur Monroy, "Oam-enhanced transmission for multimode short-range links," *Proc. SPIE*, vol. 9390, 2015. [Online]. Available: http://dx.doi.org/10.1117/12.2079795

[9] X. Shen, J. M. Kahn, and M. A. Horowitz, "Compensation for multimode fiber dispersion by adaptive optics," *Opt. Lett.*, vol. 30, no. 22, pp. 2985–2987, Nov 2005. [Online]. Available: http://ol.osa.org/abstract.cfm?URI=ol-30-22-2985

[10] L. Geng, S. Lee, K. William, R. Penty, I. White, and D. Cunningham, "Symmetrical 2-D Hermite-Gaussian square launch for high bit rate transmission in multimode fiber links," in *Optical Fiber Communication Conference and Exposition (OFC/NFOEC), 2011 and the National Fiber Optic Engineers Conference*, March 2011, pp. 1–3.

[11] H. Li, D. B. Phillips, X. Wang, Y.-L. D. Ho, L. Chen, X. Zhou, J. Zhu, S. Yu, and X. Cai, "Orbital angular momentum vertical-cavity surface-emitting lasers," *Optica*, vol. 2, no. 6, pp. 547–552, Jun 2015. [Online]. Available: http://www.osapublishing.org/optica/abstract.cfm?URI=optica-2-6-547

[12] A. Tatarczak, X. Lu, S. Rommel, S. Rodriguez, J. J. Vegas Olmos, and I. Tafur Monroy, "Radio-over-fiber transmission using vortex mode," *2015 IEEE International Topical Meeting on Microwave Photonics*, 2015.

[13] A. Jurado-Navas, A. Tatarczak, X. Lu, J. J. V. Olmos, J. M. Garrido-Balsells, and I. T. Monroy, "850-nm hybrid fiber/free-space optical communications using orbital angular momentum modes," *Opt. Express*, vol. 23, no. 26, pp. 33 721–33 732, Dec 2015. [Online]. Available: http://www.opticsexpress.org/abstract.cfm?URI=oe-23-26-33721

[14] M. Sauer, A. Kobyakov, and J. George, "Radio over fiber for picocellular network architectures," *Lightwave Technology, Journal of*, vol. 25, no. 11, pp. 3301–3320, Nov 2007.

[15] G.-K. Chang, L. Cheng, M. Xu, and D. Guidotti, "Integrated fiber-wireless access architecture for mobile backhaul and fronthaul in 5g wireless data networks," in *Avionics, Fiber-Optics and Photonics Technology Conference (AVFOP), 2014 IEEE*, Nov 2014, pp. 49–50.

[16] L. Cheng, W. Hong, and Z.-C. Hao, "Generation of electromagnetic waves with arbitrary orbital angular momentum modes," *Scientific Reports*, vol. 4, 2014.

Bibliography

[1] "IEEE Standard 802.3.bm," http://www.ieee802.org/3/bm/index.html, March 2014, IEEE 40/100 Gb/s Ethernet Standard Task Force.

[2] N. Chitica, J. Carlsson, L.-G. Svenson, and M. Chacinski, "Vertical-cavity surface-emitting lasers enable high-density ultra-high bandwidth optical interconnects," pp. 938 103–938 103–10, 2015. [Online]. Available: http://dx.doi.org/10.1117/12.2083188

[3] J. A. Tatum, D. Gazula, L. A. Graham, J. K. Guenter, R. H. Johnson, J. King, C. Kocot, G. D. Landry, I. Lyubomirsky, A. N. MacInnes, E. M. Shaw, K. Balemarthy, R. Shubochkin, D. Vaidya, M. Yan, and F. Tang, "VCSEL-Based Interconnects for Current and Future Data Centers," *Journal of Lightwave Technology*, vol. 33, no. 4, pp. 727–732, Feb 2015.

[4] A. Flatman, "Data centre link lengths. ," http://www.ieee802.org/3/NGBASET/public/nov12/flatman_01a_1112_ngbt.pdf, May 2012, IEEE 802.3ba.

[5] H. Liu, C. F. Lam, and C. Johnson, "Scaling Optical Interconnects in Datacenter Networks Opportunities and Challenges for WDM," in *2010 18th IEEE Symposium on High Performance Interconnects*, Aug 2010, pp. 113–116.

[6] C. Minkenberg, "HPC Networks: Challenges and the Role of Optics," in *Optical Fiber Communication Conference*. Optical Society of America, 2015, p. W3D.3. [Online]. Available: http://www.osapublishing.org/abstract.cfm?URI=OFC-2015-W3D.3

[7] D. Coleman, "Optical Trends in the Data Center. ," https://www.bicsi.org/uploadedFiles/BICSI_Website/Global_Community/

Presentations/Caribbean/1.07%20Corning.pdf, 2012, Corning Cable System.

[8] Infiniband , " Infiniband Roadmap. ," http://www.infinibandta.org/content/pages.php?pg=technology_overview.

[9] Fiber Channel , " Fiber Channel Roadmap. ," http://fibrechannel.org/wp-content/uploads/2015/11/FCIA_RoadMap_Front.jpg.

[10] G. K. Chang, L. Cheng, M. Xu, and D. Guidotti, "Integrated fiber-wireless access architecture for mobile backhaul and fronthaul in 5g wireless data networks," in *Avionics, Fiber-Optics and Photonics Technology Conference (AVFOP), 2014 IEEE*, Nov 2014, pp. 49–50.

[11] A. V. Krishnamoorthy, K. W. Goossen, L. M. F. Chirovsky, R. G. Rozier, P. Chandramani, W. S. Hobson, S. P. Hui, J. Lopata, J. A. Walker, and L. D'Asaro, "16x16 VCSEL Array Flip-chip bonded to CMOS VLSI Circuit," in *Optics in Computing*. Optical Society of America, 1999, p. PD3. [Online]. Available: http://www.opticsinfobase.org/abstract.cfm?URI=OC-1999-PD3

[12] I. Ukaegbu, D.-W. Kim, M. Shirazy, T.-W. Lee, M. Cho, and H.-H. Park, "Performance Analysis of Vertical and Horizontal Transmitter Array Modules Using Short- and Long-Wavelength VCSELS for Optical Interconnects," *Components, Packaging and Manufacturing Technology, IEEE Transactions on*, vol. PP, no. 99, pp. 1–1, 2013.

[13] D. M. Kuchta, A. V. Rylyakov, F. E. Doany, C. L. Schow, J. E. Proesel, C. W. Baks, P. Westbergh, J. S. Gustavsson, and A. Larsson, "A 71-Gb/s NRZ Modulated 850-nm VCSEL-Based Optical Link," *IEEE Photonics Technology Letters*, vol. 27, no. 6, pp. 577–580, March 2015.

[14] P. Dapkus, M. Mac Dougal, G.-M. Yang, and Y. Cheng, "Ultralow threshold VCSEL's for application to smart pixels," in *Advanced Applications of Lasers in Materials Processing/Broadband Optical Networks/Smart Pixels/Optical MEMs and Their Applications. IEEE/LEOS 1996 Summer Topical Meetings:*, 1996, pp. 5–6.

[15] J. Guenter, B. Hawkins, R. Hawthorne, and G. Landry, "Reliability of VCSELs for $>$ 25Gb/s," in *Optical Fiber Communications Conference and Exhibition (OFC), 2014*, March 2014, pp. 1–3.

[16] H. Li, P. Wolf, P. Moser, G. Larisch, J. A. Lott, and D. Bimberg, "Vertical-cavity surface-emitting lasers for optical interconnects. ," http://spie.org/newsroom/5689-vertical-cavity-surface-emitting-lasers-for-optical-interconnects, November 2014.

[17] R. Michalzik and K. Ebeling, "3 Operating Principles of VCSELs," *Vertical-Cavity Surface-Emitting Laser Devices*, vol. 6, p. 53, 2002.

[18] A. Ibaraki, K. Kawashima, K. Furusawa, T. Ishikawa, T. Yamaguchi, and T. Niina, "Buried Heterostructure GaAs/GaAlAs Distributed Bragg Reflector Surface Emitting Laser with Very Low Threshold (5.2 mA) under Room Temperature CW Conditions," *Japanese Journal of Applied Physics*, vol. 28, no. Part 2, No. 4, pp. L667–L668, 1989. [Online]. Available: http://jjap.jsap.jp/link?JJAP/28/L667/

[19] J. Jewell, A. Scherer, S. McCall, Y. Lee, S. Walker, J. Harbison, and L. Florez, "Low-threshold electrically pumped vertical-cavity surface-emitting microlasers," *Electronics Letters*, vol. 25, no. 17, pp. 1123–1124, 1989.

[20] A. Fox, *Optical Properties of Solids*, ser. Oxford Master Series in Physics: Condensed Matter Physics. Oxford University Press, Incorporated, 2001. [Online]. Available: http://books.google.dk/books?id=-5bVBbAoaGoC

[21] D. Huffaker, D. Deppe, K. Kumar, and T. Rogers, "Native oxide defined ring contact for low threshold vertical cavity lasers," *Applied Physics Letters*, vol. 65, no. 1, pp. 97–99, 1994.

[22] A. Gholami, D. Molin, and P. Sillard, "Physical Modeling of 10 GbE Optical Communication Systems," *Journal of Lightwave Technology*, vol. 29, no. 1, pp. 115–123, Jan 2011.

[23] K. Iga, F. Koyama, and S. Kinoshita, "Surface emitting semiconductor lasers," *Quantum Electronics, IEEE Journal of*, vol. 24, no. 9, pp. 1845–1855, 1988.

[24] A. Rissons and J.-C. Mollier, "The Vertical-Cavity Surface Emitting Laser (VCSEL) and Electrical Access Contribution," in *Optoelectronics - Devices and Applications*, P. P. Predeep, Ed. InTech, 2011.

[25] K. L. Lear, V. M. Hietala, H. Q. Hou, J. Banas, B. E. Mammons, J. Zolper, and S. P. Kilcoyne, "Small and large signal modulation of 850 nm oxide-confined vertical-cavity surface-emitting lasers," in *Conference on Lasers and Electro-Optics*. Optical Society of America, 1997, p. CWA2. [Online]. Available: http://www.osapublishing.org/abstract.cfm?URI=CLEO-1997-CWA2

[26] M. R. T. Tan, "Commercial applications of vertical cavity surface emitting lasers," in *Lasers and Electro-Optics, 2000. (CLEO 2000). Conference on*, May 2000, pp. 201–.

[27] M. Freebody, " Lasers evolve to meet the demands of optical communications. ," 2012.

[28] L. A. Coldren and S. W. Corzine, *Diode Lasers and Photonic Integrated Circuits*. New York, NY: John Wiley & Sons, 1995.

[29] Y. Satuby and M. Orenstein, "Mode-coupling effects on the small-signal modulation of multitransverse-mode vertical-cavity semiconductor lasers," *IEEE Journal of Quantum Electronics*, vol. 35, no. 6, pp. 944–954, Jun 1999.

[30] C. Cox, *Analog optical links: theory and practice*. Cambridge University Press, 2004. [Online]. Available: http://books.google.dk/books?id=wax_AyFEZDwC

[31] M. Ariga, A. Arai, T. Kageyama, C. Setiagung, Y. Ikenaga, N. Iwai, H. Shimizu, K. Nishikata, A. Kasukawa, and F. Koyama, "Noise characteristics of GaInNAsSb 1300-nm-range VCSEL with optical feedback for isolator-free module," *Selected Topics in Quantum Electronics, IEEE Journal of*, vol. 11, no. 5, pp. 1074–1078, 2005.

[32] Y. Ou, J. S. Gustavsson, P. Westbergh, A. Haglund, A. Larsson, and A. Joel, "Impedance characteristics and parasitic speed limitations of high-speed 850-nm vcsels," *IEEE Photonics Technology Letters*, vol. 21, no. 24, pp. 1840–1842, Dec 2009.

[33] E. Haglund, Å. Haglund, J. S. Gustavsson, B. Kögel, P. Westbergh, and A. Larsson, "Reducing the spectral width of high speed oxide confined VCSELs using an integrated mode filter," pp. 82 760L–82 760L–8, 2012. [Online]. Available: http://dx.doi.org/10.1117/12.908424

[34] O. Kjebon, R. Schatz, S. Lourdudoss, S. Nilsson, and B. Stalnacke, "Modulation response measurements and evaluation of MQW InGaAsP lasers of various designs," in *Society of Photo-Optical Instrumentation Engineers (SPIE) Conference Series*, ser. Society of Photo-Optical Instrumentation Engineers (SPIE) Conference Series, P. A. Morton and D. L. Crawford, Eds., vol. 2684, Apr. 1996, pp. 138–152.

[35] P. Westbergh, J. S. Gustavsson, B. Kögel, Å. Haglund, and A. Larsson, "Impact of Photon Lifetime on High-Speed VCSEL Performance," *IEEE Journal of Selected Topics in Quantum Electronics*, vol. 17, no. 6, pp. 1603–1613, Nov 2011.

[36] G. P. Agrawal, *Fiber-Optic Communication Systems*, 3rd ed. John Wiley & Sons, 2002.

[37] N. Guan, K. Takenaga, S. Matsuo, and K. Himeno, "Multimode fibers for compensating intermodal dispersion of graded-index multimode fibers," *Journal of Lightwave Technology*, vol. 22, no. 7, pp. 1714–1719, July 2004.

[38] J. M. Kahn, "Compensating Multimode Fiber Dispersion Using Adaptive Optics," in *Optical Fiber Communication and the National Fiber Optic Engineers Conference, 2007. OFC/NFOEC 2007. Conference on*, March 2007, pp. 1–3.

[39] G. D. Brown, "Chromatic dispersion measurement in graded-index multimode optical fibers," *Journal of Lightwave Technology*, vol. 12, no. 11, pp. 1907–1909, Nov 1994.

[40] R. Pimpinella, "Impact of including OM4 as a fiber type option ," http://www.ieee802.org/3/ba/public/may09/pimpinella_01_0509.pdf, May 2008, iEEE 802.3ba.

[41] P. Pepeljugoski, M. J. Hackert, J. S. Abbott, S. E. Swanson, S. E. Golowich, A. J. Ritger, P. Kolesar, Y. C. Chen, and P. Pleunis, "Development of system specification for laser-optimized 50- mu;m multimode fiber for multigigabit short-wavelength LANs," *Journal of Lightwave Technology*, vol. 21, no. 5, pp. 1256–1275, May 2003.

[42] D. Molin, M. Bigot, F. Achten, A. Amezcua-Correa, and P. Sillard, "850-950nm wideband OM4 multimode fiber for next-generation

WDM systems," in *Optical Fiber Communications Conference and Exhibition (OFC), 2015*, March 2015, pp. 1–3.

[43] D. Molin, M. Bigot-Astruc, and P. Sillard, "New MMF and VCSEL metrics for system reach predictions," in *Optical Fiber Communications Conference and Exhibition (OFC), 2014*, March 2014, pp. 1–3.

[44] D. Molin, F. Achten, M. Bigot, A. Amezcua-Correa, and P. Sillard, "WideBand OM4 multi-mode fiber for next-generation 400Gbps data communications," in *2014 The European Conference on Optical Communication (ECOC)*, Sept 2014, pp. 1–3.

[45] "EIA/TIA 568 For Fiber Optics," tIA 568. [Online]. Available: http://www.thefoa.org/tech/tia568b3.html

[46] "TIA Specification for 850 nm Laser Optimized OM4 MMF ," Sept 2009, TTIA-492ADDD.

[47] B. Kose, R. Pimpinella, J. M. Castro, Y. Huang, and A. Novick, "Zero Dispersion Modes and its Effects on Characterization of MMF Chromatic Dispersion ," March 2015, panduit Laboratories.

[48] I. Lyubomirsky, R. Motaghian, H. Daghighian, D. McMahon, S. Nelson, C. Kocot, J. A. Tatum, F. Achten, P. Sillard, D. Molin, and A. Amezcua-Correa, "100G SWDM4 transmission over 300m wideband MMF," in *Optical Communication (ECOC), 2015 European Conference on*, Sept 2015, pp. 1–3.

[49] D. M. Kuchta, T. Huynh, F. Doany, A. Rylyakov, C. L. Schow, P. Pepeljugoski, D. Gazula, E. Shaw, and J. Tatum, "A 4-wavelength 40Gb/s/wavelength bandwidth extension of multimode fiber in the 850nm range," in *Optical Fiber Communications Conference and Exhibition (OFC), 2015*, March 2015, pp. 1–3.

[50] Y. Sun, R. Lingle, roman shubochkin, K. balemarthy, D. braganza, timo gray, wenjuan fan, kent wade, deepa gazula, and J. Tatum, "51.56 Gb/s SWDM PAM4 Transmission over Next Generation Wide Band Multimode Optical Fiber," in *Optical Fiber Communication Conference*. Optical Society of America, 2016, p. Tu2G.3. [Online]. Available: http://www.osapublishing.org/abstract.cfm?URI=OFC-2016-Tu2G.3

[51] M. Bigot, D. Molin, F. Achten, A. Amezcua-Correa, and P. Sillard, "Extra-wide-band OM4 MMF for future 1.6Tbps data communications," in *Optical Fiber Communications Conference and Exhibition (OFC), 2015*, March 2015, pp. 1–3.

[52] H. Wang and Y. Cheng, "Equalization techniques for high-speed serial interconnect transceivers," in *Solid-State and Integrated-Circuit Technology, 2008. ICSICT 2008. 9th International Conference on*, Oct 2008, pp. 1589–1592.

[53] J. Proakis, *The Communication Handbook*. Davis, CA: IEEE Press, Univ. of California, 1997, channel equalization.

[54] A. V. Rylyakov, C. L. Schow, J. E. Proesel, D. M. Kuchta, C. Baks, N. Y. Li, C. Xie, and K. P. Jackson, "A 40-Gb/s, 850-nm, VCSEL-based full optical link," in *Optical Fiber Communication Conference and Exposition (OFC/NFOEC), 2012 and the National Fiber Optic Engineers Conference*, March 2012, pp. 1–3.

[55] T. Lengyel, K. Szczerba, P. Westbergh, M. Karlsson, A. Larsson, and P. Andrekson, "Sensitivity improvements in an 850 nm VCSEL transmitter using a one-tap pre-emphasis electronic filter," in *Optical Communication (ECOC), 2015 European Conference on*, Sept 2015, pp. 1–3.

[56] M. Bruensteiner, G. C. Papen, J. Poulton, S. Tell, R. Palmer, K. Giboney, D. Dolfi, and S. Corzine, "3.3-V CMOS pre-equalization VCSEL transmitter for gigabit multimode fiber links," *IEEE Photonics Technology Letters*, vol. 11, no. 10, pp. 1301–1303, Oct 1999.

[57] C. L. Schow, A. V. Rylyakov, B. G. Lee, F. E. Doany, C. Baks, R. A. John, and J. A. Kash, "Transmitter pre-distortion for simultaneous improvements in bit-rate, sensitivity, jitter, and power efficiency in 20 Gb/s CMOS-driven VCSEL links," in *Optical Fiber Communication Conference and Exposition (OFC/NFOEC), 2011 and the National Fiber Optic Engineers Conference*, March 2011, pp. 1–3.

[58] K. Szczerba, B. E. Olsson, P. Westbergh, A. Rhodin, J. S. Gustavsson, Å. Haglund, M. Karlsson, A. Larsson, and P. A. Andrekson, "37 Gbps transmission over 200 m of MMF using single cycle subcarrier modulation and a VCSEL with 20 GHz modulation bandwidth," in

36th European Conference and Exhibition on Optical Communication, Sept 2010, pp. 1–3.

[59] B. L. Kasper, "Equalization of multimode optical fiber systems," *The Bell System Technical Journal*, vol. 61, no. 7, pp. 1367–1388, Sept 1982.

[60] X. Zhao and F. S. Choa, "Demonstration of 10-Gb/s transmissions over a 1.5-km-long multimode fiber using equalization techniques," *IEEE Photonics Technology Letters*, vol. 14, no. 8, pp. 1187–1189, Aug 2002.

[61] I.-C. Lu, J.-W. Shi, H.-Y. Chen, C.-C. Wei, S.-F. Tsai, D.-Z. Hsu, Z.-R. Wei, J.-M. Wun, and J. Chen, "Ultra low power VCSEL for 35-Gbps 500-m OM4 MMF transmissions employing FFE/DFE equalization for optical interconnects," in *Optical Fiber Communication Conference and Exposition and the National Fiber Optic Engineers Conference (OFC/NFOEC), 2013*, March 2013, pp. 1–3.

[62] D. M. Kuchta, A. V. Rylyakov, C. L. Schow, J. E. Proesel, C. W. Baks, P. Westbergh, J. S. Gustavsson, and A. Larsson, "A 50 Gb/s NRZ Modulated 850 nm VCSEL Transmitter Operating Error Free to 90^oC," *Journal of Lightwave Technology*, vol. 33, no. 4, pp. 802–810, Feb 2015.

[63] J. M. Castro, R. Pimpinella, B. Kose, Y. Huang, B. lane, adrian Amezcua-Correa, M. Bigot, denis molin, and P. Sillard, "200m 2x50Gbps PAM-4 SWDM transmission over WideBand Multimode Fiber using VCSELs and pre-distortion signal," in *Optical Fiber Communication Conference*. Optical Society of America, 2016, p. Tu2G.2. [Online]. Available: http://www.osapublishing.org/abstract.cfm?URI=OFC-2016-Tu2G.2

[64] I. Lyubomirsky and W. A. Ling, "Digital QAM modulation and equalization for high performance 400 GbE data center modules," in *Optical Fiber Communications Conference and Exhibition (OFC), 2014*, March 2014, pp. 1–3.

[65] N. G. Gonzalez, D. Zibar, X. Yu, and I. T. Monroy, "Optical phase-modulated radio-over-fiber links with k-means algorithm for digital demodulation of 8PSK subcarrier multiplexed signals," in *Optical*

Fiber Communication (OFC), collocated National Fiber Optic Engineers Conference, 2010 Conference on (OFC/NFOEC), March 2010, pp. 1–3.

[66] Y. Matsui, T. Pham, W. Ling, R. Schatz, G. Carey, H. Daghighian, T. Sudo, and C. Roxlo, "55-GHz Bandwidth Short-Cavity Distributed Reflector Laser and its Application to 112-Gb/s PAM-4," in *Optical Fiber Communication Conference Postdeadline Papers*. Optical Society of America, 2016, p. Th5B.4. [Online]. Available: http://www.osapublishing.org/abstract.cfm?URI=OFC-2016-Th5B.4

[67] InfiniBandTM, "Architecture Specification," 2012, release 1.3.

[68] "Fibre Channel, Physical Interface-6 ," http://www.t11.org/ftp/t11/pub/fc/pi-6p/15-057v4.pdf, Fiber Channel Committee of INCITS.

[69] I. Reed and G. Solomon, "Polynomial codes over certain finite fields," *J. Soc. Ind. Appl. Math.*, vol. 8, no. 2, pp. 300–304, June 1960.

[70] M. Brown, M. Dudek, A. Healey, L. B. Artsi, R. Mellitz, C. Moore, A. Ran, and P. Zivny, "The state of IEEE 802.3bj 100 Gb/s Backplane Ethernet," http://www.ee.sc.edu/classes/Spring14/elct861/Class_Notes/8-TH6%20state%20of%20IEEE%20802%203bj%20100%20Backplane%20Ethernet.pdf, 2014.

[71] F. Chang, K. Onohara, and T. Mizuochi, "Forward error correction for 100 G transport networks," *IEEE Communications Magazine*, vol. 48, no. 3, pp. S48–S55, March 2010.

[72] D. M. Kuchta, A. V. Rylyakov, C. L. Schow, J. E. Proesel, C. Baks, P. Westbergh, J. S. Gustavsson, and A. Larsson, "64Gb/s transmission over 57m MMF using an NRZ modulated 850nm VCSEL," in *Optical Fiber Communications Conference and Exhibition (OFC), 2014*, March 2014, pp. 1–3.

[73] P. Westbergh, E. P. Haglund, E. Haglund, R. Safaisini, J. S. Gustavsso, and A. Larsson, "High-speed 850 nm VCSELs operating error free up to 57 Gbit/s," *Electronics Letters*, vol. 49, no. 16, pp. 1021–1023, Aug 2013.

[74] K. Szczerba, P. Westbergh, M. Karlsson, P. A. Andrekson, and A. Larsson, "70 Gbps 4-PAM and 56 Gbps 8-PAM Using an 850

nm VCSEL," *Journal of Lightwave Technology*, vol. 33, no. 7, pp. 1395–1401, April 2015.

[75] J. Castro, R. Pimpinella, B. Kose, Y. Huang, B. Lane, K. Szczerba, P. Westbergh, T. Lengyel, J. Gustavsson, A. Larsson, and P. Andrekson, "Investigation of 60 Gb/s 4-PAM using an 850 nm VCSEL and multimode fiber," *Journal of Lightwave Technology*, vol. PP, no. 99, pp. 1–1, 2016.

[76] J. M. Castro, R. Pimpinella, B. Kose, Y. Huang, B. Lane, K. Szczerba, P. Westbergh, T. Lengyel, J. S. Gustavsson, A. Larsson, and P. A. Andrekson, "48.7-Gb/s 4-PAM Transmission Over 200 m of High Bandwidth MMF Using an 850-nm VCSEL," *IEEE Photonics Technology Letters*, vol. 27, no. 17, pp. 1799–1801, Sept 2015.

[77] K. Szczerba, M. Karlsson, P. Andrekson, A. Larsson, and E. Agrell, "35.2 gbps 8-pam transmission over 100 m of mmf using an 850 nm vcsel," in *Optical Communication (ECOC 2013), 39th European Conference and Exhibition on*, Sept 2013, pp. 1–3.

[78] W. A. Ling, I. Lyubomirsky, R. Rodes, H. M. Daghighian, and C. Kocot, "Single-Channel 50G and 100G Discrete Multitone Transmission With 25G VCSEL Technology," *J. Lightwave Technol.*, vol. 33, no. 4, pp. 761–767, Feb 2015. [Online]. Available: http://jlt.osa.org/abstract.cfm?URI=jlt-33-4-761

[79] S. C. J. Lee, F. Breyer, S. Randel, D. Cardenas, H. P. A. van den Boom, and A. M. J. Koonen, "Discrete multitone modulation for high-speed data transmission over multimode fibers using 850-nm VCSEL," in *Optical Fiber Communication - incudes post deadline papers, 2009. OFC 2009. Conference on*, March 2009, pp. 1–3.

[80] R. Puerta, M. Agustin, L. Chorchos, J. Tonski, J.-R. Kropp, N. Ledentsov, V. A. Shchukin, N. N. Ledentsov, R. Henker, I. T. Monroy, J. J. V. Olmos, and J. Turkiewicz, "107.5 Gb/s 850 nm multi- and single-mode VCSEL transmission over 10 and 100 m of multi-mode fiber," in *Optical Fiber Communication Conference Postdeadline Papers*. Optical Society of America, 2016, p. Th5B.5. [Online]. Available: http://www.osapublishing.org/abstract.cfm?URI=OFC-2016-Th5B.5

[81] M. Olmedo, T. Zuo, J. Jensen, Q. Zhong, X. Xu, S. Popov, and I. Monroy, "Multiband Carrierless Amplitude Phase Modulation for High Capacity Optical Data Links," *Lightwave Technology, Journal of*, vol. 32, no. 4, pp. 798–804, Feb 2014.

[82] M. I. Olmedo, A. Tatarczak, T. Zuo, J. Estaran, X. Xu, and I. T. Monroy, "Towards 100 Gbps over 100m MMF using a 850nm VCSEL," in *Optical Fiber Communications Conference and Exhibition (OFC), 2014*, March 2014, pp. 1–3.

[83] X. Lu and I. T. Monroy, "8-dimensional Lattice Optimized Formats in 25-GBaud/s VCSEL based IM/DD Optical Interconnections," in *Asia Communications and Photonics Conference 2015*. Optical Society of America, 2015, p. AS4D.3. [Online]. Available: http://www.osapublishing.org/abstract.cfm?URI=ACPC-2015-AS4D.3

[84] J. H. Conway, N. J. A. Sloane, and E. Bannai, *Sphere-packings, Lattices, and Groups*, 3rd ed. Springer-Verlag New York, Inc., 1987.

[85] " MMF Standardization and S-WDM technology," www.ieee802.org/3/50G/public/Jan16/kolesar_50GE_NGOATH_01a_0116.pdf, January 2015, IEEE 802.3 50G and NGOATH Study Groups, Atlanta GA.

[86] J. Jewel, "MMF Capabilities or 400-GigabitEthernet, and Beyond. ," http://www.ieee802.org/3/400GSG/public/13_07/jewell_400_01a_0713.pdf, ethernet Study Group, Geneva, Switzerland.

[87] K. Nagashima, T. Kise, Y. Ishikawa, and H. Nasu, "A Record 1-km MMF NRZ 25.78-Gb/s Error-Free Link Using a 1060-nm DIC VCSEL," *IEEE Photonics Technology Letters*, vol. 28, no. 4, pp. 418–420, Feb 2016.

[88] S. Kamiya, T. Kise, M. Funabashi, T. Suzuki, A. Imamura, K. Hiraiwa, T. Nakamura, H. Shimizu, T. Ishikawa, and A. Kasukawa, "Over 25,000 hours operation of 1060 nm vertical cavity surface emitting lasers," in *2013 18th OptoElectronics and Communications Conference held jointly with 2013 International Conference on Photonics in Switching (OECC/PS)*, June 2013, pp. 1–2.

[89] J. B. Haroux, T. Kise, M. Funabashi, T. Aoki, C. L. Schow, A. V. Rylyakov, and S. Nakagawa, "Energy-Efficient 1060-nm Optical Link

Operating up to 28 Gb/s," *Journal of Lightwave Technology*, vol. 33, no. 4, pp. 733–740, Feb 2015.

[90] K. Nagashima, T. Kise, Y. Ishikawa, and H. Nasu, "1060-nm VCSEL-based 28-Gb/s 4-channnel optical signal transmission beyond 500-m MMF using high-density parallel-optical modules," in *IEEE CPMT Symposium Japan 2014*, Nov 2014, pp. 130–133.

[91] S. K. Pavan, J. Lavrencik, R. Shubochkin, Y. Sun, J. Kim, D. Vaidya, R. Lingle, T. Kise, and S. E. Ralph, "50Gbit/s PAM-4 MMF transmission using 1060nm VCSELs with reach beyond 200m," in *Optical Fiber Communications Conference and Exhibition (OFC), 2014*, March 2014, pp. 1–3.

[92] A. Tatarczak, Y. Zheng, G. A. Rodes, J. Estaran, C. H. Lin, A. V. Barve, R. Honore, N. Larsen, L. A. Coldren, and I. T. Monroy, "30 Gbps bottom-emitting 1060 nm VCSEL," in *2014 The European Conference on Optical Communication (ECOC)*, Sept 2014, pp. 1–3.

[93] H. Halbritter, M. Aziz, F. Riemenschneider, P. Meissner, M. Strassner, A. Tarraf, and O. P. Daga, "Performance evaluation of wdm components based on tunable dielectric membrane technology," *IEE Proceedings - Circuits, Devices and Systems*, vol. 150, no. 6, pp. 501–505, Dec 2003.

[94] L. Han, S. Liang, J. Xu, L. Qiao, H. Zhu, and W. Wang, "Electroabsorption-modulated widely tunable dbr laser transmitter for wdm-pons," in *Optical Communications and Networks (ICOCN), 2015 14th International Conference on*, July 2015, pp. 1–3.

[95] J. Peerlings, R. Riemenschneider, M. Strassner, V. Scheuer, V. N. Kumar, K. Mutamba, J. Pfeiffer, S. Herbst, H. L. Hartnagel, and P. Meissner, "Ingaas-inp fabry-perot pin receiver for dense wavelength division multiplex systems," in *Optical Communication, 1998. 24th European Conference on*, vol. 1, Sep 1998, pp. 65–66 vol.1.

[96] Y. Sun, M. E. Ali, K. Balemarthy, R. L. Lingle, S. E. Ralph, and B. E. Lemoff, "10 Gb/s transmission over 300 m OM3 fiber from 990-1080 nm with electronic dispersion compensation," in *2006 Optical Fiber Communication Conference and the National Fiber Optic Engineers Conference*, March 2006, pp. 3 pp.–.

[97] B. E. Lemoff, M. E. Ali, G. Panotopoulos, E. de Groot, G. M. Flower, G. H. Rankin, A. J. Schmit, K. D. Djordjev, M. R. T. Tan, A. Tandon, W. Gong, R. P. Tella, B. Law, and D. W. Dolfi, "500-Gbps Parallel-WDM Optical Interconnect," in *Proceedings Electronic Components and Technology, 2005. ECTC '05.*, May 2005, pp. 1027–1031.

[98] J. Carpenter and T. D. Wilkinson, "Characterization of Multimode Fiber by Selective Mode Excitation," *Journal of Lightwave Technology*, vol. 30, no. 10, pp. 1386–1392, May 2012.

[99] Z. Haas and M. A. Santoro, "A mode-filtering scheme for improvement of the bandwidth-distance product in multimode fiber systems," *Journal of Lightwave Technology*, vol. 11, no. 7, pp. 1125–1131, Jul 1993.

[100] G. Stepniak, J.-R. Kropp, N. N. Ledentsov, V. A. Shchukin, N. Ledentsov, G. Schaefer, and J. P. Turkiewicz, "54 Gbps OOK Transmission Using Single Mode VCSEL up to 1 km OM4 MMF," in *Optical Fiber Communication Conference*. Optical Society of America, 2016, p. Th4D.5. [Online]. Available: http://www.osapublishing.org/abstract.cfm?URI=OFC-2016-Th4D.5

[101] R. Safaisini, E. Haglund, P. Westbergh, J. S. Gustavsson, and A. Larsson, "20 Gbit/s data transmission over 2 km multimode fibre using 850 nm mode filter VCSEL," *Electronics Letters*, vol. 50, no. 1, pp. 40–42, January 2014.

[102] L. Raddatz, I. H. White, D. G. Cunningham, and M. C. Nowell, "An experimental and theoretical study of the offset launch technique for the enhancement of the bandwidth of multimode fiber links," *Journal of Lightwave Technology*, vol. 16, no. 3, pp. 324–331, Mar 1998.

[103] A. Amphawan, F. Payne, D. O'Brien, and N. Shah, "Derivation of an Analytical Expression for the Power Coupling Coefficient for Offset Launch Into Multimode Fiber," *Journal of Lightwave Technology*, vol. 28, no. 6, pp. 861–869, March 2010.

[104] L. Geng, S. Lee, K. William, R. Penty, I. White, and D. Cunningham, "Symmetrical 2-D Hermite-Gaussian square launch for high bit rate transmission in multimode fiber links," in *Optical Fiber Communication Conference and Exposition (OFC/NFOEC), 2011 and the National Fiber Optic Engineers Conference*, March 2011, pp. 1–3.

[105] E. Alon, V. Stojanovic, J. M. Kahn, S. Boyd, and M. Horowitz, "Equalization of modal dispersion in multimode fiber using spatial light modulators," in *Global Telecommunications Conference, 2004. GLOBECOM '04. IEEE*, vol. 2, Nov 2004, pp. 1023–1029 Vol.2.

[106] G. Stepniak, L. Maksymiuk, and J. Siuzdak, "Binary-Phase Spatial Light Filters for Mode-Selective Excitation of Multimode Fibers," *Lightwave Technology, Journal of*, vol. 29, no. 13, pp. 1980–1987, July 2011.

[107] F. Dubois, P. Emplit, and O. Hugon, "Selective mode excitation in graded-index multimode fiber by a computer-generated optical mask," *Opt. Lett.*, vol. 19, no. 7, pp. 433–435, Apr 1994. [Online]. Available: http://ol.osa.org/abstract.cfm?URI=ol-19-7-433

[108] X. Shen, J. M. Kahn, and M. A. Horowitz, "Compensation for multimode fiber dispersion by adaptive optics," *Opt. Lett.*, vol. 30, no. 22, pp. 2985–2987, Nov 2005. [Online]. Available: http://ol.osa.org/abstract.cfm?URI=ol-30-22-2985

[109] R. A. Panicker and J. M. Kahn, "Algorithms for Compensation of Multimode Fiber Dispersion Using Adaptive Optics," *Journal of Lightwave Technology*, vol. 27, no. 24, pp. 5790–5799, Dec 2009.

[110] I.-C. Lu, C.-C. Wei, H.-Y. Chen, K.-Z. Chen, C.-H. Huang, K.-L. Chi, J.-W. Shi, F.-I. Lai, D.-H. Hsieh, H.-C. Kuo, W. Lin, S.-W. Chiu, and J. Chen, "Very High Bit-Rate Distance Product Using High-Power Single-Mode 850-nm VCSEL With Discrete Multitone Modulation Formats Through OM4 Multimode Fiber," *Selected Topics in Quantum Electronics, IEEE Journal of*, vol. 21, no. 6, pp. 444–452, Nov 2015.

[111] B. wu, X. Zhou, N. ledentsov, and jun luo, "Towards 100 Gb/s Serial Optical Links over 300m of Multimode Fibre Using Single Transverse Mode 850nm VCSEL," in *Asia Communications and Photonics Conference 2015*. Optical Society of America, 2015, p. ASu4C.3. [Online]. Available: http://www.osapublishing.org/abstract.cfmURI=ACPC-2015-ASu4C.3

[112] R. Motaghiannezam, I. Lyubomirsky, H. Daghighian, C. Kocot, T. Gray, J. Tatum, A. Amezcua-Correa, M. Bigot-Astruc, D. Molin, F. Achten, and P. Sillard, "Four 45 Gbps PAM4

VCSEL based transmission through 300 m wideband OM4 fiber over SWDM4 wavelength grid," *Opt. Express*, vol. 24, no. 15, pp. 17 193–17 199, Jul 2016. [Online]. Available: http://www.opticsexpress.org/abstract.cfm?URI=oe-24-15-17193

[113] R. Motaghian and C. Kocot, "104 Gbps PAM4 Transmission over OM3 and OM4 Fibers using 850 and 880 nm VCSELs," in *Conference on Lasers and Electro-Optics*. Optical Society of America, 2016, p. SW4F.8. [Online]. Available: http://www.osapublishing.org/abstract.cfm?URI=CLEO_SI-2016-SW4F.8

[114] M. I. Olmedo, Z. Tianjian, J. B. Jensen, Z. Qiwen, X. Xiaogeng, and I. T. Monroy, "Towards 400GBASE 4-lane solution using direct detection of MultiCAP signal in 14 GHz bandwidth per lane," in *Optical Fiber Communication Conference and Exposition and the National Fiber Optic Engineers Conference (OFC/NFOEC), 2013*, March 2013, pp. 1–3.

[115] D. M. Kuchta, C. L. Schow, A. V. Rylyakov, J. E. Proesel, F. E. Doany, C. Baks, B. H. Hamel-Bissell, C. Kocot, L. Graham, R. Johnson, G. Landry, E. Shaw, A. MacInnes, and J. Tatum, "A 56.1Gb/s NRZ modulated 850nm VCSEL-based optical link," in *Optical Fiber Communication Conference and Exposition and the National Fiber Optic Engineers Conference (OFC/NFOEC), 2013*, March 2013, pp. 1–3.

Appendices

Appendix A

Paper 9: Optical-domain Compensation for Coupling between Optical Fiber Conjugate Vortex Modes

Lyubopytov, V. S.; Tatarczak, A.; Lu, X.; Kutluyarov, R. V.; Rommel, S.; Sultanov, A. K.; Monroy, I. T., "Optical-domain Compensation for Coupling between Optical Fiber Conjugate Vortex Modes," in *2015 Conference on Lasers and Electro-Optics Pacific Rim, Optical Society of America*, 2015, paper PDP T12 1001, 2015.

Optical-domain Compensation for Coupling between Optical Fiber Conjugate Vortex Modes

Vladimir S. Lyubopytov*, Anna Tatarczak**, Xiaofeng Lu**, Ruslan V. Kutluyarov*,
Simon Rommel**, Albert Kh. Sultanov*, and Idelfonso Tafur Monroy**

* Ufa State Aviation Technical University, Telecommunication Systems Dept., 12 K. Marx Street, Ufa, 450000 Russia
** DTU Fotonik, Technical University of Denmark (DTU), 2800 Kgs. Lyngby, Denmark

Abstract

We demonstrate for the first time optical-domain compensation for coupling between conjugate vortex modes in optical fibers. We introduce a novel method for reconstructing the complex propagation matrix of the optical fiber with straightforward implementation.

I. Introduction

Nowadays a number of applications involving the use of orbital angular momentum (OAM) of light for data transmission are under development, including classical communications approaching the nonlinear Shannon limit and OAM-based quantum communications. However, OAM modes, or optical vortices, transmitted over conventional optical fibers are subject to random mode coupling caused by fiber bending, twisting and inherent optical fiber fabrication defects [1]. Therefore, computationally heavy multiple-input multiple-output (MIMO) digital signal processing is a standard technique to compensate for such mode coupling and recover the transmitted data in current optical fiber mode-division-multiplexed (MDM) transmission systems [2, 3]. However, this approach demands great computational resources for real-time signal processing implementation. Optical-domain mitigation of crosstalk resulting from mode coupling is a more effective solution in respect to better scalability and reduced power consumption.

Compensation of the crosstalk between OAM-multiplexed channels transmitted over atmospheric turbulence has been recently demonstrated by means of adaptive optics [4]. Several adaptive techniques for multimode fiber modes control have also been proposed [5, 6], however the main goal of these works is to control the output field distribution, rather than to provide independent transmission of modes over the fiber.

We demonstrate experimentally for the first time that the intensity of conjugate OAM modes transmitted over the fiber in the presence of mode coupling can be recovered in the optical domain. A standard single mode fiber (SSMF) patch cord in 3-mode regime is used for our demonstration. We employ a novel method for reconstructing the fiber complex propagation matrix based on the output field azimuthal decomposition [7] that allows matrix elements determination by direct calculations from the beam intensities in the corresponding diffraction orders.

This work is partly supported by the Ministry of Education and Science of Russian Federation under the State assignment for higher education organizations.

II. Method Principles and Experimental Setup

Fig. 1 shows the simplified scheme of the experimental setup, where the key building blocks are two spatial light modulators (SLMs), first of those is intended for excitation of vortex beams and their superpositions, and the second one is used for the fiber propagation matrix analysis and mode coupling compensation.

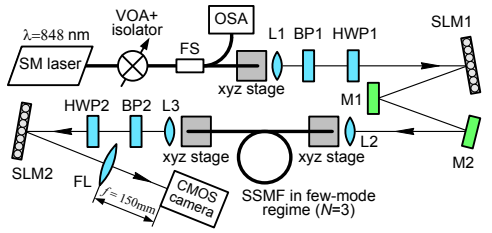

Fig. 1. Experimental setup for the fiber analysis and mode coupling compensation: SLM1, SLM2 – spatial light modulators Hamamatsu X10468-02 (792x600 pixels); OSA – optical spectrum analyzer; FS – fiber splitter; L1-L3 – lenses; FL – Fourier lens; HWP1, HWP2 – half-wave plates; BP1, BP2 – beam polarizers; M1, M2 – mirrors.

A patch cord ($L = 4$ m) made of conventional SSMF has been used as a transmission medium. It behaves as a 3-mode fiber at the wavelength 848 nm. A considered modal basis consists of the fundamental mode LP_{01} and the two conjugate vortex modes $LP_{\pm 11} = LP_{11a} \pm iLP_{11b}$.

To build the propagation matrix reconstruction, our proposed method involves only two consecutive steps. First, we transmit individual modes and determine amplitudes of all elements in the propagation matrix and phase differences within each column relative to the element on the main diagonal. Next it is sufficient to determine phase differences between matrix columns by transmitting twin-mode superpositions through adjacent modal channels. Theoretical details of our method and simulation results are presented in [8]. Here we report, for the first time, experimental verification of the proposed method. Validity and accuracy of the experimentally obtained propagation matrix is controlled by two factors: coincidence of the free space experiment data (when propagation matrix tends to be identity) with the simulation results; fulfillment of the phase loop condition, providing the determined relative phases are correct throughout the columns and rows of the propagation matrix (phase loop inaccuracy does not exceed 0.4 rad throughout all our experiments).

In order to implement inverse fiber propagation operator using SLM2, the transfer function of the computer generated hologram (CGH) is defined as:

$$\Psi_{\mathrm{SLM2}}(\mathbf{x})=\sum_{\nu=1}^{N}\left(\sum_{\mu=1}^{N}u_{\nu\mu}^{-1}e^{-il_{\mu}\varphi}\right)e^{i\mathbf{w}_{\nu}\mathbf{x}} \qquad (1)$$

where $u_{\nu\mu}^{-1}$ are the elements of the matrix inverse to the normalized propagation matrix $\mathbf{U}$, N is the number of modes, l_{μ} is the topological charge of the μ-th transmitted mode; $\mathbf{w}_{\nu}$ is the spatial carrier corresponding to the ν-th received mode; $\mathbf{x} = (x, y)$.

III. Experiment Results and Discussion

Our experimental observations show that coupling between conjugate modes which possess equal propagation constants and differ from each other only by the phase front vorticity handedness is much stronger than coupling between modes with adjacent azimuthal indices (Fig. 2 (a)-(c), (g) shows an exemplary output modal content). It may appear significant even in a fiber of short length and lead to almost complete transfer of energy between modes. But when the fiber complex propagation matrix is determined, this coupling can be compensated for (Fig. 2 (d)-(f), (h)), while energy distribution between vortex modes and fundamental modes remains almost the same. Effectiveness of the compensation in our setup was limited by the SLM property to operate with only one polarization, whereas coupling between two polarizations of OAM modes increases with the fiber length and can be compensated by their simultaneous processing. Alternatively, polarization coupling may be avoided by using polarization maintaining fiber.

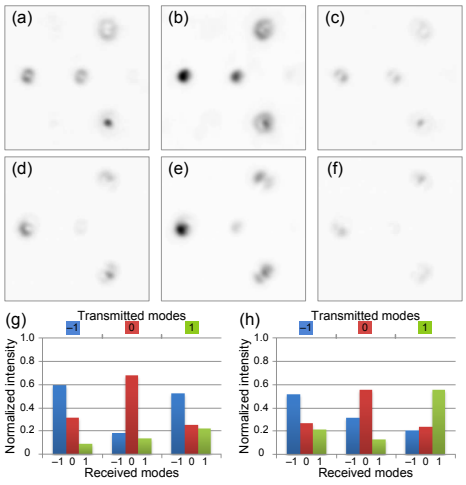

Fig. 2. (a)-(c) Intensity distribution at the Fourier lens focus plane when testing the fiber with modes LP_{-11}, LP_{01}, and LP_{11} respectively (the lower diffraction order corresponds to topological charge $l = -1$, left one – to $l = 0$, and the upper one – to $l = 1$); (d)-(f) when applying optical compensation; (g), (h) normalized intensity distribution between modes during fiber analysis and after optical compensation respectively.

Our proposed method allows for using potentially conjugate modes as independent orthogonal carriers for OAM-multiplexed data transmission systems, effectively increasing the capacity of the channel. Moreover, as conjugate modes have the same propagation constants, extension from continuous wave to modulated signal transmission should not require additional means to deal with differential mode delay.

IV. Conclusions

The presented experimental results are the first proof-of-concept demonstration that mode coupling between conjugate vortex modes can be compensated in the optical domain by means of a CGH, whose transfer function is defined to perform the inverse fiber propagation matrix. We show reconstruction of the waveguide complex propagation matrix, implemented experimentally, on the basis of azimuthal field decomposition with an accuracy level sufficient for straightforward compensation for the mode mixing. Our demonstrated approach allows a potential utilization of the conjugate vortex modes as signal carriers in MDM communication systems using efficient optical-domain signal processing.

References

[1] V.P. Garitchev, M.A. Golub, S.V. Karpeev, S.G. Krivoshlykov, N.I. Petrov, I.N. Sissakian, V.A. Soifer, W. Haubenreisser, J.-U. Jahn, and R. Willsch, "Experimental investigation of mode coupling in a multimode graded-index fiber, caused by periodic microbends using computer-generated spatial filters," *Opt. Commun.*, vol. 55(6), pp. 403-405, October 1985.

[2] C. Koebele, M. Salsi, D. Sperti, P. Tran, P. Brindel, H. Mardoyan, S. Bigo, A. Boutin, F. Verluise, P. Sillard, M. Astruc, L. Provost, F. Cerou, G. Charlet, "Two mode transmission at 2x100Gb/s, over 40km-long prototype few-mode fiber, using LCOS-based programmable mode multiplexer and demultiplexer," *Opt. Express*, vol. 19(17), pp. 16593-16600, 2011.

[3] S. Randel, R. Ryf, A.H. Gnauck, M.A. Mestre, C. Schmidt, R.-J. Essiambre, P.J. Winzer, R. Delbue, P. Pupalaikis, A. Sureka, Y. Sun, X. Jiang, R. Lingle, Jr., "Mode-Multiplexed 6×20-GBd QPSK Transmission over 1200-km DGD-Compensated Few-Mode Fiber," *Optical Fiber Communication Conference and Exposition and the National Fiber Optic Engineers Conference (OFC/NFOEC)*, PDP5C.5, March 2012.

[4] Y. Ren, G. Xie, H. Huang, C. Bao, Y. Yan, N. Ahmed, M.P.J. Lavery, B.I. Erkmen, S. Dolinar, M. Tur, M.A. Neifeld, M.J. Padgett, R.W. Boyd, J.H. Shapiro, and A.E. Willner, "Adaptive optics compensation of multiple orbital angular momentum beams propagating through emulated atmospheric turbulence," *Opt. Lett.*, vol. 39(10), pp. 2845-2848, May 2014.

[5] P. Lu, M. Shipton, A. Wang, and Y. Xu, "Adaptive control of waveguide modes using a directional coupler," *Opt. Express*, vol. 22(17), pp. 20000-20007, August 2014.

[6] R.N. Mahalati, D. Askarov, J.P. Wilde, and J.M. Kahn, "Adaptive control of input field to achieve desired output intensity profile in multimode fiber with random mode coupling," *Opt. Express*, vol. 20(13), pp. 14321-14337, June 2012.

[7] I.A. Litvin, A. Dudley, F.S. Roux, and A. Forbes, "Azimuthal decomposition with digital holograms," *Opt. Express*, vol. 20(10), pp. 10996-11004, May 2012.

[8] V.S. Lyubopytov, V.K. Bagmanov, A.K. Sultanov, "Adaptive SLM-based compensation of intermodal interference in few-mode optical fibers," *Proc. SPIE 9216, Optics and Photonics for Information Processing VIII*, 92160I, August 2014.

Appendix B

Paper 10: Towards 100 Gbps over 100m MMF using a 850 nm VCSEL

Iglesias Olmedo, M.; Tatarczak, A.; Tianjian Zuo; Estaran, J.; Xiaogeng Xu; Tafur Monroy, I., "Towards 100 Gbps over 100m MMF using a 850 nm VCSEL," *Optical Fiber Communications Conference and Exhibition (OFC)*, 2014, pp.1,3, March 2014.

Towards 100 Gbps over 100m MMF using a 850nm VCSEL

Miguel Iglesias Olmedo[(1,3)], Anna Tatarczak[(1)], Tianjian Zuo[(2)], J. Estaran[(1)], Xiaogeng Xu[(2)], Idelfonso Tafur Monroy[(1)]

(1) Department of Photonics Engineering, Technical University of Denmark (DTU), 2800 Kgs. Lyngby, Denmark.
(2) Transmission Technology Research Department, Huawei Technologies Co., Ltd., Shenzhen, 518129, China.
(3) Optics division, Royal Institute of Technology (KTH), Electrum 229, Kista, SE-164 40, Sweden.
molm@fotonik.dtu.dk

Abstract: Employing MultiCAP signaling, successful 70.4 Gbps transmission over 100m of OM3 MMF using off-the-shelf 850 nm VCSEL with 10.1 GHz 3-dB bandwidth is experimentally demonstrated indicating the feasibility of achieving 100 Gbps with a single 25 GHz VCSEL.
OCIS codes: (060.2330) Fiber optics communications; (060.4080) Modulation

1. Introduction

Active optical cables (AOC) for datacenter interconnect and supercomputer applications are forecasted to surpass a market of 40 million units per year by 2015 and to evolve from current 40 Gbps to 100 Gbps capacity [1]. Furthermore, AOC are required to meet the growing bandwidth demands while keeping the cost at minimum, providing longer reach, lighter weight and smaller form factor [2]. AOCs typically use vertical-cavity surface-emitting lasers (VCSEL) and photodiodes operating at 850 nm, combined with multi-mode fiber (MMF) of 1 to 100 m length. This combination offers a good tradeoff between capacity and cost. Although the objective is very clear, how to increase capacity without increasing the cost, the power consumption and the form factor is a timely and challenging research question. Moving towards longer wavelength would provide more bandwidth at the cost of more expensive light sources, whereas increasing the number of lanes incurs in more complex designs and bigger form factors. Therefore, more spectrally efficient modulation formats are now being researched. The highest error-free bitrates reported for 850 nm VCSELs-based links are 60 Gbps over 2 m OM4 using 4 level pulse amplitude modulation (4-PAM) [3], 55 Gbps over 5m OM2 using on-off keying (OOK) [4], and 35.2 Gbps over 100m OM4 using 8-PAM [5]. All of which require very fast electrical interfaces, and suffer from low tolerance towards modal dispersion as compared to pass-band modulation formats [6].

We report on a 100 m MMF OM3 link that achieves below-FEC 70.4 Gbps (65.7 Gbps net rate) using a VCSEL with a bandwidth of 10.1 GHz. We use multiband and multilevel approach to carrierless amplitude phase (CAP) modulation [7]. Our proposed MultiCAP signaling has the prospect of achieving 100 Gbps over 100 m MMF with emerging 25 GHz 850 nm VCESLs. This solution overcomes both electrical and optical bandwidth limitations towards single lane 100 Gbps AOC employing cost efficient 850 nm MMF technologies.

2. Experimental Setup

Fig. 1 shows the experimental setup. The transmitter is composed of a digital-to-analog converter (DAC), a linear driver amplifier, a bias-tee and a commercially available 850 nm VCSEL. The fiber is a 100 m MMF OM3 compliant. The receiver consists of a photodiode, a linear amplifier and a digital-storage-oscilloscope (DSO). Signal generation and demodulation is performed off-line using Matlab.

For signal generation, we choose a 6 band configuration of MultiCAP [8] with different modulation orders per band depending on the aimed bitrate (see Tab. 1). The first configuration enables a total throughput of 70.4 Gbps

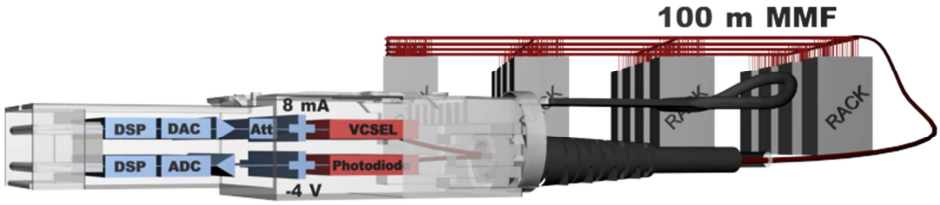

Fig. 1: Experimental Setup as in a CXP connector. Digital Signal Processing (DSP), digital-to-analog converter (DAC), attenuator (Att), analog-to-digital converter (ADC).

978-1-55752-993-0/14/$31.00 ©2014 Optical Society of America

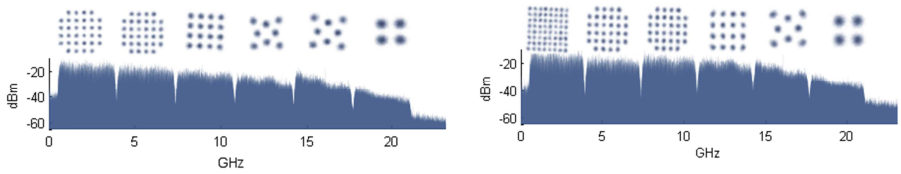

Fig. 2: Received spectrum and constellations MultiCAP signals for a)70.4 Gbps over 100 m and b) 80 Gbps over 1 m.

(65.7 Gbps after 7% overhead forward error correction (FEC) decoding), whereas the second configuration enables 80 Gbps (74.7 Gbps after 7% FEC). Received electrical spectrum and constellations are presented in Fig. 2. Each band was constructed from a pseudo-random binary sequence (PRBS) of 2^{13}-1 bits and delivers a baud rate of 3.2 Gbaud. The CAP filters were 20 symbols long with 0.05 and 0.08 roll-off factors for transmitter and receiver respectively, and the number of samples per symbol and band was 20. Each band is equally spaced 4.28 GHz. The electrical signal generation is performed by a 64 GSa/s DAC with 5 effective number of bits (ENOB).

The DAC output is amplified to a 1.2 Vpp signal that is used to drive an 850 nm VCSEL biased at 8 mA. Fig. 3a shows the light-intensity-voltage (LIV) curve of the VCSEL together with its operation region. Fig. 3b shows optical spectrum of the VCSEL driven with a MultiCAP signal. An optical power of 6 dBm is launched into 100 m of MMF with a total link loss of 0.5 dB for 100 m. The signal is photo-detected with an 850 nm photodiode reverse biased at 4 V. The signal is then amplified to a Vpp of 1 V and digitally stored with an 80 GSa/s DSO with a resolution of 8 bits. Offline processing is performed as described in [8]. Multimode dispersion and other linear impairments are compensated by using a 15 tap decision-directed (DD) equalizer per band.

Tab. 1: Modulation order per band for different bitrates

Bitrate (Gbps)	B1	B2	B3	B4	B5	B6
70.4	32	32	16	8	8	4
80	64	32	32	16	8	4
108	64	64	32	16	16	4

3. Results

Fig. 4b shows the measured bit error rate (BER) curves. We define the sensitivity at a BER of 4.4 10^{-3} which is below the theoretical limit of 7% FEC based shortened BCH (Bose - Chaudhuri - Hocquenghem) components [9]. Thereby, we can observe sensitivities of 2.1, 4.7 and 5.4 dBm for experimentally obtained 70.4 Gbps over 1 m, 70.4 Gbps over 100 m, and 80 Gbps over 1 m respectively. The measured transmission penalty after 100m MMF is 2.5 dB; a significantly low penalty considering the high bitrate.

Fig. 4a shows the end-to-end frequency response of the transmission link as well as electrical B2B. A 3 dB bandwidth of 10.1 GHz was measured for the optical end-to-end link and 11 GHz for the electrical B2B. However, a difference of up to 10 dB can be observed between the electrical and optical frequency responses at 20 GHz. Such a

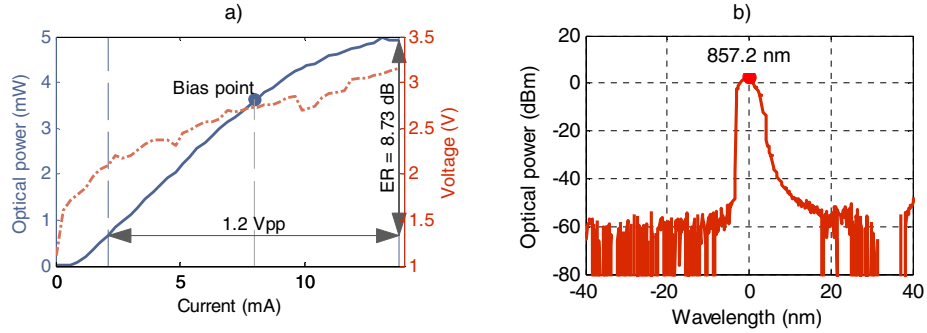

Fig. 3: a) LIV curve for VCSEL. b) Measured optical spectrum.

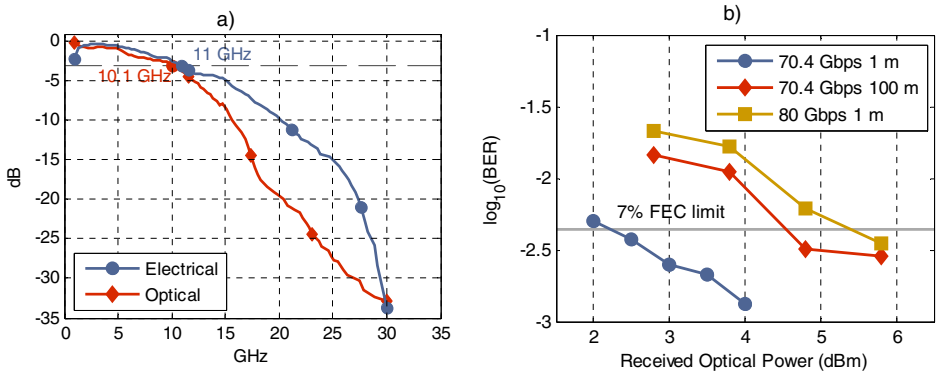

Fig. 4: a) Frequency response of the end-to-end link with and without the optical subsystem b) BER curves

steep roll-off drastically reduces the achievable capacity. We use the bit loading and power loading features of MultiCAP to overcome those limitations, at the cost of worsening the sensitivity. This can be directly observed as 3.1 dB penalty introduced by increasing the capacity from 70.4 to 80 Gbps. The latency of a MultiCAP system is mainly governed by the group delay of the CAP filters at both the transmitter and the receiver side:

$$Latency = 2 \times \frac{N_{sym}}{2} \frac{1}{R_b}$$

Where N_{sym} is the length of the filter in symbols, and R_b is the baud rate of each subband. For our reported configuration, the calculated latency value is 6.25 ns, which is a much lower value compared to the latency due to FEC processing (~100 ns) [10].

4. Conclusions

We have achieved record transmission of 70.4 Gbps (65.7 Gbps net rate) over 100m, and 80 Gbps (74.7 Gbps net rate) over 1 m for 850 nm MMF data links. The advantageous feature of MultiCAP approach of being able to assigning parallel electrical interfaces of smaller bandwidth into different frequency bands overcomes both electrical and optical bandwidth limitations, and eases the DSP pipelining. Its pass-band nature and multi-band structure greatly increase tolerance towards multimode dispersion, while retaining the same complexity as in baseband approaches. And the added latency is considerably low in comparison to other DSP processes such as FEC.

5. References

[1] "The Active Optical Cable Market Analysis & Forecast Report," 2013.

[2] A. Benner, "Optical Interconnect Opportunities in Supercomputers and High End Computing," in *Optical Fiber Communication Conference*, 2012, p. OTu2B.4.

[3] P. Westbergh, M. Karlsson, A. Larsson, P. a. Andrekson, and K. Szczerba, "60 Gbits error-free 4-PAM operation with 850 nm VCSEL," *Electron. Lett.*, **49**, 15, pp. 953–955, Jul. 2013.

[4] D. M. Kuchta, A. V Rylyakov, C. L. Schow, J. E. Proesel, C. Baks, C. Kocot, L. Graham, R. Johnson, G. Landry, E. Shaw, A. MacInnes, and J. Tatum, "A 55Gb/s directly modulated 850nm VCSEL-based optical link," in *IEEE Photonics Conference*, 2012, p. PD1.5A.

[5] K. Szczerba, M. Karlsson, P. Andrekson, A. Larsson, and E. Agrell, "35.2 Gbps 8-PAMTransmission Over 100 m of MMF Using an 850 nm VCSEL," in *39th European Conference and Exhibition on Optical Communication*, 2013, p. Th.1.F.1.

[6] L. Raddatz and I. H. White, "Overcoming the modal bandwidth limitation of multimode fiber by using passband modulation," *Photon. Technol. Lett.*, **11**, 2, pp. 266–268, Feb. 1999.

[7] M. Iglesias Olmedo, Z. Tianjian, J. Bevensee Jensen, Z. Qiwen, X. Xu, and I. T. Monroy, "Towards 400GBASE 4-lane Solution Using Direct Detection of MultiCAP Signal in 14 GHz Bandwidth per Lane," in *Optical Fiber Communication, National Fiber Optic Engineers Conference (OFC/NFOEC)*, 2013, p. PDP5C.10.

[8] M. Iglesias Olmedo, T. Zuo, J. Jensen, Q. Zhong, X. Xu, S. Popov, and I. Tafur Monroy, "Multiband Carrierless Amplitude Phase Modulation for High Capacity Optical Data Links," *J. Lightw. Technol.*, **PP**, 99, 2013.

[9] J. Justesen, "Performance of Product Codes and Related Structures with Iterated Decoding," *Trans. Commun.*, **59**, 2, pp. 407–415, Feb. 2011.

[10] A. Szczepanek, "FEC Latency Considerations," in *IEEE P802.3bm 40 Gb/s and 100 Gb/s Fiber Optic Task Force*, 2012.

Appendix C

Paper 11: SWDM Strategies to Extend Performance of VCSELs over MMF

Tatarczak, A.; Reza Motaghiannezam, S. M.; Kocot, C.; Hallstein, S.; Lyubomirsky, I.; Askarov, D.; Daghighian, H.M.; Nelson, S.; Tatum, J.A., "SWDM Strategies to Extend Performance of VCSELs over MMF," *Optical Fiber Communications Conference and Exhibition (OFC)*, paper Tu2G.1, 2016.

SWDM Strategies to Extend Performance of VCSELs over MMF

C. Kocot[1], S.M.R. Motaghiannezam[1], A. Tatarczak[1], S. Hallstein[1], I. Lyubomirsky[1], D. Askarov[1], H. Daghighian[1], S. Nelson[1], and J.A. Tatum[2]
(1) Finisar Corp., 1389 Moffett Park Dr., Sunnyvale, CA, 94089, USA
(2) Finisar Corp., 600 Millennium Dr., Allen, TX, 75013, USA
Chris.kocot@finisar.com

Abstract: Experimental data is presented demonstrating 100GbE (4x25.8 Gbps) SWDM4 VCSEL technology, and SWDM4 transmission over 200m and 300m of wideband OM4 fibers. All NRZ SWDM4 channels achieved error-free transmission at 200m, and BER < 1e-9 at 300m. In addition, successful 180 (4x45) Gbps transmission is demonstrated over 300m wideband OM4 fibers using a 45-Gbps-PAM4 chip. Real time BERs < 2e-4 were achieved for all four SWDM grid channels in the 850-950nm wavelength range. Precise modal excitation in MMF fibers for improving the fiber bandwidth by minimizing modal dispersion is also discussed. Using our novel modal excitation method, 25 Gbps NRZ transmission over 300m OM3 is shown.
OCIS codes: (060.0060) Fiber optics communications; (060.4080) Modulation

1. Introduction

Multimode fiber (MMF) optical modules based on vertical cavity surface emitting laser (VCSEL) technology provide a low cost and power efficient solution for 100 Gbps data center networks based on parallel multimode fiber [1]. The IEEE recently standardized these systems as 100GBASE-SR4 (100GbE), providing a maximum reach of 100m on OM4 fiber. It would be desirable to extend the reach to 300m OM4, while also saving on fiber plant costs by reducing or eliminating the need for parallel fiber. In addition, 300m OM3 reach is attractive for data center networks. Higher transmission rates and longer reach can be achieved for data center networks by leveraging of electronic or/and optical technologies such as four-level Pulse Amplitude Modulation (PAM4) [2] and electronic equalizers [3] as well as short wavelength division multiplexing (SWDM) and novel wideband MMFs [4]. However, powerful DSP based modulation and equalization techniques suffer from high power consumption.

In this paper, we describe SWDM4 transmission over wideband OM4 fiber as well as selective mode excitation in OM3 fiber to increase data rate and extend reach without using DSP based modulation and/or equalization techniques. We demonstrate that the extended reach, high capacity, fiber efficiency, and low power consumption are achievable by simultaneous use of 4 x 25.8 Gbps SWDM (SWDM4) VCSEL technology and novel wideband OM4 fiber. Successful 100 GbE SWDM4 transmission is shown over 300m wideband OM4 by utilizing only conventional low-power NRZ electronics and low-cost SWDM optics. We also show that the selective mode excitation enables us to increase the 3 dB transmission bandwidth of MMF. In conjunction with simple equalization, this method extends the reach of OM3 fiber to over 300m at 25.8 Gbps; a distance objective for the extended reach data center applications. By combining optical and electronic technologies, we experimentally demonstrate the potential application of 200GBASE-SWDM4 over wideband OM4 fiber using a single chip PAM4 generator and equalizer. The measured average optical powers (AOPs) are shown at IEEE standard KP4 FEC with a BER threshold of 2e-4 for 180/204 Gbps PAM4-SWDM transmission over 100m and 300m wideband OM4 fiber as well as 200m conventional OM4 fiber.

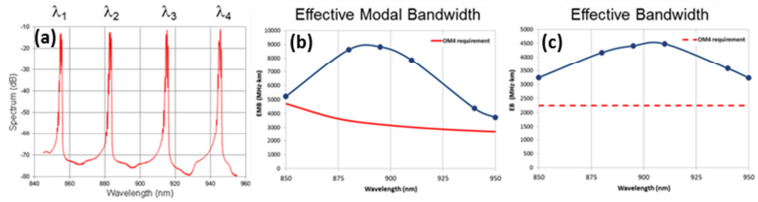

Fig. 1 (a) Measured SWDM4 spectrum, (b) measured effective modal bandwidth (EMB) and (c) effective bandwidth (EB) of the wideband OM4 (blue) and OM4 bandwidth requirement (red).

2. Experimental Setups and Results

A set of four 25G VCSELs and photodetectors (PDs) are designed and fabricated for SWDM application in the 850-950nm band. The VCSELs and PDs are assembled into conventional 25.8 Gbps TOSA and ROSA packages. For this initial demonstration, we employ separate SFP+ modules for each channel. The modules include conventional 25G NRZ CDR, and there is no DSP or adaptive technology, the channel spacing is 30nm, the external wavelength multiplexer has passbands of ~20nm to accommodate the wavelength accuracy specifications for uncooled VCSEL operation. The four-channel SWDM spectrum measured at output of the multiplexer is shown in Fig. 1 (a). The VCSEL center wavelengths are measured at 855, 883, 915, and 945nm, and RMS spectral bandwidths (SBWs) are in the range 0.34 to 0.41.The link includes a mode preserving VOA to adjust the optical power, and various lengths of wideband OM4 fiber. The measured effective modal bandwidth (EMB) is shown in Fig. 1 (b). This fiber is designed for peak EMB at ~ 890nm. Note that chromatic dispersion bandwidth tends to shift the peak of net effective bandwidth (EB) to slightly longer wavelengths at ~ 905nm. The EB shown in Fig. 1 (c) is calculated from the EMB data (Fig. 1 (b)) and chromatic dispersion bandwidth, assuming a VCSEL SBW of 0.4 nm, without taking into account modal and chromatic dispersion interaction.

Figure 2 shows the measured BER curves for 4 x 25.8 Gbps NRZ-SWDM (SWDM4) over the link with wideband OM4 fiber as a function of the received AOP measured at the receiver. The BER was measured simultaneously on the SWDM4 channels using a four-channel BERT. We used pseudo-random bit sequences (PRBS) of length 2^{31}-1 in all tests. For clarity, the BER data is organized into four separate plots, one for each wavelength channel. We show BER waterfall curves measured B2B (black squares), after 200m (blue triangles), and after 300m (red diamonds) for each wavelength channel. The B2B receiver sensitivities at BER=1.e-12 are approximately in the range of -10 to -10.5 dBm. At 200m, we achieve error-free transmission on all channels when the received power is > - 8 dBm. The 200m power penalties relative to B2B are modest, approximately ranging from 1 to 2 dB at BER=1.e-12. We believe this SWDM transmission result demonstrates acceptable performance over 200m wideband OM4 without the need for FEC. At 300m, the penalties increase significantly as expected from the measured eye diagrams. Nevertheless, all channels achieve BER < 1.e-9. This BER performance provides adequate margin to achieve error-free transmission in data center systems employing IEEE standard KR4 FEC with a BER threshold at 5.e-5.

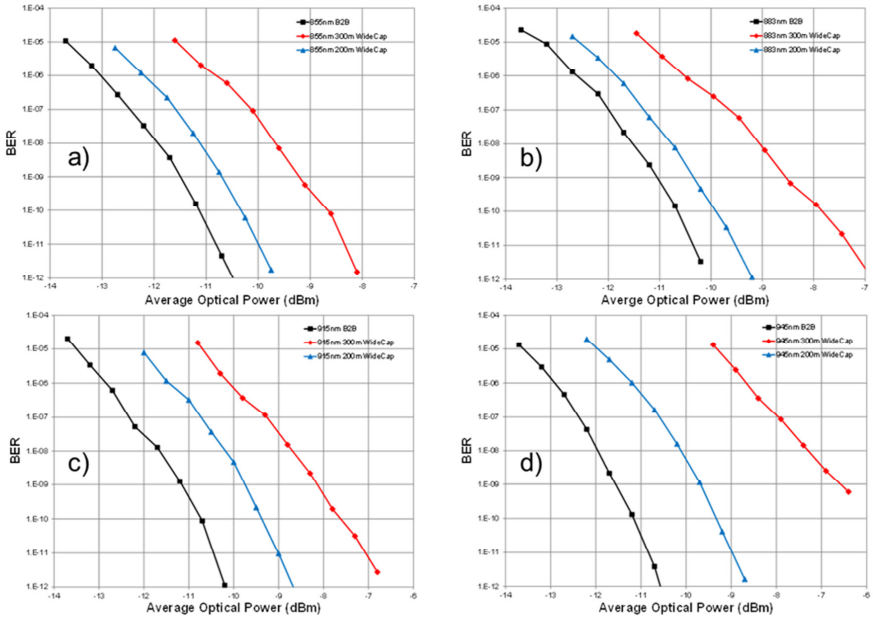

Fig. 2 Measured BER B2B (black), 200m (blue), and 300m (red) for a) 855nm, b) 883nm, c) 915nm, and d) 945nm channels.

To improve 3dB MMF bandwidth and extend the reach, a selective mode VCSEL beam launcher was used at the output of a 25.8 Gbps NRZ TOSA at 850nm. Figures 3 (a-b) show the received NRZ eye diagrams at 25.8 Gbps after transmission over OM3 fiber. The eye diagram (Fig. 3 (a)) was measured using a standard launch and no equalization. In this case, the eye at the output of a 300m link of OM3 fiber is completely closed. The eye in Fig. 3 (b) was measured using a selective mode launcher and simple Feed-Forward Equalization (FFE). This eye demeonstartes enhanced data transmission through a 300m OM3 fiber link at 25.8 Gbps.

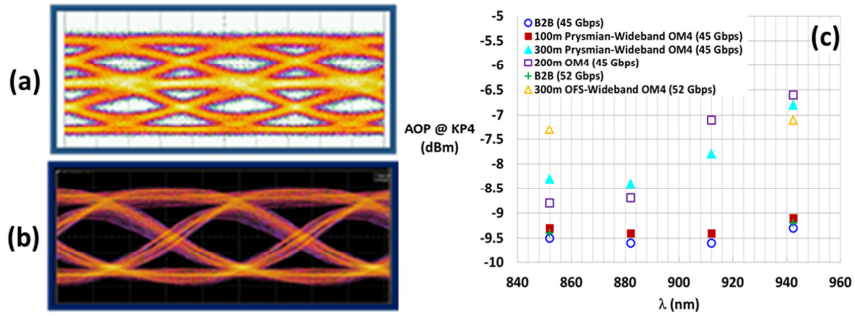

Fig. 3 Received optical eye diagrams after transmission over 300m OM3 fiber (a) using standard launch and no equalization and (b) using selective mode launch with simple FFE equalization. (c) AOPs at IEEE standard KP4 FEC with a BER threshold of 2e-4for four 45 Gbps PAM4 channels at 851.9, 882.0, 912.1, and 942.4nm and two 51.6 Gbps PAM4 channels at 851.9 and 942.4nm.

To study PAM4 SWDM4 receiver sensitivities, a single chip was used to generate 45 (or 51.6) Gbps PAM4 optical data stream. The 25G VCSELs were directly and differentially driven by 22.5-Gbaud (or 25.8-Gbaud) PAM4 PRBS of length 2^{31}-1 produced by integrated DACs, with ~0.8 Vpp electrical signal. The chip also performed the main functions, such as 45 Gbps PAM4 clock and data recovery, pulse shaping at the transmitter, adaptive modal and chromatic dispersion equalization at the receiver, and real-time BER measurement. Two sets of MMF types and various fiber lengths were used for this experiment including: 200m conventional OM4 fiber and wideband OM4 fibers (100m/300m). The wideband OM4 fibers are manufactured by Prysmian Group and OFS Corporation. The 25G VCSELs used in this experiment were production-grade Finisar VCSELs. The measured VCSEL center wavelengths were 851.9, 882.0, 912.1, and 942.4nm. RMS SBWs were 0.558, 0.370, 0.5011, and 0.527nm from the short wavelength to the long wavelength, respectively. The measured average RINs were ~-141 dB/Hz. In this study, a Finisar ROSA operating over the SWDM grid was used. The chip DSP provided functionality for digital pre-emphasis compensation. Using 22.5-Gbaud and 25.8-Gbaud PAM4 chips, the measured transmitter ERs were around 3.1 dB and 4.5 dB at four wavelengths, respectively. Figure 3 (c) shows the measured AOPs at IEEE standard KP4 FEC with a BER threshold of 2e-4for four SWDM 45 Gbps channels over 200m conventional OM4 as well as 100m and 300m Prysmian and OFS wideband OM4 fibers. The measured AOPs were ~-9.5 dBm for back-to-back over all SWDM 45 Gbps and 51.6 Gbps PAM4 channels at BER of 2e-4. Negligible AOP penalty (<0.2 dB) was captured over 100m Prysmian wideband OM4 fiber for all SWDM 45 Gbps PAM4 channels at KP4 level. Less than 0.5 dB AOP penalty was observed over 300m Prysmian wideband OM4 fiber in comparison with 200m conventional OM4 fiber for two short wavelength 45 Gbps PAM4 channels (850 nm and 880 nm). Long wavelength PAM4 channels (910 nm and 940 nm) over 300m Prysmian wideband OM4 fiber showed better receiver sensitivities at KP4 BER threshold compared to 200m conventional OM4 fiber. The required AOPs were ~-7.2 dBm over 300m OFS wideband fibers at 51.6 Gbps PAM4 channels at 850 nm and 940 nm.

3. Acknowledgement

We wish to thank Dr. Julie Eng at Finisar, Prysmian group, and OFS Corporation for their supports of this research.

4. References

[1] J. A. Tatum, et al., "VCSEL-Based Interconnects for Current and Future Data Centers," J. Lightwave Technol., **33**, 727-732 (2015).
[2] I. Lyubomirsky, et al., "Digital QAM Modulation and Equalization for High Performance 400 GbE Data Center Modules," OFC'14, W1F.4.
[3] R. Motaghian, et al., "45Gb/s PAM4 VCSEL 850/940nm Transmission over OM3 and OM4 Multimode Fibers," FIO'15, FM2E.3.
[4] D. Molin et al., "WideBand OM4 Multi-mode Fiber for Next-Generation 400Gbps Data Communications," ECOC'14, P.1.6.